Simulation of Nanostructure Formation in Rigid-Chain Polyelectrolyte Solutions

Dissertation

Zur Erlangung des Doktorgrades Dr. Rer. Nat.
der Fakultät für Naturwissenschaften
der Universität Ulm
vorgelegt von

Olga A. Gus'kova

aus Tver, Rußland

Ulm, 2008

CONTENTS

INTRODUCTION

Many synthetic macromolecules containing various functional groups are capable of self-organizing in three-dimensional assemblies. Self-assembling polymer systems are of great interest in nanotechnology. This is defined by the ability of macromolecules to form stable and well-ordered nanostructures. On the other hand, it may be easy to modify their self-organizing forms with small environmental changes.

In aqueous systems, both hydrophobic and electrostatic interactions are the most important for the self-organization processes. The presence of the charged groups is characteristic of both low-molecular amphiphils and many synthetic and natural polymers. At strong dissociation their monomer units became negatively charged. In this case, each macromolecule can be considered as a polyanion. Also, there are polycations with positively charged units.

Specificity of macromolecules consists in covalent connectivity of the large number of monomer units, which cannot move independently from each other. The connectivity sharply decreases translational entropy of the system. This fact is responsible for a higher ability of polymers, including polyelectrolytes, to form well-ordered nanostructures in comparison with low-molecular compounds.

The list of areas in which self-organizing polyelectrolyte systems find the feasibility is extremely wide. This list includes both traditional problems related to the design of innovative organic materials and more recent applications such as "organic electronics".

One of the most important features of ion-containing polymers is an ability to form regular nanostructures with well-ordered distribution, in essence, polymer component as well as counterions, usually Na^+ or K^+ for polyanions. Furthermore, these counterions can be replaced via ion-exchange by more complex ones (e.g. ions of noble and rare-earth metals) which represent the inorganic component showing controlled regular microheterogeneity distribution within the organic polymer matrix. Further reduction of metal ions to atoms allows to obtain regular metal nanostrucrures or nanoparticles inside the polymer matrix. Having the well-developed metallic surface with the controlled shape and size of microinhomogeneities, such systems are certainly of interest as catalysts with manageable activity. On the same principle, it is possible to create both the nanowires and nanocomposite metal-polymeric materials which have properties of electroconductivity or magnetism as well as

polymer – semiconductor type nanocomposites, which are potentially interesting objects for molecular microelectronics.

Ionomers with strongly associating groups are actively applied as organic fluid flow regulator (fuels, oil). Even very small amount of such polymers can drastically influence the flow characteristics of fluids. It is caused by the ability of high-molecular ionomers in dilute solution to form a thermoreversible-associated network. Under changes of temperature, this network can arise, thereby yielding system curdling, or can disintegrate, returning in system fluidity.

An active interest in different nanostructures of ion-containing polymers is also stems from the fact that they often play the dominating role in numerous biological systems. In this connection, it should be mentioned DNA collapse transition or chromatin formation, or *F*-actin spatial network formation.

Over the past few years, considerable progress in the polyelectrolyte theory has been achieved. Among the most important attainments it should be mentioned the development of the microphase separation theory (Erukhimovich, Khokhlov [1,2]), cascading collapse of hydrophobic-modified polyelectrolytes (Rubinstein, Dobrynin [3]), a giant overcharge of surfaces (Shklovskii, Grosberg [4]), polyelectrolyte nematic ordering (Potemkin [5]), description of both charged networks and gels behavior (Vasilevskaya, Starodoubtsev [6,7]), the elucidation of the role of counterion condensation and counterion correlation in like-charged ions attraction (Holm, Kremer [8], Winkler and Reineker [9]), etc. In spite of significant advances in this field, many critical problems in the polyelectrolyte theory are still under question.

The main theoretical challenges are related to the presence of two types of interactions, electrostatic and van der Waals, whose spatial scales are greatly different from each other. Because of this difference, analytical models can usually be developed only for weakly-charged polyelectrolyte chains, at small fraction of dissociating groups. However, many important polyelectrolytes are strongly-charged macromolecules. For example, the linear charge density of actin reaches 4 e/nm, DNA - 6 e/nm, M13 virus - 7 e/nm, fd-virus - 10 e/nm. To examine such systems, the computer simulations are more successful.

In computer simulation of polyelectrolytes, flexible charged chains and interpolyelectrolyte complexes based on them have been the subjects of extensive investigation. On the other hand, rigid and semiflexible charged chains were modeled much less. However, just

these polyelectrolytes are able to demonstrate the most interesting and practically important self-organization forms. Therefore, the investigation of rigid and semirigid strongly-charged polyelectrolytes is a highly topical problem.

In this thesis, the different polyelectrolyte systems have been studied, using computer simulation. The aim of this thesis is the investigation of nanostructure formation in rigid and semirigid strongly-charged polyelectrolyte solutions by means of computational approach.

Specific targets involve:

1. The study of aggregation and stability of complexes formed by rigid polyanions as well as the collapse transition of strongly-charged polyanions under the action of chain condensing agents;

2. The analysis of self-organization processes in solutions comprising both rigid polyelectrolyte chains and double hydrophilic block copolymers with opposite charged block; the investigation of stoichiometric complexes formation as well as their spatial ordering in dilute and semi-dilute regimes;

3. The examination of the processes of network formation in solutions comprising rigid polyelectrolyte chains and multivalent counterions.

The novelty of our study is related to the fact that for the first time, we used computer simulation to predict the properties of solutions of rigid strongly-charged polyelectrolytes. In particular, the following main results have been obtained:

- The state diagrams of complexes based on rigid polyelectrolytes have been built, depending on the temperature, solvent quality and condensing agents;

- Network structure formation in polyelectrolyte solutions in the presence of multivalent counterions have been predicted;

- Both polyelectrolyte chains stiffening in complexes with double hydrophilic block copolymers and liquid-crystalline ordering such ionic micelles having well-pronounced shape anisotropy, have been predicted.

The thesis is organized as follows.

The literature review is presented in the first Chapter. It includes common information about ion-containing macromolecules, short description of computer simulation methods, etc.

The Chapters 2-4 include original results.

In the second Chapter, the structure and stability of complexes formed by oppositely charged rigid-chain macromolecules and their response to variation in external conditions were studied using molecular dynamics. The conditions of conformational transitions were considered, depending on the chain length, temperature, and dielectric permittivity of the medium. It was shown that the chains involved in a complex can take various conformations having shape of torus, tennis racket, etc.

In the third Chapter, the complexation in solutions of strongly charged polyelectrolytes and diblock copolymers composed of oppositely charged and neutral blocks was studied. The main aim here was to explore in detail the structural properties of stoichiometric micellar complexes formed in a dilute solution.

In the fourth Chapter, the results of molecular dynamics simulation of solutions of strongly charged rigid-chain polymers in the presence of multivalent counterions are presented. The processes of macromolecule self-assembly which occur during the condensation of counterions were studied, depending on temperature, dielectric permittivity of the medium, and charge of counterions. Various conformational rearrangements induced by changing the parameters of the medium were examined.

Chapter I.   Objects and Methods.

I.1   Ion-containing Polymer Systems.

Ion-containing polymer molecules are those having charged units. A monomer unit can become charged due to dissociation; as a result, there are a charged unit and a low-molecular counterion. Usually, the dissociation occurs when molecules are dissolved in highly polar solvents, of which water is the most important (dielectric constant is $\varepsilon_r \approx 81$). For this reason, by ionic polymer systems one mostly means the aqueous polymer solutions [10,11].
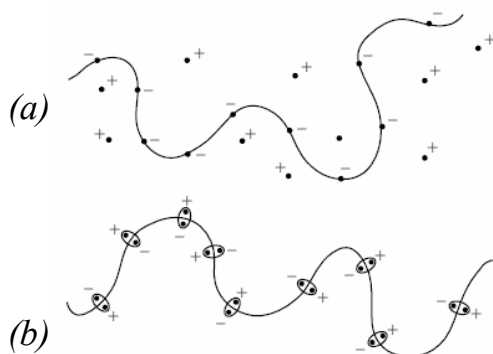
Figure 1. Polymer coil with charged units in (a) the polyelectrolyte and (b) ionomeric regimes. Dots are negatively charged monomer units and positively charged counterions [10].

In this case, a polymer coil can be schematically depicted as that shown in **Fig. 1***a*, with charged units and counterions being relatively independed of one another. The corresponding behavior of ion-containing macromolecules is called polyelectrolyte behavior, and polymer chains are polyelectrolytes. An alternative behavior can be observed when counterions are condensed on oppositely charged monomer units of a polymer chain with the formation of the so-called ion pairs (**Fig. 1***b*). Such situation is known as ionomeric regime. It is realized in a low-polar media.

As mentioned in the Introduction, polyelectrolytes can carry both negative (polyanions) and positive (polycations) charges. Typical examples of anionic units are sodium acrylate and sodium metacrylate. An example of cationic unit is diallyldimethylammonium chloride. Polymer chains consisting merely of charged monomer units are called strongly charged polyelectrolytes. The fraction of charged units can be smaller, e.g. in copolymers consisting of charged and neutral units or in chains with a pH-dependent charge (acrylic and metacrylic acids). These units are not charged at low pH; however, they can acquire a charge at higher

pH. Charged macromolecules with a small fracton of charged units are called weakly charged polyelectrolytes.

For strongly charged polymer chains, the long-range Coulomb interactions are of great importance. These interactions strongly influence the system's behavior. For the first time, it had been shown by Staudinger [12] that some characteristic properties of the solutions of proteins and nucleinic acids can be caused by their high ionic charge.

Also, polyelectrolytes can be subdivided into flexible and rigid-rod types. Kuhn's statistical segment A is an important characteristic in this classification [13,14]. It is accepted that polymers having $A \approx$ 15-50Å are flexible; for semiflexible macromolecules, A is ~50-170Å. For rigid polymers, the A value can essentially exceed 100-1000Å [15]. Typical examples of semiflexible and rigid polyelectrolytes are presented in **Table 1**.

Table 1. Rigid and semirigid polyelectrolytes and their persistence length

Polyelectrolyte	*Persistence length*	*Ref.*
Alginate	50-170 Å	[16]
Xylinan	300 Å	[17]
DNA	500 Å	[18]
Xanthan	1200 Å	[19]
Actin	2-20 μ	[20]
PE based on poly(*p*-phenylene)	130 Å	[21]

Rigidity of polymer backbone significantly changes the majority of polyelectrolyte properties. In Ref. 22, it was assumed that in the case of flexible polyelectrolytes, a decrease in

ionic strength of a solution can lead to polymer coil swelling due to significant intramolecular forces and strong intermolecular electrostatic interactions. On the other hand, conformationally rigid rod-like polyelectrolytes remain in an extended form at any ionic strength or can collapse and form torus-like globules if their countour length essentially exceeds Kuhn's statistical segment length [22].

Active works on synthesis of rigid polyelectrolytes started only in the middle of 1980 [23]. In particular, both poly(1,4-phenylene-2,6-benzobisthiazole) and poly(1,4-phenyl-ene-2,6-benzobisoxazole) were synthesized. Afterwards effective synthesis ways were developed for others rigid polyelectrolytes, e.g. for PE based on poly(*p*-phenylene) [24,25]. These polymers have been successfully applied in solubilization processes [26] and catalysis [27]. Based on these polymers it was subsequently possible to receive carboxylated and sulphonated poly(*p*-phenylene) derivatives with homogeneous structure and controllable degree of polymerization. Such polymers have the potential to combine environmental and thermal stability with their high charge density (up to four ionic groups per monomer unit). For this reason, such polyelectrolytes were often investigated as an ideal model of rigid strongly charged polyelectrolytes [28,29]. The main aim of those investigations was to explore in detail the counterion of correlations near a strongly charged macroion. These effects can be directly measured in experimental studies of counterion activity and spatial distribution of small ions around a macroion. Because of the cylindrical symmetry and well-defined conformation, such polyelectrolytes represent also the simplest system for which the counterion correlations near to macroion can be described analytically [8].

I.2   Self-Organization Processes in Ion-Containing Polymers.

The molecular self-assembly is widespread phenomena associated with both well-ordered aggregation and various cluster formation. By selecting a chemical structure of synthesized molecules and the nature and distribution of functional groups, it is possible to control over molecular assembly process in order to construct the complex supramolecular structures with unique properties. At a given polymer concentration and environmental conditions, this process occurs spontaneously, and the formed structure is thermodynamically stable because of associative bonding interaction. There are some polymer systems which have the ability to form thermodynamically stable microdomain structures. Usual representatives are many synthetic copolymers, some types of polymer networks, ion-containing polymer

systems (the mixture of weakly-charged PEs, PE gels [3,6], solutions and melts of ionomers, etc.). What all such objects have in common is that they are characterized by two competing factors, one of which causes macroscopic separation in the system, and another factor hinders this tendency with energetic, entropic or kinetic reasoning. The fine sensibility of these systems with respect to the environment and wide range of the structural motifs and molecular architectures, and the possibility to monitor of assembly in the bulk makes this investigation of the nanostructure formation in ion-containing polymers one of most interesting direction in polymer science.

Lyotropic liquid crystaline PEs. Semiflexible PEs in a solution can generate liquid-crystal order. The representative examples of macromolecules for which this effect was revealed are ion-modified polysaccharides (see Table 1) and nucleic acids in double helix conformation. The ability of PEs to form well-defined structures in dilute solutions has been stressed by many authors [30]. In this case, an abnormal viscosity growth was observed at some polymer concentration, which is concerned with the liquid-crystalline order formation. In Refs. [31,32], the behavior of concentrated PE solutions has been studied. The transition "LC – isotropic solution" has been established for xanthan, cellulose sulfate and carboxy-methyl cellulose.

Hydrophobic PEs. Three general types of hydrophobic PEs are recognized: charged block copolymers, associating PEs, and polysoaps. The simplest block copolymer types are copolymers containing two covalently linked blocks. Diblock-PEs, including both hydrophilic A-block (PE) and hydrophobic B-block have the "tadpole" conformation in water, because water is a good solvent for PE blocks and a poor solvent for B blocks. Several B blocks aggregate with each other forming the micellar core which is stabilized by PE shell. The ability of PECs to form the different micelle structures is similar to that characteristic of low-molecular tensides. The sizes of such micelles in aqueous solutions are determined by competition between core surface tension and electrostatic repulsion between chains in the shell [33]. The control over hydrophilic-lipophilic balance provides opportunities of morphology design under changes of the ionic strength or pH value. Recent experiments have demonstrated a wide variety of micellar morphologies, spherical or cylindrical micelles, and vesicles [34,35]. Using the scaling approach, the state diagram of such systems has been proposed [36]. These theoretical predictions are well correlated with the corresponding experimental data [35].

Water-soluble polymers having a hydrophilic backbone, which contains the minor amounts of hydrophobic groups, can form high viscosity solutions. It is related to a trend of hydrophobic groups to make the intermolecular aggregates of micellar type [37], which can act as physical gel cross-links (thermoreversible associating gel consists of PE chains). Rheological properties of such polymers determine their common use as dye component, in cosmetic chemistry, paper coating and oil recovery [38].

Self-organization in PE-surfactant systems. In many experimental papers devoted to PE-surfactant complexes, interaction between either PEs and opposite charged tensides or associating polymers and micelle-forming surfactants have been considered [30]. It was established that the chemical structure of PEs, linear charge density, charge arrangement, PE hydrophobicity, and chain flexibility/rigidity influence not only the cooperativity of complexation process and surfactant aggregation numbers, but also determine final conformation of the complexes [39,40].

The processes of self-assembly in the systems of opposite charged PE chains, PEs interacting with double hydrophilic block copolymers, as well as the structure formation in PE solutions involving multivalent ions are discussed in Chapters II, III and IV, respectively.

I.3 Polyelectrolyte in Solution: Theoretical Predictions.

In this section, we present some theoretical fundamentals that are related to the results of our simulations which will be discussed in the corresponding Chapters.

Electrostatic interactions make the properties of PE solutions qualitatively different from those known for neutral polymer solutions [3,9]. For example,

(1) The crossover from dilute to semidilute solution regime occurs at much lower polymer concentrations than that in solutions of neutral chains.

(2) There is a well-pronounced peak in the scattering function of the homogeneous polyelectrolyte solutions. The magnitude of the wave vector corresponding to this peak increases with concentration as $c^{1/2}$. There is no such peak in solutions of neutral polymers.

(3) The osmotic pressure of PEs in salt-free solutions exceeds the osmotic pressure of neutral polymers at comparable polymer concentrations by several orders of magnitude. It increases almost linearly with polymer concentration and is independent of the chain mo-

lecular weight in a wide range of polymer concentrations. This almost linear concentration dependence of the osmotic pressure together with its strong dependence on added salt demonstrates that osmotic pressure is mainly due to the counterion contribution.

(4) The viscosity of polyelectrolyte solutions is proportional to the square root of polymer concentration $\eta \sim c^{1/2}$ (Fuoss' law), while for solutions of uncharged polymers at the same concentration, the viscosity is proportional to polymer concentration. There is no concentration regime where reduced viscosity η/c of solutions of neutral polymers decreases with polymer concentration ($\eta/c \sim c^{-1/2}$ for PEs in the Fuoss regime) [3,9].

(5) PE chains in semidilute regime follow unentangled dynamics in a much wider concentration range and the crossover to the entangled dynamics occurs further away from the chain overlap concentration than in solutions of uncharged polymers [3,9].

The origin of the differences listed above with neutral polymers can be traced back to the difficulty to apply renormalization group theories and scaling ideas to systems in which long-range (Coulomb) forces are present. The success of the modern theories of neutral polymer solutions is based on the fact that the range of the interactions between molecules is much smaller than the scale determining the physical properties of the solution, which is the size of the polymer chain or the correlation length. If, as it is in general the case in polymer physics, the main issue is the variation of solution properties with molecular weight, the interactions only affect prefactors that can be adjusted to experimental results. The theories [41,42] developed in this spirit have proven extremely powerful for the interpretation of experimental data on neutral polymer solutions. Polyelectrolyte solutions are more complex, both short range (excluded volume) and long-range (Coulomb) interactions are simultaneously present. The screening of the electrostatic interactions introduces an intermediate length scale in the problem that can be comparable to the chain size or to the correlation length. Moreover, the details of the local chain structure are important and control such important phenomena as counterion condensation [43]. The counterion condensation in turn modifies the long-range part of the interaction. The long range interactions also have a nontrivial influence on the local structure [44] (e.g., stiffness) of the polymer chains. The implication of this complicated coupling between small and large length scales is that the theoretical results for polyelectrolytes can be expected to be more "model-dependent" than for neutral polymers. In particular, the functional dependence of several physical properties on molecu-

lar weight or concentration depends in some cases on the local description that is used for the polymer chain. Such situations never occur in neutral polymers.

In the theoretical limit of infinite dilution and zero salt concentration, a PE chain can be modeled as a connected sequence of charged and uncharged monomers in a "dielectric vacuum" that represents a solvent. This model is not very realistic to describe actual PE solutions but it serves here to introduce some important concepts important for charged polymer chains. In particular, within the framework of this model, the following expression is valid [41,42]

$$R \sim N f^{2/3} \left(l_B b^2 \right)^{1/3} . \tag{1.1}$$

This establishes the well-known result that the mean chain size R is proportional to the number of monomers N and to a $1/3$ power of the charge fraction f. This result was first obtained by Katchalsky and coworkers [45] using a distribution function approach. The electrostatic interactions tend to swell the chain; therefore, the equilibrium radius of a weakly charged PE chain must be larger than the Gaussian radius, $R_0 \sim N^{1/2}$. A more refined calculation of the electrostatic energy, accounting for the fact that the shape of the chain is rodlike rather than spherical, only yields a logarithmic correction to Eq. (1.1):

$$R \sim N f^{2/3} \left(l_B b^2 \ln(N) \right)^{1/3} . \tag{1.2}$$

Because of this rodlike character, the polyelectrolyte chain is often described as being a "fully extended" object. Short-range molecular flexibility does not have to be frozen in a locally stretched configuration to obtain such relations. To get a deeper insight into the meaning of Katchalsky's calculation, it is useful to introduce the concept of the so-called electrostatic blob [41].

An electrostatic blob is a chain subunit within which the electrostatic interactions can be considered as a weak perturbation. The size ξ_e and the number of monomers g in such a subunit are thus related by $\frac{(fg)^2 l_B}{\xi_e} \cong 1$. The blob picture is particularly useful to discuss the structure of a charged chain in a good or poor solvent. In a good solvent, the only modification compared to the theta solvent case (when $R_0 \sim N^{1/2}$) is the good solvent statistics characterized by a swelling exponent $\upsilon \neq 1/2$ must be used in the relation that relates the blob size to

the number of monomers in a blob, $\xi_e \sim g^\upsilon$. The result is still a linear string of blobs $R \sim N f^{(2-2\upsilon)/(2-\upsilon)}$.

In a poor solvent, the problem has first been analyzed in detail by Khokhlov [46]. In that case, the chain would be completely collapsed into a globular state in the absence of electrostatic interactions. The effect of these interactions is to break up the globular structure into a string of "globular blobs". For this case Eq. (1.1) is replaced by

$$R \sim (N/g)\xi_e \sim N\tau^{-1}\left(f^2 l_B /b\right)^{2/3}$$
$$\xi_e \sim b\left(f^2 l_B /b\right)^{-1/3}; \quad g \sim \tau\left(f^2 l_B /b\right)^{-1}, \tag{1.3}$$

where $n \sim \tau b^{-3}$ is density of the collapsed chain.

The Flory-type calculation discussed above is a typical mean-field approach. Similar approaches that have been successfully applied to the charged bead spring model include the "chain under tension" model [41] and the "Gaussian variational method" [47]. Both methods are mean-field approaches formulated in a variational fashion. For long-range interactions it was shown [48] that the variational Gaussian approach predicts the same asymptotic behavior as Flory's theory and as the "chain under tension" method. As for the chain under tension model, the quantitative agreement with numerical simulation results is good.

The success of variational and mean-field methods for chains with long-range interactions is not unexpected. As pointed out in Ref. [48], these methods usually fail because a poor approximation of the monomer-monomer correlation function is used in the calculation of the potential energy. In ither words, we observe here a compensation of different errors.

When a finite concentration of salt is present in solution (which is always the case in experiments, at least because of water dissociation), the solution becomes a conducting, rather than dielectric, medium. The fundamental implication is that the Coulomb interaction between charged monomers is screened by the salt solution, i.e. the electrostatic potential created by a monomer, or a group of monomers, falls off exponentially rather than algebraically with distance. Thus, distant parts of the chain do not interact, and the chain can be expected to behave, in the asymptotic limit $N \to \infty$, as a random walk with short-ranged repulsive interactions.

The resulting interaction is in general a complex function of the monomer coordinates, involving many body interactions. In the case of dilute salt solutions and sufficiently

weak perturbations, however, the linear response (or Debye-Hückel) theory can be used, and the salt can be treated as an ideal gas. The screening length $\kappa^{-1} = \lambda_D$ is then given by

$$\kappa^2 = 4\pi l_B I ,\tag{1.4}$$

where I is the ionic strength of the solution defined as $I = \sum_{\substack{ionic \\ species}} Z_i^2 \cdot c_i$, Z_i being the valence and c_i the concentration of species i.

The effective interaction can in this limit be written as a sum of pairwise additive interactions between the monomers. The effective pair potential is given by the Debye- Hückel formula:

$$v_{DH}(r) = k_B T \frac{l_B}{r} \exp(-\kappa r).\tag{1.5}$$

Although the potential (1.5) is short-ranged, its range κ^{-1} can be much larger than the monomer size, which is the typical interaction range in neutral polymers. Depending on the ionic strength, the value of κ^{-1} can vary typically from less than 1 nm to more than 100 nm. At distances smaller than κ^{-1}, the screened potential (1.5) is close to the unscreened Coulomb potential. The behavior and properties of PE chains can therefore be markedly different from those of neutral chains over rather large length scales.

The Flory-like model discussed above considers only the interactions between charged monomers along the PE chain and ignores the role of the small counterions that neutralize the PE charge. When the PE is strongly charged, the electrostatic potential on the chain is large and some of the counterions remain bound to the chain. This phenomenon is known as counterion condensation, or Manning condensation [43].

Within the framework of this theory, PE chain has an effective charge due to the charged monomers and to the sheath of bound, or condensed, counterions. As a result, the effective charge is lower than the nominal charge of the monomers. Counterion condensation can be effective even at infinite dilution and reduces the electrostatic interactions between monomers. The condensed counterion sheath around a PE chain is electrically polarizable (each monomer-counterion pair behaves like a dipole); this can induce attractive interactions between polyelectrolyte chains. The possible mechanisms for attractive electrostatic interactions in PE solutions will be discussed in Chapter IV.

Fuoss, Katchalsky, and Lifson [49] have studied the interaction between the PE chains and their counterion clouds using the Poisson-Boltzmann equation. They consider a solution of infinite rodlike molecules, which are all parallel. Around each of these molecules, there exists an equipotential surface where the electric field vanishes. This surface can be approximated by a cylinder parallel to the polyelectrolyte chains with a radius R. The average density of counterions in the cylinder is $c_i = fc = 1 \big/ \left(\pi R^2 A \right)$ where A is the distance between charges along the chain. From an electrostatic point of view, each chain with its counterions in the cylinder of radius R is independent of all the other chains. The electrostatic potential in this cell satisfies the Poisson equation

$$\Delta \psi = -4\pi l_B c_i \left(r \right) \tag{1.6}$$

where $c_i(r)$ is the local counterion concentration at a distance r from the chain. The local counterion concentration is obtained from Boltzmann statistics $c_i \left(r \right) = c_i \exp\left(-\psi\left(r \right) \right)$. This leads to the Poisson-Boltzmann equation:

$$\Delta \psi \left(r \right) = -\kappa^2 \exp\left(-\psi\left(r \right) \right) \tag{1.7}$$

The Debye screening length is defined here as $\kappa^2 = 4\pi l_B c_i$; it is such that $\kappa^2 R^2 = 4u$ where u is the charge parameter ($u = \dfrac{l_B}{A}$). The Poisson-Boltzmann equation can easily be solved exactly in this geometry [49]. The expression of the potential critically depends on the value of the charge parameter.

The Manning theory describes the condensation of the counterions as a transition between two states, a bound state and a free state. On the contrary, in the Poisson-Boltzmann approach, the distribution of the counterions is continuous and there is no bound state. However, close to the PE chain, the interaction energy between one counterion and the polyelectrolyte chain becomes much larger than $k_B T$ (in the region where electrostatic potential $\psi \gg 1$). One could then divide space into two regions, a region close to the chain where the interaction energy is larger than $k_B T$ (with a size of the order of a few times the monomer size b) and where the counterions can be considered as bound and a region further away from the chain where the interaction between a counterion and the chain is smaller than $k_B T$ and where the counterions can be considered as unbound.

The counterions condensed on a PE chain move essentially freely along the chain; they more or less form a one dimensional gas of average density g/b, where $g = b/l_B$ is the fraction of condensed counterions. The charge density along the chain is therefore not a frozen variable and shows thermal fluctuations due to the mobility of the counterions. When two chains are sufficiently close, the charge density fluctuations on the two chains are coupled by the electrostatic interactions; this leads to effective attraction between the polymers which is very similar in nature to the van der Waals interactions between polarizable molecules. A fluctuation induced attraction can be expected for all polyelectrolytes where the charges are mobile along the chain. This is for example the case above the Manning condensation threshold but also for annealed polyelectrolytes, which are polyacids or polybases, where the charge can be monitored by tuning the pH of the solution (for more detail, see Chapter IV).

In spite of variety of modern theoretical approaches used for description of charged polymer systems (including scaling concepts [41], PRISM[1]-model [50], mean-field methods [1] or others [51]) many problems are not well understood. In the context of theory, the main problem of description of PEs consists in long-range nature of electrostatic interaction, as discussed before. The problem is complicated by the presence in the system more than one typical interaction scales what is connected with both electrostatic and short-range potentials.

Most of aforementioned methods are unable to predict adequately the behaviuor of PE concentrated solutions as well as to take into account all details of PE chemical structure. In this respect, the use of computer simulations is very important.

I.4 Computer Simulation of Charged Polymer Systems.

I.4.1 Single Polymer Chain Models.

In a computer simulation, a real system is replaced by some simplified model. The choice of the model is determined by the task under consideration. The modeling of polymer chains can be carried out by either in continuum (continuous model) or on a lattice.

In *lattice model,* a realistic macromolecule is replaced by the polygonal path which is restricted by points of a perfect lattice (cubic, tetrahedral, etc.) [52]. Occupied lattice points

---

[1] PRISM - Polymer-reference-interaction-site model

correspond to polymer units, and segments joining them correspond to chemical links. The volume interactions, i.e. short-range repulsion which arises between non-connected monomer units when they are close to each other owing to bending of the chain, are modeled by a self-avoiding random walk. The variety of ways of chains arrangement on the lattice corresponds to different conformations. There are various modifications of lattice models, but all of them are discontinuous, i.e. the number of possible conformations is always finite. The lattice models possess high computational power, but as a rule, they can be investigated only by means of Monte Carlo techniques.

In *continuous model*, the polymer chain can change its conformation in continuous manner. The simplest example is the chain consisting of hard spheres sequentially linked by rigid or elastic bonds. Such models can be simulated both with Monte Carlo techniques and molecular dynamics methods (MD). In continuous models, where particle coordinates are continuously varied, the mobility of the system can be provided by vibrational and rotational motions of valence bonds and valence angles. In computer simulation of polymers a great number of models have been utilized which are applicable to both continuous and discrete space [53-56].

Since flexible polymers in solution can take large number of different configuration, their shape and size can be understood and described statistically. Quantitative charachteristics of molecule chain size are the mean square end-to-end distance R^2, the mean square radius of gyration R_g^2 and the contour length L_C.
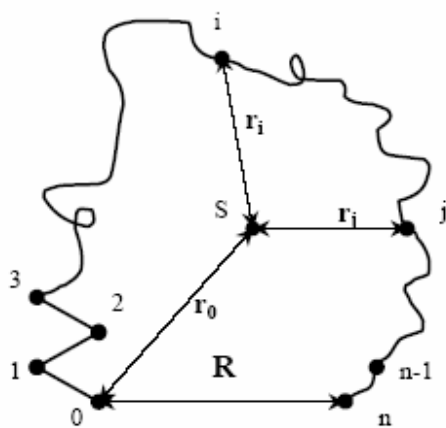
Figure 2. Sketch of a linear polymer chain. End-to-end distance R, the center of mass of the chain S, and distance of *i-th* monomer from the center of mass r_i are indicated.

The mean square radius of gyration is a quantity that one can obtain experimentally (e.g., from light scattering):

$$R_g^2 = \frac{1}{N}\sum_{i=1}^{N} r_i^2 \,.$$

(1.8)

It is defined as a mean square distance of all segments r_i (monomers) from the center of mass of the chain (**Fig. 2**).

The simplest model for the description of the shape of macromolecule in solution is the Kuhn segment model (freely jointed chain) [13,57]. For this model, the mean square end-to-end distance is

$$R^2 = N \cdot A^2 \,,$$

(1.9)

with N being the number of statistical segments of length A

$$A = \frac{R^2}{L_C} \,.$$

(1.10)

The extension of the freely jointed chain come out with consideration of fixed valence angle. The end-to-end distance becomes larger due to fixation of the bond angles

$$R^2 = N \cdot A^2 \frac{1+\cos\vartheta}{1-\cos\vartheta} \,,$$

(1.11)

where ϑ is the bond angle.

The next refinement of the model takes into account of hindered rotation around the connection axle. In this case, the end-to-end distance reads

$$R^2 = N \cdot A^2 \frac{1+\cos\vartheta}{1-\cos\vartheta} \cdot \frac{1+\langle\cos\Phi\rangle}{1-\langle\cos\Phi\rangle} \,.$$

(1.12)

A model suggested by Kratky and Porod [58] for stiff or semiflexible polymers in a solution is the so-called worm-like chain model. The main characteristic quantity in this model is persistence length. It determines the stiffenes of the chain and represents the distance over which the memory of the initial orientation of the polymer persists. The intrinsic persistence length ($l_{p,0}$) due to monomer structure and non-electrostatic interactions of the polymer is defined as:

$$l_{p,0} = \frac{d}{1+\cos\theta} \,.$$

(1.13)

Here, d is the segment length between points s and s' on the chain, θ the angle between two adjacent unit vectors tangential to the chain at position s and s' (see **Fig. 3**). For this model, the R, R_g, and ℓ_p values are connected by the following equations:

$$R^2 = 2\ell_p L_C - 2\ell_p^2 \left(1 - e^{-L_c/\ell_p}\right), \tag{1.14}$$

$$R_g^2 = \frac{1}{3}\ell_p L_C - \ell_p^2 + \frac{2\ell_p^3}{L_C}\left[1 - \frac{\ell_p}{L_C}\left(1 - e^{-L_c/\ell_p}\right)\right]. \tag{1.15}$$

The two limiting cases are:

1. $L_C/\ell_p \gg 1$ (Gaussian coil limit), $R^2 = 6R_g^2 = 2\ell_p L_C$;

2. $(L_C/\ell_p \ll 1)$ (rigid rod limit), $R^2 = 12R_g^2 = L_C^2$.
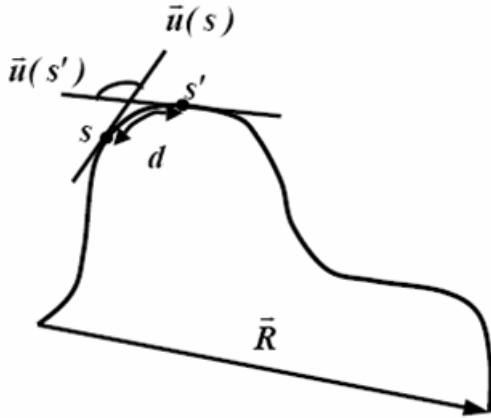
Figure 3. Sketch of a worm-like chain. Unit vectors $\vec{u}(s)$ and $\vec{u}(s')$ tangential to the chain at position s, s'; bend angle θ between unit vectors $\vec{u}(s)$ and $\vec{u}(s')$, and end-to-end vector $\vec{R}$ are indicated.

From these equations, the following well-known relation can be established

$$A = 2\ell_p. \tag{1.16}$$

However, in the case of PEs, the persistence length increases additionally due to electrostatic repulsion between monomers. Thus, the theoretical description of the persistence length should include this effect. This leads to an additional contribution to the persistence length, the electrostatic persistence length $l_{p,e}$ due to longe-range intrachain repulsion [59,60]. As a result, the effective persistence length is given by

$$\ell_p \cong l_{p,0} + l_{p,e}. \tag{1.17}$$

I.4.2 Interaction Potentials.

Understanding the interactions within and between the polymer chains can help in predicting macroscopic properties of the polymeric systems. That is why a proper choice of

the potentials governing the interactions (force field) is crucial in computer simulation. The forces between particles have to be as realistic as possible and also suitable for feasible simulations since their calculation is the most time consuming part of any simulation algorithm.

Generally, interaction potentials can be divided into two parts: the potentials which describe short-range intramolecular interactions, and non-bonded interactions. The first part includes the contributions that due to valence bonds, bond angles, and dihedral angles. The second part takes into account van der Waals and electrostatic forces, hydrogen bonding, and solvent interaction.

In most cases, van der Waals forces are described by a Lennard-Jones potential [61]:

$$V_{LJ}(r) = \begin{cases} 4\varepsilon\left[\left(\dfrac{\sigma}{r}\right)^{12} - \left(\dfrac{\sigma}{r}\right)^{6}\right] + c, & r \leq r_c \\ 0, & r > r_c \end{cases}$$

(1.18)

Here, σ and ε are parameters, r_c is a cutoff radius. Also, the Morse potential is frequently used [62].

The interaction of charged atoms is characterized by Coulomb potential

$$V_C(r) = \sum_{i \neq j} \frac{q_i q_j}{r_{ij}},$$

(1.19)

as well as by Debye-Hückel potential that takes into account the charge screening effects:

$$V_C(r) = k_B T q_i q_j \ell_B \frac{\exp(-\lambda_D r)}{r_{ij}},$$

(1.20)

where q_i is the charge of i-th particle, k_B is Bolzmann constant , ℓ_B is the Bjerrum length. The Bjerrum length is given by:

$$\ell_B = \frac{e^2}{4\pi\varepsilon_r\varepsilon_0 k_B T}.$$

(1.21)

Here, e is the elementary charge, ε_0 is the electrical permittivity of vacuum, and ε_r is the permittivity of medium.

The problem of correct description of long-range electrostatic interactions is the most important in molecular simulations. A category long-ranges forces consists of the charge-charge interaction between ions ($V^{zz}(r) \sim r^{-1}$) and dipole-dipole interaction between mole-

cules ($V^{\mu\mu}(r) \sim r^{-3}$). These forces are a serious problem for the computer experiment, since their range is always greater than half the box length[2].

A variety of methods have been developed to handle long-range forces [63]. The lattice methods, such as the Ewald sum (ES), include the interaction of an ion or molecule with all its periodic images. In some cases, these methods tend to overemphasize the periodic nature of the model [64,65]. The reaction field (RF) methods assume that the interaction from molecules beyond a cutoff distance can be handled in an average way, using macroscopic electrostatics.

The ES is a technique for efficiently summing the interaction between an ion and all its periodic images. The potential energy can be written as

$$V^{zz} = \frac{1}{2} \sum_{\mathbf{n}} \left(\sum_{i=1}^{N} \sum_{j=1}^{N} z_i z_j \left| \mathbf{r}_{ij} + \mathbf{n} \right|^{-1} \right), \tag{1.22}$$

where z_i, z_j, are the charges. The sum over $\mathbf{n}$ is the sum over all simple cubic lattice points, $\mathbf{n} = \left(n_x L, n_y L, n_z L \right)$ with n_x, n_y, n_z being integers and L denoting the box size.
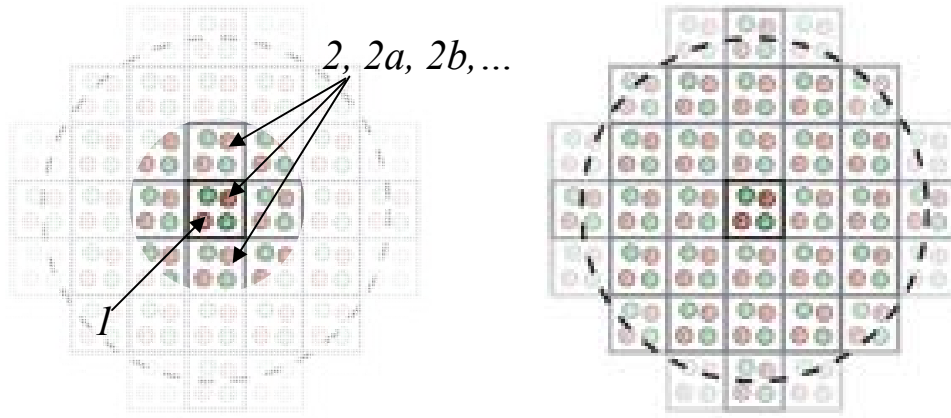
Figure 4. The construction of a system of periodic cells in the Ewald method. Ion *1* interacts with ion *2* and all its periodic images, *2a*, *2b*, …, etc.

The unit cells are added in sequence: the first term has $|\mathbf{n}| = 0$, i.e., $\mathbf{n} = (0,0,0)$; the second term $|\mathbf{n}| = L$ comprises the six boxes centered at $\mathbf{n} = (\pm L,0,0)$, $\mathbf{n} = (0,\pm L,0)$, $\mathbf{n} = (0,0,\pm L)$; etc. As soon

---

[2] In most cases, computer simulations are performed with periodic boundary conditions (PBC). Upon that the objects being examined are put into the computational box. This system is placed in a central model box which is surrounded by an infinite array of its periodic images [64].

as further term is added to the sum, an infinite system is building up in roughly spherical layers (**Fig**. **4**).

For this approach the nature of the medium surrounding the sphere, in particular its relative permittivity ε_r, must be specified. The results for a sphere surrounded by a good conductor such as metal ($\varepsilon_r = \infty$) and for a sphere surrounded by vacuum ($\varepsilon_r = 1$) are different [64]:

$$V^{zz}(\varepsilon_r = \infty) = V^{zz}(\varepsilon_r = 1) - \frac{2\pi}{3L^3}\left|\sum_i z_i\mathbf{r}_i\right|. \tag{1.23}$$

The mathematical frameworks of ES are given in Ref. [66]. In the ES method, each point charge is surrounded by a charge distribution of equal magnitude with an opposite sign, which spreads out radially from the charge. This distribution is conveniently taken to be Gaussian

$$\rho_i^z(\mathbf{r}) = \frac{z_i\alpha^3}{\pi^{3/2}}\exp\left(-\alpha^2 r^2\right), \tag{1.24}$$

where the arbitrary parameter α determines the width of the distribution and $\mathbf{r}$ is the position relative to the centre of the distribution. This extra distribution acts like an ionic atmosphere, to screen the interaction between neighboring charges. The screened interactions are now short-ranged, and the total screened potential is calculated by summing over all the molecules in the central cube and all their images in the real space lattice of image boxes. This is illustrated in **Fig**. **5***a*.
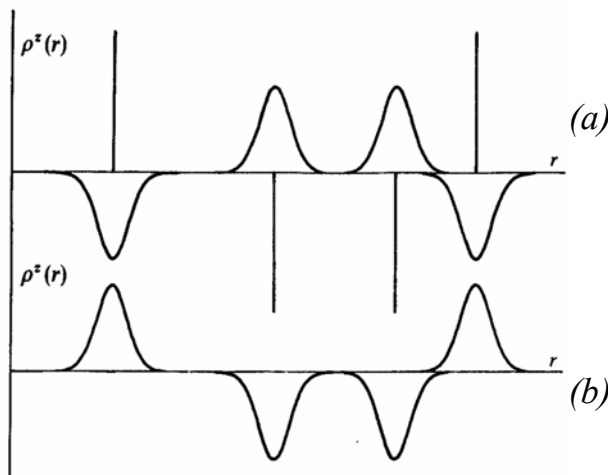
Figure 5. Charge distribution in the Ewald sum (*a*) – Original point charges and screening distribution; (*b*) Canceling distribution [64].

A charge distribution of the same sign as the original charge and the same shape as the distribution $\rho_i^z(\mathbf{r})$ is also added (**Fig. 5b**). This canceling distribution reduces the overall potential to that due to the original set of charges. The canceling distribution is summed in reciprocal space. It should be noted that the recipe includes the interaction of the canceling distribution with itself (**Fig. 5b**), and this self term must be subtracted from the total energy . The final results is [64]:

$$V^{zz}(\varepsilon_r = 1) =$$
$$\frac{1}{2}\sum_{i=1}^{N}\sum_{j=1}^{N}\left(\sum_{|\mathbf{n}|=0}^{\infty}\frac{z_i z_j}{4\pi\varepsilon_0}\frac{\text{efrc}(\alpha|\mathbf{r}_{ij}+\mathbf{n}|)}{|\mathbf{r}_{ij}+\mathbf{n}|} + (1/\pi L^3)\sum_{\mathbf{k}\neq 0}\frac{z_i z_j}{4\pi\varepsilon_0}(4\pi^2/k^2)\exp(-k^2/4\alpha^2)\cos(\mathbf{k}\cdot\mathbf{r}_{ij})\right) \quad (1.25)$$
$$-(\alpha/\pi^{1/2})\sum_{i=1}^{N}\frac{z_i^2}{4\pi\varepsilon_0} + (2\pi/3L^3)\left|\sum_{i=1}^{N}\frac{z_i}{4\pi\varepsilon_0}\mathbf{r}_i\right|^2$$

Here, $\text{erfc}(x) = (2/\pi^{1/2})\int_x^\infty \exp(-t^2)dt$ is the complementary error function which falls to zero with increasing x.

There are other widely used techniques which are the extension of the ES method, viz., P3M and PME (or SPME)[3] [67]. Along with the ES method, in these procedures a common force applied to i-th ion is separated into "short-ranged" $V^r = \frac{f(r)}{r}$ and "long-ranged" parts $V^m = \frac{1-f(r)}{r}$. The function $V^r = \frac{f(r)}{r}$ (first term in Eq. 1.25) is calculated in a regular manner [64]. The parameter α is chosen sufficiently large by computation of this sum so that the specific cutoff radius can be applied (α is a cutoff radius function). It is necessary in order to reduce calculation complexity of direct sum from $O(N^2)$ to $O(N)$, where $O(N^j)$ is the number of operations. To compensate the potential cutoff during the calculation of direct sum, the number of $\mathbf{k}$-vectors in reciprocal space can be increased proportionally to the number of charges N. The second sum is estimated by means of 3D fast Fourier transform technique in which common operation number is of the order of $N\log(N)$. As distinguished from conventional ES method, in PME the summation in reciprocal space is carried out as follows [68]:

1.   The charge density in the system is approximated by assigning charges to a finely-spaced mesh in the simulation box:

---

[3] P3M = Particle-Particle-Particle-Mesh, PME = Particle-Mesh Ewald, SPME = Smooth PME.
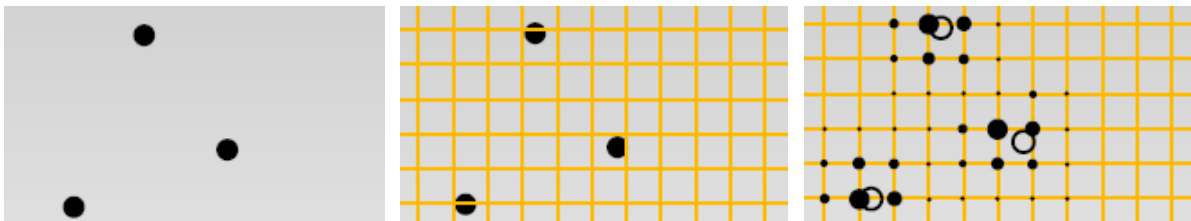
2.   The fast Fourier transform technique is then used to solve Poisson's equation for the electrostatic potential due to the charge distribution on the mesh. This gives the potential at each mesh point.

3.   The field at each mesh point is calculated by numerical differentiating the potential, and then the force on a particular particle *i* is calculated from the mesh field by interpolation. The relative force measurement error is approximately 10^{-6} for PME method. The Lagrange interpolation polynomial is used for charge exploration between mesh points [68].

        The SPME method is the modification of PME. In this approach, B-spline approximation is applied as an interpolation function. With the use of this method, the computational accuracy can be increased as well as the computational cost can be reduced owing to deflating of the interpolation function. In this case, the electrostatic potential differentiation at the force determining is carried out more precisely as compared to the method of finite differences. The SMPE scheme is the main method used in our simulations.

        In the reaction field method, a sphere $\Re$ is constructed around the molecule with a radius equal to the cutoff distance r_{RF} (**Fig**. **6**). The interaction with molecules that are within the sphere is calculated explicitly. This value is added to the energy of interaction with the medium beyond the sphere, which is modeled as a homogeneous medium with dielectric constant ε_r. (**Fig**. **6**) [69].

Solvent
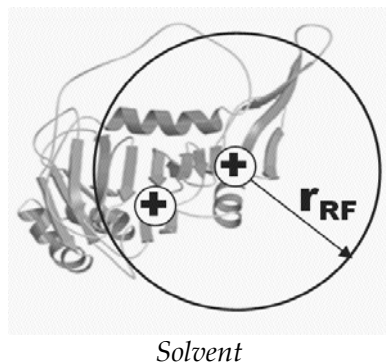
Figure 6. A cavity and reaction field.

27

The electrostatic field due to the surrounding dielectric medium is given by

$$\mathbf{E}_i = \frac{2(\varepsilon_r - 1)}{2\varepsilon_r + 1} \frac{1}{r_{RF}^3} \sum_{j \in \Re} \mathbf{\mu}_j \,,$$

(1.26)

where $\mathbf{\mu}_j$ are dipoles of the neighboring molecules that are within the cutoff distance r_{RF} of the molecule i. The interaction between the molecule i and the reaction field equals $\mathbf{E}_i \cdot \mathbf{\mu}_i$, which is added to the total electrostatic interaction.

Similar approaches employ a single boundary for the entire system. This boundary may be spherical or may have a more complicated shape that better approximates the true molecular surface of the molecule. In the image charge method, a spherical boundary is employed and the reaction field due to a charge inside the boundary is considered to arise from a so-called image charge situated in the continuous dielectric beyond the sphere [68].

I.4.3   Molecular Dynamics Method (MD).

Molecular dynamics is a specific computer simulation method employed for molecular systems, from ideal gases and liquids to biomacromolecules and composite materials. The systems studied by molecular dynamics are modeled as ensembles of interacting particles under specific internal and external conditions. Given the initial coordinates and velocities of an ensemble of particles that interact in an explicit manner, this method integrates the equation of motion numerically, providing new sets of coordinates and velocities at each integration time step. From the obtained particles trajectories one can calculate various global system properties as statistical averages.

The conventional MD technique consists in the stepwise time integration of Newton's equations of motion for a set of N particles:

$$\frac{d^2\mathbf{r}_i}{dt^2} = \mathbf{F}_i\left(\mathbf{r}_1, \mathbf{r}_2, ..., \mathbf{r}_N\right)$$

(1.26)

where

$$\mathbf{F}_i\left(\mathbf{r}_1, \mathbf{r}_2, ..., \mathbf{r}_N\right) = -\nabla_{\mathbf{r}_i} V\left(\mathbf{r}_1, \mathbf{r}_2, ..., \mathbf{r}_N\right)$$

(1.27)

Here, $\mathbf{r}_i$ is the position vector of particle i, $\mathbf{F}_i$ is the total force acting on particle i and V is the total potential energy from which the force is derived. By solving Newton's equations the total energy of the simulated system is conserved and the time averages obtained during

the simulations are equivalent to averages in micro-canonical NVE ensemble. But most often this ensemble is not practical when comparing with experimental or theoretical results that traditionally use other ensembles. So, other ensembles are preferred depending on what thermodynamic quantity is kept constant (number of particles, volume, pressure, temperature or chemical potential). All the results presented in this thesis are obtained by performing MD simulations at constant N, V and T.

One way to obtain this ensemble is by replacing Newton's equations (Eqs. 1.26) with the Langevin equation (stochastic MD):

$$\frac{d^2\mathbf{r}_i}{dt^2} = -\nabla_{\mathbf{r}_i} V - \Gamma \frac{d\mathbf{r}_i}{dt} + \mathbf{R}_i \tag{1.28}$$

Two additional forces are included in Eq. (1.28) to introduce kinetic energy of the system: a frictional force, proportional to the velocity (Γ being the friction constant of the particle) and a stochastic force $\mathbf{R}$. The strength of the noise is related to Γ via the fluctuation dissipation theorem (for more detail see, Chapter II).

There are many algorithms for integrating the equations of motion using finite difference methods or predictor-corrector methods, several of which are commonly used in molecular dynamics calculation. The Verlet algorithm [70] is probably the most widely used method for integrating the equation of motion. In this algorithm, the position and velocity of each particle are updated from time t to time $t + \Delta t$ using an intermediate half-time-step at $t + \frac{1}{2}\Delta t$:

$$\mathbf{r}(t + \Delta t) = \mathbf{r}(t) + \mathbf{v}(t)\Delta t + \frac{1}{2}\mathbf{a}(t)\Delta t^2 \tag{1.29}$$

$$\mathbf{v}\left(t + \frac{1}{2}\Delta t\right) = \mathbf{v}(t) + \frac{1}{2}\mathbf{a}(t)\Delta t. \tag{1.30}$$

Using the updated positions and velocities from Eq. (1.29) and Eq. (1.30), the force $\mathbf{F}(t + \Delta t)$ is evaluated. Several variation of the Verlet algorithm have been developed (the leap-frog technique, the velocity Verlet method, Beeman's algorithm) [64].

Solving the Langevin equations Eq. (1.28) the MD simulations sample the canonical ensemble by keeping the system temperature constant at a desirable value T. This method is known also as the Langevin thermostat and reflects the weak coupling of each particle with a virtual heat bath represented by the combination of frictional and random forces. A Langevin thermostat has two major advantages that make it very suitable for simulating polymeric ma-

terials for which long simulation time is needed. One is that it accepts larger time steps than other thermostats without causing instabilities. The other is that by coupling the system to the background, the inevitable effect of accumulating numerical errors is diminished with the direct consequence of improving the systems' stability over long runs.

The stochastic MD is the central method in this study. Its details are discussed in the methodical part of Chapter II.

Chapter II.   Complexes Based on Rigid-Chain Polyelectrolytes and
**   Oppositely Charged Polyions.**

II.1   Introduction.

A very important aspect of the behavior of PEs is their interaction with counterions, as this interaction determines many properties of such polymers, beginning from diffusion coefficients in solution to specific ion binding and their complexation with polyions [73,74]. In latter case, interaction between unlike macromolecules can yield polymer-polymer complexes. Polyelectrolyte complexes (PECs) are usually formed as a result of cooperative electrostatic interactions between oppositely charged polyions.

PECs play a fundamental role in biological systems. An example is DNA, which binds to histones (chromatin formation). DNA-cationic polymer [75,76] and DNA-charged dendrimer [77-80] complexes have recently attracted attention. Hybrid systems containing DNA molecules adsorbed onto positive charged small latex particles can be applied as gene delivery systems.

An important means of detailed investigation of PECs on a molecular scale is computer simulation. In reported studies, the complexes of PE chains with counterions and colloid particles [81-82], as well as complexes formed by oppositely charged flexible chains of equal lenght [81,83-87] were considered.

Of the experimental techniques what make it possible to study directly the structure of PECs, fluorescence microscopy is of special note. Using this method, the process of DNA compaction involving various agents (histones [88,89], polyamines [89], multiply charged inorganic cations [90], etc. [91,92]) can be directly visualized.

In any case, the PECs formation is concerned with conformational rearrangements of molecules. In some instances such structural reorganizations can be quite considerable down to the collapse of charged chains. The collapse of a single polymer chain – the transition from a random coil to a dense globule state – takes place when the solvent quality reduces [93,94]. The results of the collapse of a flexible-chain polymer is an approximately spherical globule if the conditions of a minimum surface energy are fulfilled; however, the situation for the semiflexible-chain polymers can be more complicated [96,97]. The local structure of aggregates in this case is always composed of extended chains, most frequently, with their parallel

packing to minimize the fold energy and to maximize the density. Therefore, the following typical conformations are characteristic of semiflexible polymers in a poor solvent: toroidal, rodlike, and cylindrical. Some theoretical studies also predict the existence of various intermediate conformations such as rackets [98,99] and bent cylinders [100]. Despite significant achievements in experimental and theoretical studying of these structures, many aspects are still remained in abeyance.

It is known that the DNA acquires the toroidal structure after addition of condensing agents, which are special substances and cause the collapse of this molecule. It has been already noted that these agents are salts containing miltivalent cations, polyamines, neutral flexible-chain polymers, etc.

It is commonly believed that DNA toroids have constant inner (150 Å) and outer (500 Å) diameters [101]. Toroids of approximately this size were observed for DNA of 400 to 56000 base pairs in length. This fact indicates that several small molecules or one large molecule form isolated particles. It was displayed by the example of T5 bacteriophage that large toroids of condensed DNA can be obtained [102].

In some studies [103,104], it was shown that the size variations of toroids can be even more significant than those above mentioned. It was found that toroids and rods form under identical conditions; usually complexes with similar geometric characteristics are produced. However, not only the environmental conditions of experiment but also the concentration of solution [103] and length of DNA molecules [104] determine the torus dimensions. Many investigators associate the invariability of the size of obtained aggregates with the intristic rigidity of the DNA molecule.

The stability of the aggregates under question was studied experimentally; several theoretical approaches for description of possible deformations of tori under exposure to external factors were proposed [105-116]. For example, Ubbink and Odijk [106] calculated the toroid energy associated with a change in surface tension. It was shown that the outer diameter of the torus and its thickness increase and the inner diameter decreases as the surface tension decreases. Park et al. [107] theoretically studied the problem of the optimal size of toroidal DNA with allowance for interactions between topological defects which affect the stretching of the molecular chain in the torus. The stability of tori in the mean-field approximation with emphasis on the coil-compact toroidal globule transition is described in Ref. [108]. It was found [109] that the free energy of the hollow sphere becomes lower than the

free energy of the toroid because of a decrease in the characteristic parameter α, which was first introduced in Ref. [106]. On the basis of this finding, it was supposed that the conformational transition of a single semiflexible chain from the coil to the toroidal globule state may be interpreted in terms of the first-order phase transition between random and ordered states [115]. It was shown that the toroidal structure is destabilized when the polymer chain length becomes infinitely large. Thus, the surface energy plays a substantial role in the determination of the stable structure of the compact state for an individual semiflexible chain.

As has been noted above, condensed DNA exists in various characteristic conformations. In addition to tori, rodlike (cylindrical) [116-118], flower-like [104,119], and globular structures [120], structures resembling a tennis racket (TR) (**Fig. 7**) [121-122] were observed in the experiment.

Martemyanova et al. [100] studied the transitions between the globular, cylindrical, and racket-like conformations of a rigid-chain polymer using a Monte Carlo method. The cylinders, tori, and rackets were characterized in terms of their energy. It was found that, e.g., the cylinders have a certain length and a certain number of strands. The TR conformation is an intermediate state between the cylinder and torus and is a kind of transient, metastable conformational state. In addition, the form factors were calculated to attribute chain conformations to certain structures [123,124].

Such conformations were observed not only for neutral rigid-chain polymers, when the solvent quality deteriorated, but also for PECs [125-126].
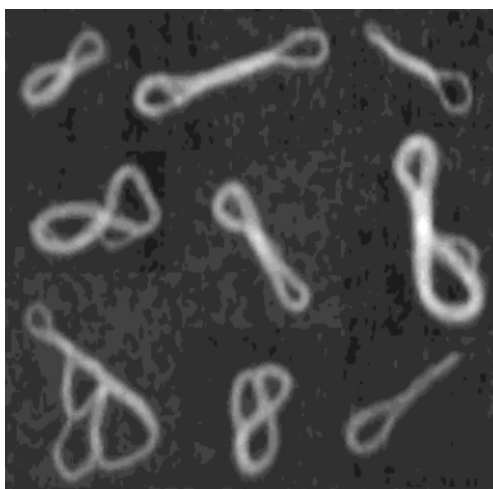
Figure 7. Metastable structures detected for xanthan-chitosan complexes [122].

The objective of the computer simulation reported in this charter was to study the conformational structure of complexes formed by a rigid-chain polyanion and polycations of different length, the stability of these complexes against external impacts, and the collapse of a strongly charged chain under the acting of condensing agents. The novelty of investigation lies in the fact that as opposed to previous works in which PE condensation effects have been considered only by involving of spherical (pointlike) ions in solution, in the present research the chain counterions of various lengths are used.

II.2   Model and Computational Method.

The system under question included salt-free dilute solution of semiflexible PE chains with a fixed value of charge on each monomer unit, as well as oppositely charged flexible-chain oligocations. In the model, each chain unit was assumed to be charged. In actual experiments, this assumption corresponds to the conditions when practically complete ionization of functional groups (e.g., —COOH groups in polyacids) takes place with varying the pH of solution.

We use rather simple model, which nevertheless contains the most essential aspects of the real PECs because the basic features of the charge complexation behavior are quite robust and, to a large extent, independent of details. The main approximations involved are as follows: (i) For simplicity, the salt effects are omitted from the study in order to examine the fundamental nature of the electrostatic interaction between the oppositely charged species in the strong Coulomb coupling regime within the primitive electrostatic model. (ii) The solvent is treated as a dielectric continuum, and it enters the model only through its dielectric permittivity, ε_r. (iii) All other constituents are described in terms of Lennard-Jones spherical particles (beads) of diameter σ connected by bonds of fixed length b and arranged in a linear manner. (iv) The net bare charge of a polyanion bead, represented by a LJ sphere, is replaced by negative point charge in the center of the sphere.

The simulated systems were composed of polymers of two types: strongly charged N_p-unit polyanions (N_p = 128) and oligocations (their chain length N_C was varied from 2 to 128). The time evolution of the system is determined by Newton's equations that are solved using the method of Langevin molecular dynamics. Monomer units (chain beads) are linked

by rigid bonds of a fixed length, $b = \sigma$, to form linear polymer chains. The employed interaction potentials of polymer units modeled the conditions of a good solvent for both types of macromolecules.

The potential energy of the system is given by

$$V = \sum_{i}^{N}\sum_{i \neq j}^{N}[v_{ev}(r_{ij}) + v_{C}(r_{ij})] + V_{\Theta} \tag{2.1}$$

where N is the total number of monomer units in the system, v_{ev} takes into account excluded volume, v_C is the unscreened Coulomb potential characterizing electrostatic interaction between charged monomers, and V_{Θ} is the bond-angle bending energy term.

Excluded volume between any nonbonded monomers is included via a repulsive soft core Lennard-Jones potential (1.18):

$$v_{ev}(r_{ij}) = \begin{cases} 4\varepsilon\left[\left(\dfrac{\sigma}{r_{ij}}\right)^{12} - \left(\dfrac{\sigma}{r_{ij}}\right)^{6} + \dfrac{1}{4}\right], & r_{ij} \leq r_0 \\ 0, & r_{ij} > r_0 \end{cases} \tag{2.2}$$

where $\sigma = \varepsilon = 1$ and $r_0 = 2^{1/6}\sigma$ is a cutoff distance. The normalized parameter ε entering this equation controls the energy scale, σ determines the interaction length between particles.

Electrostatic energy is given by

$$v_C(r_{ij}) = k_B T \ell_B \sum_{\mathbf{m}} \frac{z_i z_j}{\left|\mathbf{r}_{ij} + \mathbf{m}L_{box}\right|}, \tag{2.3}$$

where ℓ_B is the Bjerrum length, which measures the distance at which two elementary charges interact with thermal energy $k_B T$ (see Eq. 1.21); ε_r is the relative permittivity of the medium; and the sum over $\mathbf{m}$ takes into account the periodic images of the charged particles in a cubic simulation box of length L_{box}. Since in the simulations all charges are treated explicitly, the ε_r value was set to $\varepsilon_r = 1$. To take into account long-range electrostatic interactions, we used the highly optimized particle mesh Ewald method (SPME) [127,128] and the fast Fourier transform algorithm (see Chapter I). The truncation distance for electrostatic interactions in Eq. (2.3) was set to $R_C = 10$, and long-range corrections to the potential energy were made. The Ewald convergence parameter was $\alpha = 0.3766\sigma^{-1}$; the order of B-splines was $n_B = 5$; the number of grid points in each direction was 72. These parameters ensured consistency be-

tween the Coulomb energy obtained through the pair potential and the Coulomb energy calculated through the virial [129,130].

The bond-angle bending potential, which determines the equilibrium stiffness of an N_p-unit polyanion chain, is defined as follows:

$$V_\Theta = \frac{k_1}{2} \sum_{i=2}^{N_p-1} (\Theta_i - \Theta_0)^2 + \frac{k_2}{2} \sum_{i=1}^{N_p-3} \sum_{j=i+3}^{N_p} \frac{\left(r_{ij} - r_{ij}^0\right)^2}{j-i-2},$$

(2.4)

where k_1 and k_2 are the force constants ($k_1 = 4\varepsilon$ and $k_2 = \varepsilon$), Θ_i is the angle between neighboring bond vectors $\mathbf{r}_{i-1}$–$\mathbf{r}_i$ and $\mathbf{r}_{i+1}$–$\mathbf{r}_i$, Θ_0 is the equilibrium angle ($\Theta_0 = 180°$), and $r_{ij}^0 = b(i-j)$ is the equilibrium distance between beads i and j. The value of r_{ij} in Eq. (2.4) is the distance between beads i and $j = i + 3$; it defines the magnitude of the angle Θ. If the force parameters k_1 and k_2 are high, i.e., the deviation of Θ from the corresponding equilibrium value Θ_0 is small, then $\Theta \approx \Theta_0 = 2\arcsin(r_{ij}/2b)$. The use of this potential prevents the appearance of sharp bends in the polyanion chain. The same behavior characterizes, for example, the DNA chain [131].

The Kuhn segment length A was used as a measure of the chain flexibility (rigidity). According to the concept of equivalent chain [132], a polymer chain can be replaced by a random flight chain that is composed of n_A effective bonds of length A and has a mean-square end-to-end distance R^2 equals the one of unperturbed chain (i.e., the chain without excluded volume interaction): that is, $R^2 = n_A A^2$. The value of n_A may be determined with the additional condition that both chains have the same end-to-end distance: $L_C = n_A A = (N_p - 1)b$. The effective "bond length" A of an equivalent chain is called the Kuhn statistical segment length. It defines persistent length $\ell_p = A/2$ (Eq. 1.14) [133].

Note that A and ℓ_p depend on temperature and charge of a chain bead. In this study the value ℓ_p is varied from 12 to $\approx 250\sigma$. This corresponds to semirigid and rigid chains (see examples shown in Table 1).

The linear charge density of anionic beads was fixed at a value $-e/\sigma$ ($z_C = -1$), and for cationic units was e/σ ($z_C = 1$).

Explicitly, no solvent particles are included in the simulations; i.e., the solvent is represented by a dielectric continuum. In order to simulate solvation effects and the time evolution of the solution in contact with a heat bath of temperature T, the equations of motion are augmented by the friction force $-m\gamma_i\dot{\mathbf{r}}_i$ and the Langevin uncorrelated noise term $\mathbf{R}_i$, which

is connected with the viscosity of the solvent γ through the fluctuation-dissipation theorem: $\left\langle R_{\alpha i}(0) \cdot R_{\alpha j}(t) \right\rangle = 2m\gamma k_B T \delta_{ij}\delta(t)$ [64], where γ_i is the friction constant, $m = 1$ is the mass of a single chain bead, T is the reference temperature, and $\alpha = x, y, z$; $i, j = 1,2,\ldots,N$. These terms ensure that the temperature is kept constant. In the MD simulations, the equations of motion of a polymer system in the presence of fixed constraints are:

$$m_i \ddot{\mathbf{r}}_i = -\nabla_i \left[V(\mathbf{r}) - \sum_{s=1}^{n(N-1)} \lambda_s G_s(\mathbf{r}_1,\ldots,\mathbf{r}_{nN}) \right] - \gamma_i \dot{\mathbf{r}}_i + \mathbf{R}_i, \quad i = 1, 2,\ldots, N,$$

(2.5)

$$G_s(r_1,\ldots,r_{nN}) \equiv \frac{1}{2}\left[(r_{s+1} - r_s)^2 - b^2 \right] = 0, \quad s = 1, 2,\ldots N-1,\ldots,n(N-1),$$

(2.6)

where n is the number of chain and λ_s are Lagrangian multipliers that take into account the presence of rigid bonds.

Because in this study we mainly focus on dense PECs, we take the parameter γ to be dependent on solvent-accessible surface areas (SASA). To find the values of SASA for a given configuration, an analytical computation of the surface areas S_i for each specified bead was performed [134]. Having S_i, one can define γ_i as $\gamma_i = \gamma_0 S_i / S_{max}$, where S_{max} is the maximum solvent-accessible surface area of a bead and the corresponding value of γ_0 is taken to be equal to unity (for more detail, see Refs. 130,136). The weighting factor S_i / S_{max} represents the degree of exposure of the bead i to the solvent. When the value of SASA for a given chain bead is zero, the frictional and random forces are zero and the Langevin equation reduces to Newton's equation of motion. For the chain in a compact conformation, this typically happens when a given monomer is screened by other chain segments. On the contrary, a monomer located at the surface of a PEC is strongly solvated; it means that S_i should be close to S_{max} and, as a result, the value of γ_i is close to its reference value γ_0. The selected value of solvent viscosity ensured the invariability of a preset temperature within the limits of required accuracy (± 5%).

The equations of motion (2.5) in conjunction with the constraints of fixed bond lengths (2.6) are solved iteratively using the RATTLE iteration procedure [137] with the time step $\Delta t = 0.01 \sigma\sqrt{m/\varepsilon}$. The initial systems were equilibrated for about 10^6 time steps and then the production runs were performed. Typically, each production run was from 10^6 to 2×10^6 time steps, depending on the system density and temperature. Throughout the simulation, snap-

shots of the systems were collected. The number density of the polyanion beads, $\rho = n_p N_p / V$, was $\rho = 2.05 \times 10^{-3} \sigma^{-3}$ (salt-free dilute polyelectrolyte solution).

The main calculation parameters were the temperature and the dielectric permittivity of medium ε_r. When the temperature was varied, the value of ε_r was fixed at $\varepsilon_r = 1$; when ε_r was varied, it was assumed that $T = 1\ \varepsilon / k_B$, where k_B is the Boltzmann constant. Note that a change in ε_r in this model had an effect only on electrostatic interactions, whereas a change in temperature also affected the chain rigidity.

II.3 **Results and Discussion.**

II.3.1 Structural and Energetic Criteria.

In the present section, the results of MD simulation of PECs based on semi-rigid and rigid polyanions are discussed. The conformational behavior of the macromolecules in dilute solution and their self-organization into PECs is studied at various T, N_c and ε_r, where N_c – chain length of polycations.

Several equilibrium characteristics of the formed PECs were calculated. They include the mean-square radius of gyration, R_g^2, polycation-polyanion static structure factors, $S_{+-}(q)$, the corresponding pair correlation functions, $g_{+-}(r)$, etc. These quantities were calculated as a function of T, N_c and ε_r. The average numbers of contact, n_{+-}, between the subsystems A and B, the average distance between their center-of mass, R_{+-}, and counterion coordination numbers, z, were also found.

Some of the results obtained for 128-unit chains are shown in **Fig. 8**. It is seen that the distance R_{+-}, plotted as a function of the polycation chain length of N_c at different values of T and ε_r increases as the value N_c decreases This quantity shows how far the subsystems are from one another. As the value of R_{+-} increases, the system is further from the condensed state. It can be stated that condensation processes in the system are more intensive when N_c >16 and at low temperatures and small ε_r.
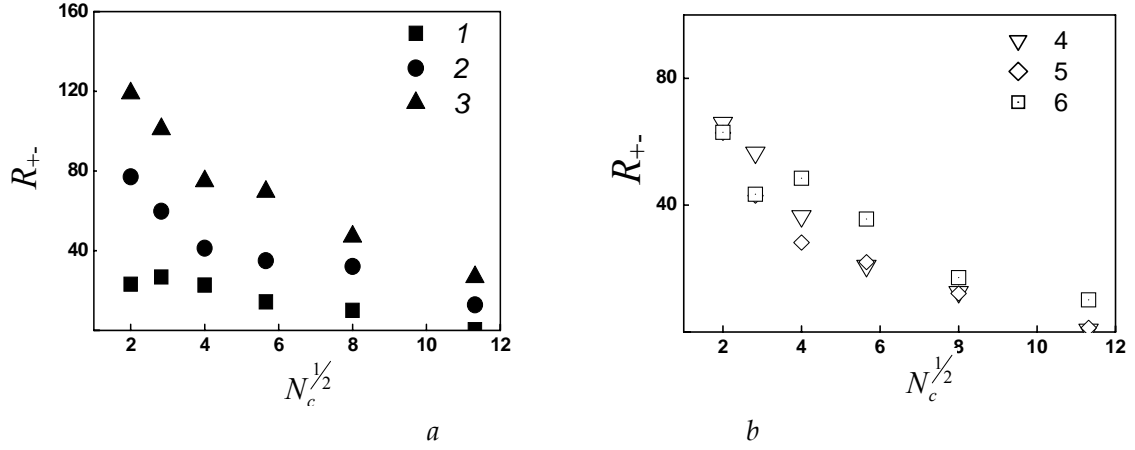
Figure 8. Average distance between the centers of mass of the subsystems A and B as a function of the polycation chain length, at $T = 0.5$ (*1*), 2.5 (*2*), 5 (*3*), 1 (*4-6*) and $\varepsilon_r = 1$ (*1-3*), 2 (*4*), 4 (*5*), 12 (*6*).

Short-chain cations act as condensing agents only at small temperatures and low ε_r values. This is due to their higher translation mobility as compared to long-chain cations, which actively enter into complexation even at rather high temperatures and make the polyanion chain more compact.

To describe the local environment formed near the polyanion monomeric units, we calculated the polycation–polyanion pair correlation functions $g_{+-}(r)$. The influence of the permittivity ε_r on the condensation of 16-unit cations onto the polyanion is illustrated in **Fig. 9**.
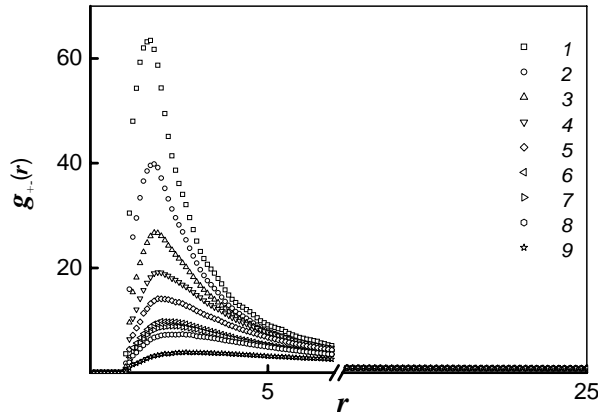
Figure 9. Polyanion-polycation pair correlation functions at $\varepsilon_r = 2$ (1), 3 (2), 4 (3), 5 (4), 6 (5), 7 (6), 8 (7), 9 (8), 16 (9). $N_c = 16$, $T = 1$.

It is seen that the probability of occurrence of polycation monomers near the polyanion decreases with a growth in ε_r. This is explained by the fact that the Bjerrum length decreases. Correlations in the arrangement of subsystems practically disappear at $\varepsilon_r \geq 6$ (in **Fig. 8b**, this is manifested by an increase in the R_{+-} value from 40 to 85σ at the increase of ε_r from 2

to 12). At such values of ε_r, the unbound state when the system does not experience complexation is stable.

In addition to pair correlation functions, the counterion coordination numbers $z(r)$ were also calculated [129]:

$$z(r) = 4\pi\rho_C \int_0^r g_{+-}(x)x^2dx, \tag{2.7}$$

where ρ_C is the number density of positive charges in the system. The value of $z(r)$ in Eq. (2.7) is the average number of positive charges about an individual monomer unit of the polyanion at a distance r from this unit. In these calculations, r was set to 4σ.

Figure 10 shows the values of z as a function of temperature at fixed ε_r (**Fig. 10***a*) and dielectric permittivity at fixed T (**Fig. 10***b*).
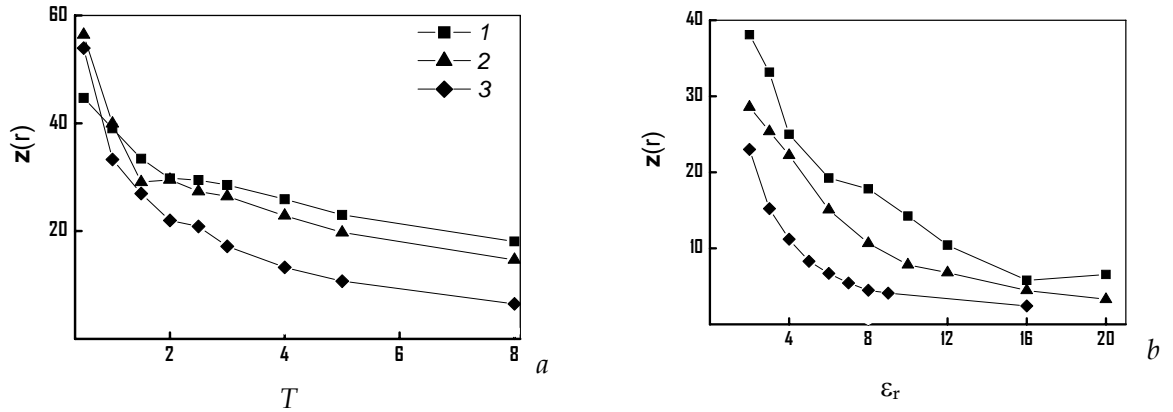
Figure 10. Coordination number z as functions of (*a*) temperature (ε_r.=1) and (*b*) permittivity of the medium ε_r (*T*=1) for N_c = 128 (*1*), 32 (*2*), 8 (*3*).

As seen, at low temperatures *T*, the complexes formed in the presence of polycations with a sufficiently long chain, $N_c \geq 8$, can be stable. As temperature increases, PECs disintegrate. This behavior is well-seen in Fig. 10, where we observe a sharp decrease in z in the range $0.1 < T \leq 2$ (Fig. 10a) or $1 < \varepsilon_r \leq 4$ (Fig. 10b). Also, we would like to stress that the disintegration of complexes proceeds at least in two stage: when *T* < 1.5, the z value demonstrates a very sharp decrease, while in the temperature range 1.5<*T*<2.5, this value decreases slowly and even can reveal a plateau if the condensing oligocations are sufficiently long, $N_c \geq 8$. A further increase in temperature, at *T*>2.5, leads to a gradual decay of $z(r)$, thereby indicating the complete dissociation of PECs. Such a behavior is associated not only with the "desorption" of polycations from the polyanion, but also with the simultaneous conformational rear-

rangements of the polyanion. In the presence of short-chain cations, we observe only very weakly pronounced complexation under whatever temperatures and dielectric constants within examined ranges (see Fig. 10).

In order to characterize the structure of the aggregates and to attribute it to certain morphology, the snapshots of the systems were also analyzed. **Figure 11** provides a general idea of possible structures of rigid-chan polyelectrolyte complexes.

In stable polyelectrolyte complexes, the observed structure can have the form of a bent superhelical bundle (**Fig. 11***a*) in which the oppositely charged chains are braided, a folded cylinder, a tennis racket, a torus (**Fig. 11***b*) or a double torus (**Fig. 11***c*).


| *a* | *b* | *c* |
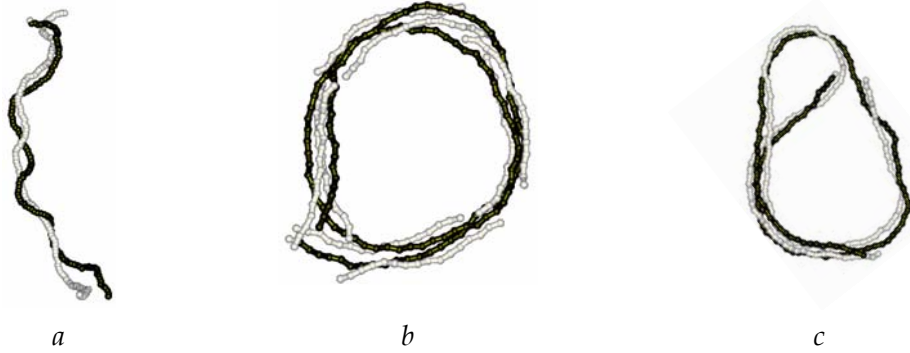
Figure 11. Snapshots of the PEC at $N_c = 128$ (*a*, *c*) and 16 (*b*), for $T = 1$ (*a*) and 0.5 (*b*, *c*) and $\varepsilon_r = 10$ (*a*), 1 (*b*, *c*).

From the visual inspection of snapshots (**Fig. 11**) and also from the dependences presented in **Figs. 8** and **10**, it follows that at low T and $N_c \geq 16$ the tori are formed. When the value of ε_r is small, a small increase in temperature leads to the formation of rather specific aggregates that have TR-like shape. In addition, in this region of parameters, we can identify stable "shapeless" aggregates having a coil-like structure. We will call these "strongly bound state". It can be concluded from the data shown in Figs. 8 and 10 that the "strongly bound state" is characterized by small values of R_{+-} and large values of z. It is important to note that the potential energy of these conformations is considerably higher as compared to that of torus-like conformations (see Fig. 12). The formation of coil-like structures can also be observed at high T and ε_r. In this case, however, we deal with a "weakly bound state". In other words, the complexes formed under these conditions typically are not stable. The same is true when the systems containing low-molecular-weight cations are simulated: the complexes become progressively less stable with decreasing N_C. Similar evolution of conformations and complex stability was also observed in experimental works [122].
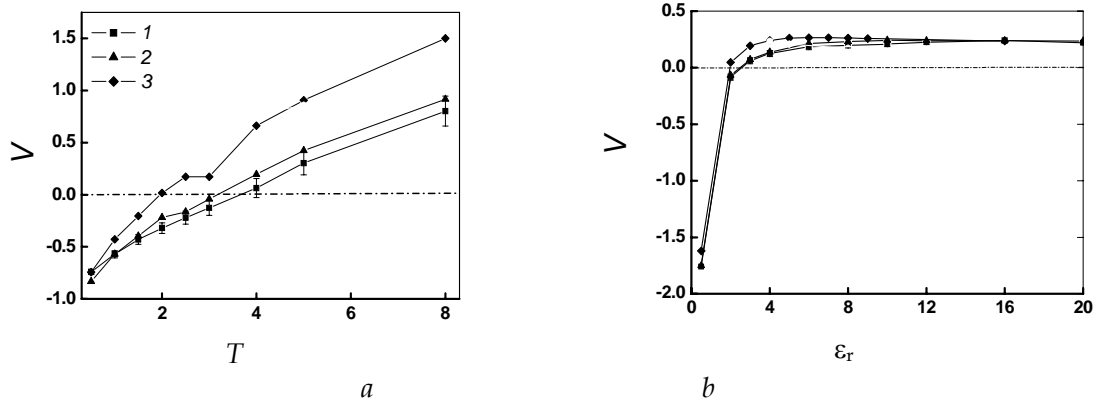
Figure 12. Potential energy of the system as a function of (*a*) temperature (ε_r=1) and (*b*) ε_r (*T*=1) for N_c = 128 (*1*), 32 (*2*), 8 (*3*).

The formation of a complex and its stability can also be characterized in terms of the number of contacts between positively and negatively charged sites, n_{+-}. In our study, we assume that two monomeric units of the subsystems *A* and *B* are in contact if the distance between them does not exceed r= 2σ.
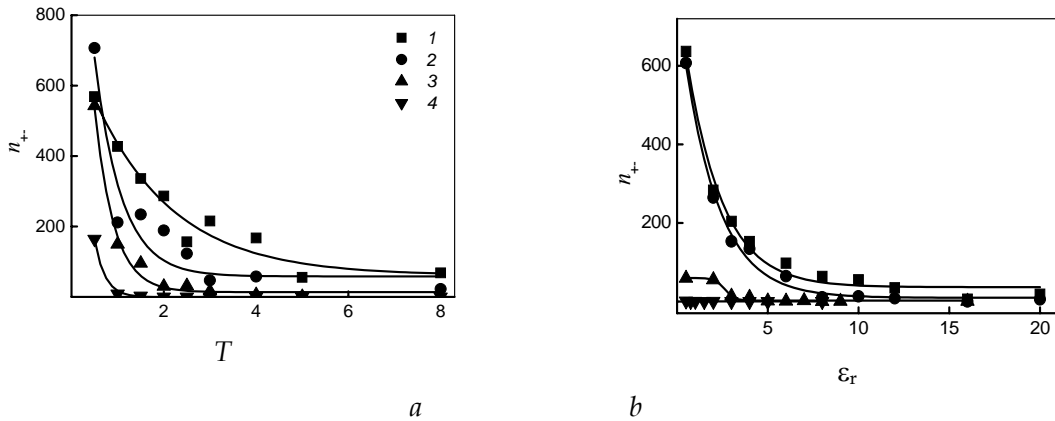
Figure 13. Number of contacts between unlike monomeric units as a function of (*a*) temperature (ε_r=1) and (*b*) ε_r (*T*=1) at N_c = 128 (*1*), 32 (*2*), *8* (*3*) and 2 (*4*).

The n_{+-}– *T* and n_{+-} –ε_r plots are shown in **Fig. 13**. At low temperatures, the number of contacts is high at any N_c. This means that the formation of the complex (bound state) takes place. At *T* = 1 and any value of ε_r, complex formation in the systems with short-chain cations is not observed.

The results presented above allow to assert that due to different self-assembly conditions the formed PECs have various conformations. Also the calculation data show that

formed tori have the different radii ($R_g^2 = 86 - 140\sigma$). This conclusion agrees with recent experimental investigations [103,104].

II.3.2   State Diagrams.

The simulation data discussed above can be used to construct state diagrams. To this end, we should introduce some structural and energy criteria which define the complex formation. It is natural to expect that a PE complex begins to form when its energy becomes negative ($V < 0$) and the number of contacts between negatively and positively charged sites, n_{+-}, is sufficiently large. Also, the deviation of geometrical parameters of PEC from the corresponding "ideal" structures can be used as an additional criterion. After some experimentation, we have chosen the following simple criteria: $V < 0$ and $n_{+-} > 10$. The calculated state diagrams are shown in **Figs. 14a** and **14b**. They illustrate how a change in the variables T, ε_r, and N_c influences the complex formation. It should be remembered that the variation in T values influences both rigidity of a polyanion chain and electrostatic interactions whereas change in ε_r at T=constant changes only the interaction of charged units.


a b
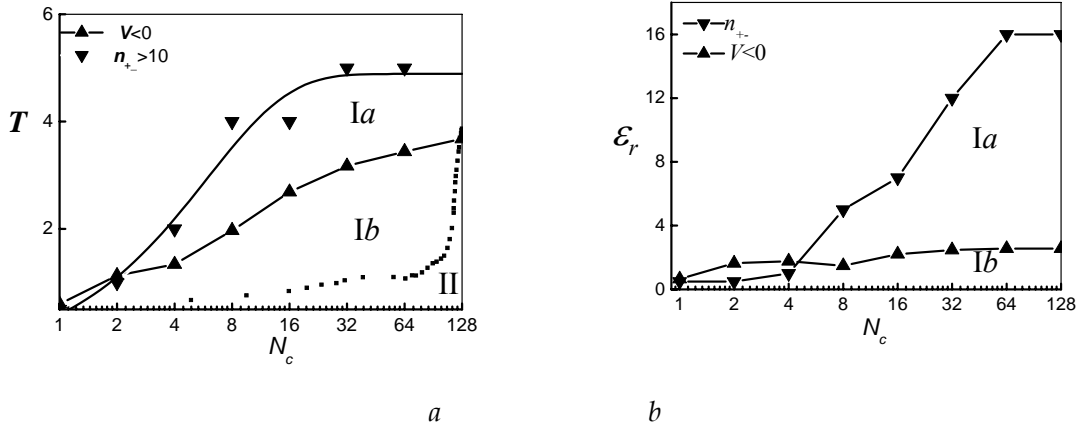
Figure 14. State diagrams polyanion-polycation complexes in terms of the number of contacts n_{+-} and the energy criterion V.

The state diagrams presented in **Fig. 14** consist of several regions. The regions Ia and Ib correspond to the bound state, i.e., complexes. In **Fig. 14a**, the region II is the region of tori and rackets. It was found that the tori formed by oppositely charged chains are stable at low temperatures. This result agrees with MC simulation data of Martemyanova et al. [100]. The regions above the curves on the diagram in **Fig. 14a** are the regions of existence of the unbound state; i.e., complexes degrade under these conditions.

The second type of state diagram characterizes the equilibrium morphology of PECs. In this case, we should compare the shape (size) of a complex formed under a given condition with that of an "ideal" complex. For example, we can define the size of an "ideal" torus, R_g^0, formed by the chain of the same length, N_p, as that used in the simulations. In doing that we assumed that the value of R_g^0 depends only on chain length, N_p, and on excluded volume interaction but not on electrostatic interactions. Based on this, we calculated the ratio

$K = \left(R_g \middle/ R_g^o \right)^2$ for different values T and N_c. In essence, the ratio K is a measure of the deviation of the simulated structures from their "ideal" counterparts. The "morphological" state diagram is shown in **Fig. 15**.

The region (I) corresponds to toroidal conformations. Here, the ratio K is $K \leq 2$. The region (II) includes the TR-like complexes at low temperatures and coil-like PECs at higher temperatures and large N_c values. The region (III) is characterized by the maximum deviation degree $K > 6$. As a result, the formation of toroidal and TR-like PECs does not occur in the systems under these conditions. In this region, the polyanion can accept the extended conformation.
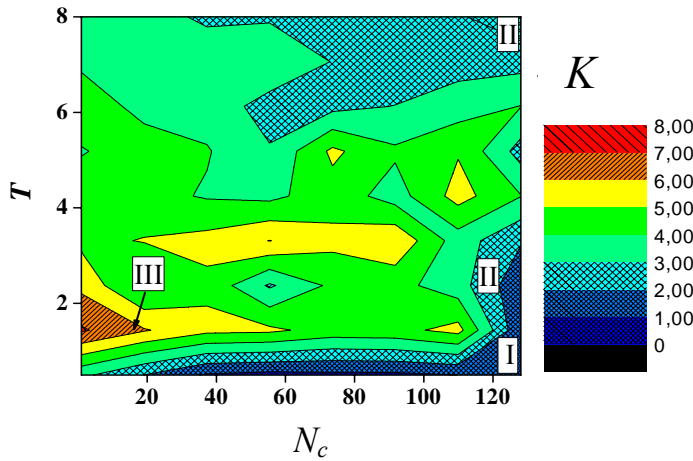
Figure 15. State diagram of the systems with emphasis on distinguishing the regions of existence of complexes with a certain morphology.

Thus, our analysis has shown that depending on T and N_c, the formed PECs have various conformations. Tori and "plaits"-like complexes are more stable. The double torus and TR-shape conformations are metastable states. At low temperatures, the collapse transition of these structures can be observed. This result is in agreement with the experimental data about conformational state of DNA complexes [103,104,117]. Besides, the results of calculations show that tori with different radii are formed. It means that not only the nature of

PE (rigidity or flexibility), but also the electrostatic interaction define the geometrical sizes of final complexes. This fact accords with recent experimental studies of systems of DNA-spermidin [138].

Therefore, it is possible to control the self-assembly process and the conformation of resulting aggregates by varying chain length of condensing agents, temperature and solvent quality. There are a series of papers in which well-defined aggregates have also been observed based on theoretically predicted state diagrams, by modifying only one parameter of the system [34,36,139].

II.4   Conclusions.

The structure and stability of complexes formed by oppositely charged rigid-chain macromolecules, as well as their response to variation in external conditions, were studied using the molecular dynamics method. The conditions of conformational transitions depending on the chain length and configuration, temperature, and dielectric permittivity of the medium were considered. It was shown that the chains involved in a complex may take various conformations of the torus, tennis racket, etc. types.

Chapter III.   Molecular Bottle Brushes in a Solution of Semiflexible

                           Polyelectrolytes and Block Copolymers with

                           Oppositely Charged Blocks.
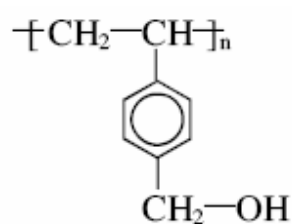
III.1   Introduction.

Ionic self-assembly through noncovalent electrostatic interactions give advantages over chemical synthesis where it does not involve complicated preparative procedures, equilibrium structures can often be realized, and adaptive rearrangement of the structure may be possible if the external conditions (e.g., solvent, temperature, or pH) are changed. In addition, self-assembled structures, in general, can self-repair and self-optimize, as the relevant structural bonds are reversible. Charge density and charge strength result in variable long-range electrostatic interactions, which are mainly responsible for the physicochemical properties of PECs and their peculiarities in aqueous solution. However, the typical properties of PECs do not depend exclusively on the electrostatic forces. Many of their solution properties are due to a complex interplay between short-range hydrophobic attraction, long-range Coulomb effects, and the entropic degrees of freedom. The balance of these factors determines the solubility and equilibrium conformation of PECs in water. Differences between the flexibility of charged polymer chains and, especially, a molecular architecture also play an important role.

In recent years, much attention has been focused on the complexes formed by rigid-chain PEs with the so-called double-hydrophilic block copolymers (DHBC). These copolymers consist of two water-soluble blocks where one (charged) block can interact with an oppositely charged polyelectrolyte and the other (neutral) block just provides water solubility and these polymers serve as a tool to provide nanometer sized building blocks for further self-assembly into complex structures (**Table 2**) [140,141]. This type of charge complexation is especially interesting for DNA or oligonucleotide delivery [142,143]. In addition, DHBCs were recently identified as highly active additives for inorganic crystallization [144]. DHBCs were also used for the preparation of nanosized metal particles and for nanoparticle stabilization in water [145]. The range of supramolecular architectures for numerous PEC systems using DHBCs is extremely wide and can be further extended by the combination of DHBCs with surfactants [140].

Table 2. Blocks used in DHBCs and their functions.

Block	Structure	Remarks
Solvating blocks		
Poly(ethylene oxide)	$+CH_2\!-\!CH_2\!-\!O\!+_n$	Temperature responsive block, hydrophilic at $T \leq 80°C$, strong hydrated, mainly non-interacting with substrates
Dihydroxypropyl methacrylate	(structure shown)	Hydrophilic, mainly noninteracting with substrate
Poly(vinyl alcohol)	(structure shown)	Hydrophilic, mainly noninteracting with substrate
Poly(vinyl ether)s	(structure shown)	Temperature responsive block
Poly[(oligoethylene glycol)methacrylate]	(structure shown)	Hydrophilic, salt responsive block
Poly(N-isopropylacrylamide)	(structure shown)	Temperature responsive block, hydrophilic at $T < 30{,}9°C$

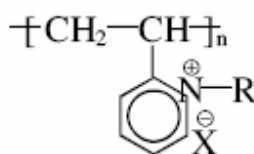| Poly(4-vinyl benzyl alcohol) | $+CH_2-CH+_n$ (with phenyl ring and CH_2-OH) | Hydrophilic, mainly noninteracting with substrate |

Funktional Blocks
Polycationic

| Poly(2-vinylpyridine) in quaternized form | $+CH_2-CH+_n$ (pyridine ring, $\overset{\oplus}{N}-R$, $\overset{\ominus}{X}$) | Strong polyelectrolyte, very hydrophilic, R = H, Me, Et, Bz; X = Br, I |

| Poly(4-vinylpyridine) in quaternized form | $+CH_2-CH+_n$ (pyridine ring, $N_\oplus$, R, $X^\ominus$) | Strong polyelectrolyte, very hydrophilic, R = H, Me, Et, Bz; X = Br, I |

| Poly(aminoethyl methacrylate) | $+CH_2-\underset{}{C}+_n$ with CH_3, $C=O$, $(CH_2)_2-O$, $R-N-R$ | Polyelectrolyte, R = CH3, R = C2H5, R = CH3-CH-CH3 |

| Poly(2-ethyloxazoline) Poly(2-methyloxazoline) | $+N-(CH_2)_2+_n$ with $C=O$, R | Polyelectrolyte, R = CH$_3$, C$_2$H$_5$ |

| Poly[4-(N,N-dimethylamino methylstyrene] | $+CH_2-CH+_n$ (phenyl ring, CH_2-N with two CH_3) | Polyelectrolyte |
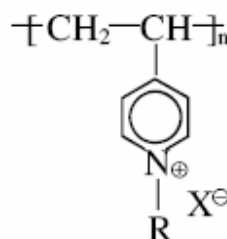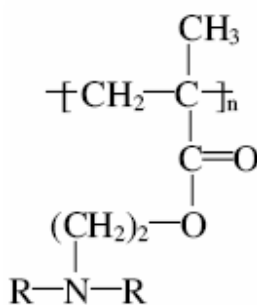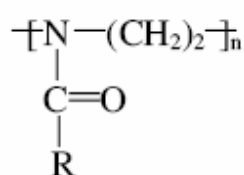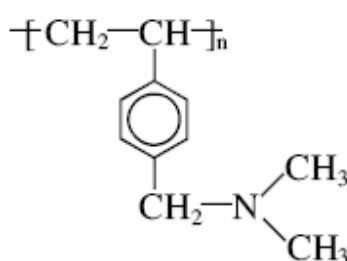
Polyanionic

48

Poly(methacrylic acid) Poly(acrylic acid)		Polyelectrolyte, R = H, Me
	$\begin{array}{c} R \\ | \\ +CH_2-C+_n \\ | \\ COOH \end{array}$	
Poly(styrene sulfonic acid)	$+CH_2-CH+_n$ with phenyl ring and SO_3H	Strong polyelectrolyte, very hydrophilic, also Na, K-salts
Poly(vinyloxy-4- butyric acid)	$\begin{array}{c} +CH_2-CH+_n \\ | \\ O \\ | \\ (CH_2)_3-COOH \end{array}$	Polyelectrolyte, hydrophilic, also Na-salts
Poly(sodium 4-vinylbenzoate)	$+CH_2-CH+_n$ with phenyl ring and $COONa$	Polyelectrolyte, pH responsive, as Na-salt
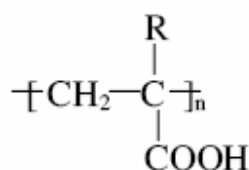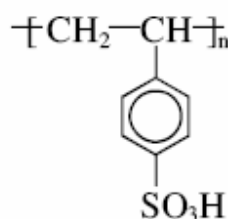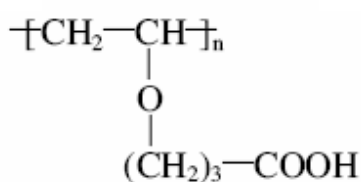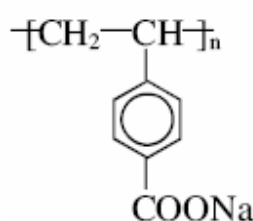
Typical examples of electrically neutral water-soluble blocks in DHBCs are poly(ethylene oxide), poly(vinyl ether), and poly(*N*-isopropylacrylamide). Cationic blocks can be poly(2-vinylpyridine), poly(4-vinylpyridine), and poly(aminoethyl methacrylate). Examples of anionic blocks are polyacrylic and poly(styrene sulfonate) blocks (**Table 2**) [140].

DHBC macromolecules with ionizable groups do not self assemble in water; they behave as normal polymers or polyelectrolytes and do not exhibit the properties of amphiphiles. In particular, they are incapable to form micelles. However, the presence of oppositely charged PEs in DHBC solutions can lead to different forms of self-assembly owing to strong electrostatic interactions. Depending on concentration, either stoichiometric or non-stoichiometric complexes are formed [140]. The schematic structure of these complexes is shown in **Fig. 16**.
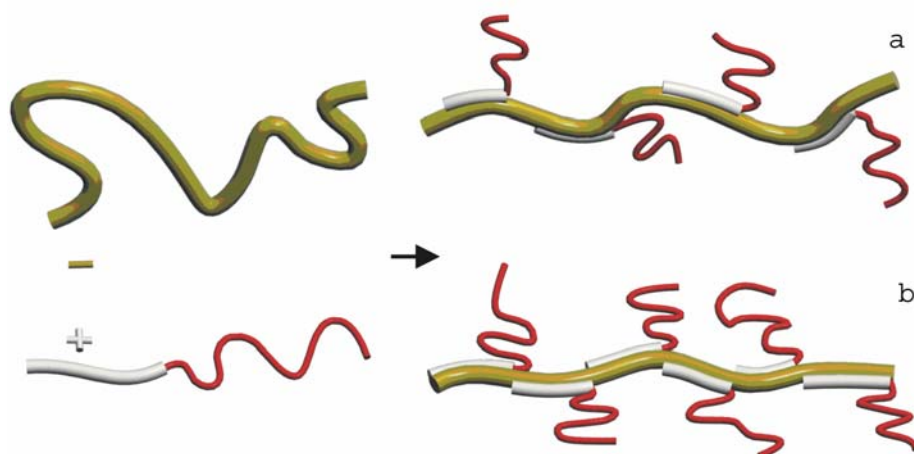
Figure 16. Schematic representation PEC formation and (*a*) nonstoichiometric complex and (*b*) stoichiometric complex.

The nonstoichiometric complexes are usually well soluble in water. The stoichiometric (or equimolar) complexes, as a rule, are sparingly soluble in water but dissolve in organic solvents of low polarity forming in many cases well-defined supramolecular structures. The insoluble complexes concentrate in liquid coacervate droplets that further coalesce and phase separate to form a separate coacervate layer. One of the attractive features of the stoichiometric PECs is the simplicity of their synthesis, which simplifies the "fine-tuning" of the resulting structures. In most experimental studies dealing with the properties of such systems, different morphologies of complexes were observed [146-154]. However, many details of their structure and formation are poorly understood at the nanometer scale.

The electrostatic-driven aggregation processes in PE solutions are usually explored in the presence of small spherical counterions or oppositely charged homopolymers [3,155,156]. However, one anticipates that the chemical structure of charged DHBC heteropolymers should crucially affect the final structure of PECs. Thus, the question of how to control the spatial organization of PECs formed in an aqueous solution of charged polymers by means of chemical modification of oppositely charged species is of great importance. This fact motivates intensive experimental [157-160] and theoretical studies of the DHBC-based PECs [161]. In addition, considerable effort has recently been directed toward the computer simulation of model PECs with the purposes of obtaining a basic understanding of the mechanism of self-assembly [162-167]. Kramarenko et al. have developed the theory of complex formation in a salt-free solution of flexible-chain polyelectrolytes and DHBCs [161].

Their model describes the process of micelle formation as an association-dissociation reaction [168]. It was assumed that the length of neutral hydrophilic block of DHBC, N_B, is larger than the one of charged block, N_C ($N_B \gg N_C \gg 1$), while the length of oppositely charged polyelectrolyte is $N_p < N_C$. In this case, spherical ionic micelles with nearly fully neutralized core are stable. This theoretical prediction is in agreement with experimental observations [159]. It should be stressed that for rigid polyelectrolytes with long chain, when $N_p \gg N_C \gg 1$ and $N_B \approx N_C$, the mechanism of self-assembly and the morphology of the DHBC-based PECs can be different. As it will be shown below, precisely this conclusion springs out results of computer simulation.

There are a number of studies where computer simulations of complexes composed of a single flexible-chain polyelectrolyte and surfactants were carried out [162-166]. It is known that environmental changes or external stimuli can cause drastic changes in conformation and molecular assembly of the polymer-surfactant aggregates due to the noncovalent bond and large difference of polarity between polymer and surfactant [152]. In particular, Groot has studied the formation of a polymer-surfactant complex in bulk solution using dissipative particle dynamics simulation of a system containing polymer, surfactant, and water [162] Using a Monte Carlo method, von Ferber and Löwen have simulated the formation of molecular bottle-brush architectures of the resulting PE-surfactant complex [163]. Depending on the hydrophilic–hydrophobic balance of the surfactants, the formation of spherical micelles or comb-shaped micelle complexes having an extended conformation was observed [163,164]. The comblike structure of complexes, which is the most probable in the case of bonding of charged ionic surfactants to a PE chain, was found to be in many respects similar to the one well-known for an electrically neutral cylindrical polymer brush [152]. Since the side chains are noncovalently connected with the main chain in the comblike complex, the properties or phase behavior in the comblike polymer-surfactant complexes should be much different from those of the covalently bonded comblike polymers. Neutral comb-shaped associates are also formed during the addition of side chains to the backbone by virtue of strong hydrogen bonding [153,169,170]. The conformation of these complexes becomes more extended with an increase in the linear density of attached side chains. This phenomenon has been studied for cylindrical brushes [171]. Using Monte Carlo simulations and the lattice bond-fluctuation model, Kramarenko et al. have studied the conformational behavior of comb polymers in the

strong segregation regime for neutral side chains [172]. Such a system may be considered a coarse-grained model of a stoichiometric PECs. However, the role of electrostatic effects and charge complexation was not studied. Recently, Komarov et al. have simulated the formation of PECs in a dilute salt-free solution of rodlike polyanions in the presence of anisotropic (chain) cations consisting of neutral tails and charged heads [173,174]. Within the framework of the primitive electrolyte model, different Coulomb coupling regimes were considered. In the strong coupling limit, the formation of ribbonlike nanostructures was observed. At strong electrostatic interaction, the system was found to undergo the self-organization resulting in the formation of planar aggregates that looks like a "ladder" of polyanions sandwiched between cationic chains. Winkler et al. have carried out a molecular dynamics simulation of the complex formation for systems with two flexible, oppositely charged polymer chains [175].

The objective of this Chapter is to simulate the self-assembly processes caused by strong electrostatic interactions in solutions containing semiflexible PE chains and flexible-chain DHBCs with an oppositely charged block. Semiflexible PE is characterized by its bending stiffness and linear charge density. The formation of stoichiometric PE-DHBC complexes is simulated in both a dilute and a semidilute solution

III.2   Model of System and Simulation Procedure.

The simulated systems were composed of polymers of two types: strongly charged N_p-unit polyanions and DBHC copolymers with a cationic block (of length N_C) and a neutral block (of length N_B). In this study we assume that $N_C = N_B$. The linear charge density of cationic DHBC blocks was fixed at a value e/σ ($z_C = 1$) while the linear polyanion charge density L_q is varied in the range from e/σ to $8e/\sigma$ with σ being the monomer size.

It should be borne in mind that a single monomeric unit of the model chains corresponds to a group of atoms or a segment of a real polymer; therefore, its charge can be substantially greater than the elementary charge. In order to map the chosen value of L_q to some suitable real system, let us consider double helix DNA. Its diameter is about 20 Å. The chain fragment of such length, which can be considered as an effective monomeric unit, includes ≈6 bp and therefore its effective charge is $2e{\times}20/3.4 = 11.7e$/monomer at the maximal possible degree of dissociation of two charges per base pair of size 3.4 Å.

For computational efficiency, chains with relatively short length, $N_p = 64$ and $N_C = N_B = 8$, were used for the simulations The cubic computational box contained n_p polyanions (total number of negatively charged chain beads is $n_p N_p$) and $n_{\text{DHBC}} = n_p(N_p/N_C)(z_p/z_C)$ positively charged diblock copolymers to ensure electroneutrality of the system and stoichiometry of the formed PECs. The entire system of n_p polyanions plus n_{DHBC} diblocks was enclosed in a periodic box with side length $L_{box} = 100$ and volume $V = L_{box}^3$. The number density of the polyanion beads, $\rho = n_p N_p / V$, was varied from $\sim 10^{-4} \sigma^{-3}$ (salt-free dilute polyelectrolyte solution) to $2.2 \times 10^{-3} \sigma^{-3}$ (semidilute solution). It should be noted that neglecting the electrostatic screening due to salt means that in the simulation, the Debye-Hückel screening length λ_D is comparable to the simulation box size. In this case, the ionic strength for a polyelectrolyte solution is as low as 10^{-5} to 10^{-6} M. This is only slightly higher than pure water. Such ionic strengths, which are typical for many experimental studies involving the salt-free solutions of charged rigid macromolecules, can be achieved using deionization and electrochemical dialysis techniques (see, e.g., Ref. [176]). For example, light scattering studies on solutions of charged rodlike fd virus at very low ionic strength (~10[-6]) [176] showed that the experimental values for the scattering vector fit very well to Monte Carlo simulations of highly coupled systems in the low-salt limit [177]. Although the present simulation describes aggregation processes in a salt-free solution, we expect it to be applicable in the wider range of salt concentrations, where the average concentration of DHBC copolymers in the aggregates exceeds considerably the one in the bulk of the solution. As we will see, this is indeed the case for PE-DHBC complexes. Also, we would like to emphasize that at present there is no satisfactory theory for strongly charged systems at very low salt concentrations.

III.3   Results and Discussion.

First, the structural properties of single PE-DHBC complexes in a dilute solution were studied. It is clear that for zero Bjerrum length, there are no charge interactions in the system and everything is governed by excluded volume; hence the chains behave like a swollen coil in a good solvent. **Figure 17** shows typical snapshots of polyelectrolyte complexes formed at a sufficiently low temperature $T = 0.5$, which correspond to $\ell_B = 2$. From analysis of these data, it may be concluded that practically complete binding of block copolymers to the oppositely charged chains takes place under these conditions, leading to the formation of

stoichiometric PE-DHBC complexes. It is also seen that the structure of the complexes is strongly dependent on the value of charge on the polyanion chain. At small values of L_q the complex has a nonregular bent brush configuration in which the polycation blocks and the polyanion chain are wound round each other and linked together by electrostatic attraction, while neutral DHBC blocks are exposed to the solvent (**Fig. 17a**).
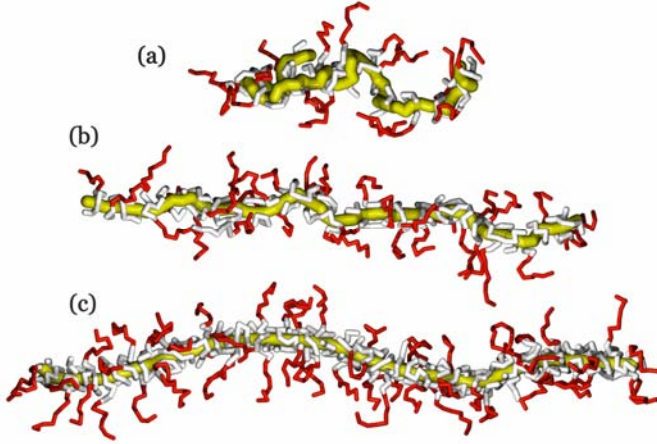

Figure 17. Snapshots of cylindrical ionic micelles at $\ell_B = 2$ and $L_q =$ (*a*) $2e/\sigma$, (*b*) $4e/\sigma$, and (*c*) $8e/\sigma$. The yellow sticks depict the polyanion chain; light-gray and red sticks represent positively charged and neutral sections of DHBC chains, respectively.

Under these conditions, when $L_q \sim 1$ and ℓ_B is sufficiently large, the local structure formed oppositely charged chains resembles a double helix, which is schematically shown in **Fig. 18a**. However, the chains do not form perfect helices. Very similar strictures were observed by Winkler et al. [175] who studied the complex formation in systems with two oppositely charged flexible chains, and by Jeon and Dobrynin [178], who simulated complexation between polyelectrolyte and polyampholyte chains.

When the strength of electrostatic interactions increases but the linear charge density is not too large ($L_q \lesssim 4e/\sigma$), the cationic sections of DHBC chains tend to be stretched and aligned along the polyanions. This complex structure, schematically depicted in **Fig. 18b**, allows maximizing the electrostatic attraction between oppositely charged sections of the polyanion and copolymers while at the same time minimizing the electrostatic repulsion between positively charged monomer units of the copolymers. As L_q further increases, the polyanion binds a larger number of DHBC chains. Visual inspection of the recorded structures indicates that the polyanion chain is extended under these conditions; clearly, a cylindrical bottle-brush architecture due to strongly attractive ion-pair interaction is visible (**Fig. 17c**). At the same time, due to strong steric conflicts between positively charged beads densely packed at the surface of the polyanion backbone, the cationic sections of DHBC chains crumple at small

length scales and show a tendency to wind around the polyanion, thus forming a solenoid-like conformation in which neighboring turns repel each other (see the scheme in **Fig. 18c**). Globally, however, perfect solenoid structure is destroyed by thermal fluctuations.
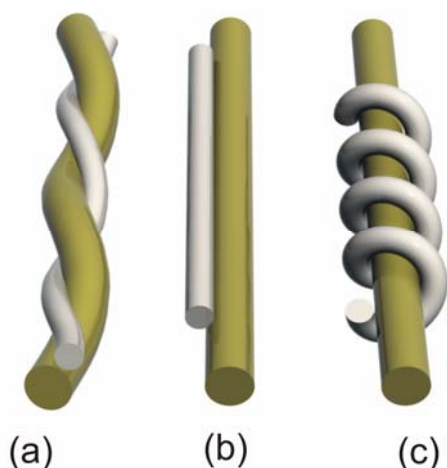

Figure 18. Schematic representation of (*a*) helix-like, (*b*) elongated, and (*c*) solinoid-like conformations.

The quantitative information about the change in each chain's conformation as they form a complex can be obtained by analyzing the mean-square end-to-end distance R^2. **Figure 19** depicts the R^2 value calculated for polyanion chains as a function of ℓ_B for different values of L_q. As expected, the chain size increases with increasing L_q and ℓ_B (or, vice versa, with decreasing temperature). On the one hand, this increase can be related to the growth of negative charge on the chain so that the chain is stiffened electrostatically. However, as follows from the snapshots (**Fig. 17**) and charge distribution functions (see below), practically complete neutralization of opposite charges is attained in the complexes under the given conditions. This is due to low translational entropy of DHBC chains, which allows them to readily bind to the polyanion chain even at a relatively high temperature or small Bjerrum lengths. Consequently, the influence of electrostatic repulsion between uncompensated negative charges during the formation of extended conformations should be very insignificant because in the condensed state screening is present.

Therefore, we can conclude that the behavior of cylindrical PE-DHBC complexes having the polyanion as their backbone is basically determined by steric repulsion between the block copolymers linked to the polyanion chain through ionically attached charged DHBC sections.

Note that polyelectrolyte chains, both flexible and semirigid ones, in the presence of small counterions exhibit a different behavior [179]. They start to collapse at certain electrostatic interaction strength due to counterion condensation.
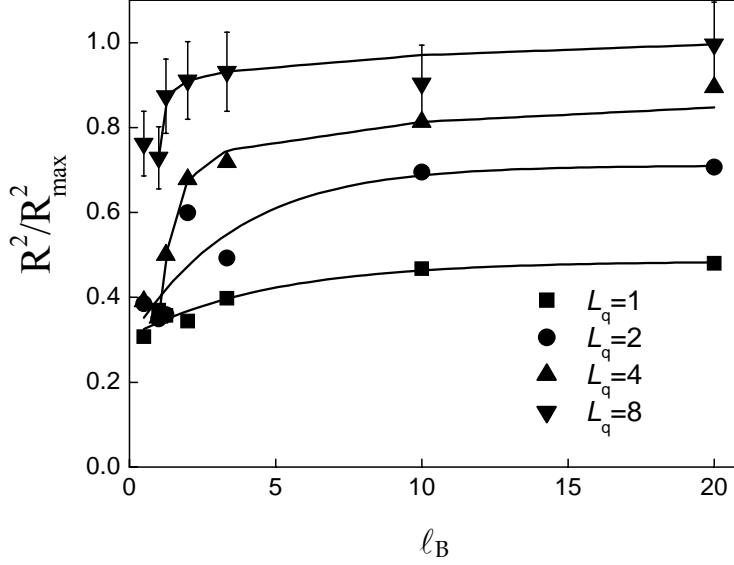

Figure 19. Ratio R^2 / R^2_{max} as a function of Bjerrum length for different linear charge densities ($L_q = e/\sigma$, $2e/\sigma$, $4e/\sigma$, and $8e/\sigma$); $R_{max} = b(N_p\text{-}1)$. Error bars indicate the statistical deviations.

The mechanism responsible for the collapse is related to the effective dipolar attraction among different ionic pairs formed in the condensed state. For the PE-DHBC systems, the charge density of the chains is very large and leads to the complex formation even at very weak Coulomb interaction. For example, for $L_q = e/\sigma$ we observe the formation of ionic aggregates even at $\ell_B \approx 0.2$. This electrostatic interaction strength is by far too small to lead to a condensation of spherical monovalent counterions on a PE chain [179]. Oppositely charged flexible-chain polyelectrolytes also exhibit a collapse and dense structures are formed for sufficiently large interaction strengths. When the Coulomb interaction is strong enough, collapsed structures were found for all chain lengths [175]. Polarization-induced attractive interactions between flexible polyelectrolyte and polyampholyte chains also lead to the formation of collapsed structures [178]. As has been mentioned above, rigid-chain polyelectrolytes can collapse in the presence of small counterions to form toroidal structures [180]. On the other hand as it appears from performed calculation, the condensation of long diblocks on the polyelectrolyte backbone leads to complexes with a molecular bottle-brush architecture for which the Coulomb collapse is significantly blocked by the excluded volume of the DHBC solvophilic tails causing a more elongated conformation of the complex.

It is reasonable to expect that in the ionic PE-DHBC complex, the persistence length (Kuhn segment) of the polyanion chain will increase owing to steric interactions between bound diblocks. Indeed, our calculation shows a growth in the persistence length ℓ_P (Eq. 1.14) with increasing Bjerrum length or/and polyanion charge density L_q (**Fig. 20**).
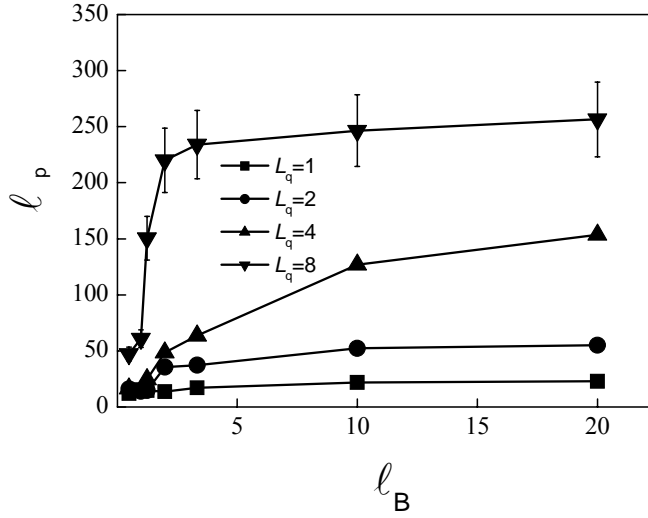
Figure 20. Persistence length of a polyanion chain as a function of Bjerrum length at $L_q = e/\sigma$, $2e/\sigma$, $4e/\sigma$, and $8e/\sigma$. Error bars indicate the statistical deviations.

As it has been noted above, the equilibrium stiffness of a single polyanion chain depends on temperature (or Bjerrum length). However, this effect is weakly pronounced for relatively small $L_q \lesssim 2e/\sigma$. Indeed, at $L_q = e/\sigma$ and $2e/\sigma$ an increase in ℓ_B leads only to an insignificant growth in ℓ_P. At $L_q \geq 4e/\sigma$, the effect of chain stiffening becomes very strong. **Figure 20** shows that ℓ_P also increases at a constant Bjerrum length when the polyanion charge density increases. For $\ell_B > 10$ the persistent length is independent of the strength of electrostatic interaction within the accuracy of our simulation. Under these conditions, the plateau-like regime is clearly present. Thus, the stiffening effect observed for the PE-DHBC complexes emerges mainly due to the specific structural features of the DHBC chains: the combination of charged and neutral blocks promotes both the formation of PE complexes and sterically-mediated stiffening of the polyanion chain in the complexes.

Additional data that confirm the observed effect of the complexation-induced steric stiffening of a polyanion chain can be obtained through analyzing the order parameter η, which characterizes the relative orientation of bond vectors **b** in a chain. The value of η is determined by the largest eigenvalue of the symmetrical matrix with the elements:

$$\eta_{\tau\upsilon} = \frac{1}{2n_p(N_p-1)}\sum_{j=1}^{n_p}\left\langle\sum_{i=1}^{N_p-1}\left[3\frac{b_{i,\tau}^{(j)}b_{i+1,\upsilon}^{(j)}}{b^2}-\delta_{\tau\upsilon}\right]\right\rangle \qquad (3.1)$$

where τ, υ = x, y, z; n_p is the number of polyanion chains in the system; $b_{i,\tau}$ and $b_{i+1,\upsilon}$ are the projections of neighboring (in the chain) bond vectors **b** of the jth polyanions on the τ and υ axes, respectively; and $\delta_{\tau\upsilon}$ is the Kronecker delta. Note that averaging in Equation 3.1 is performed independently for every chain of the system. The η function can have a value between 1 indicating parallel orientation of bonds and -0.5 indicating perpendicular orientation. **Figure 21** shows the orientational order parameter as a function of the Bjerrum length for a few values of L_q. In general, we observe an increase in the orientational order parameter as the strength of electrostatic interactions increases. As the value of L_q is larger, the the observed effect is stronger.

An analysis of the snapshots (**Fig. 17**) shows that during the formation of PE complexes, considerable conformational changes in block copolymers also take place. **Figure 22** presents the mean-square end-to-end distance R_C^2, calculated for charged DHBC sections as a function of the Bjerrum length ℓ_B. It is seen that in the range $\ell_B \gtrsim$, the value of R_C^2 increases with increasing ℓ_B, which indicates the elongation of the charged blocks.

This behavior suggests that flexible positively charged blocks tend to arrange themselves along the polyanion chain in the extended conformation during the complexation.
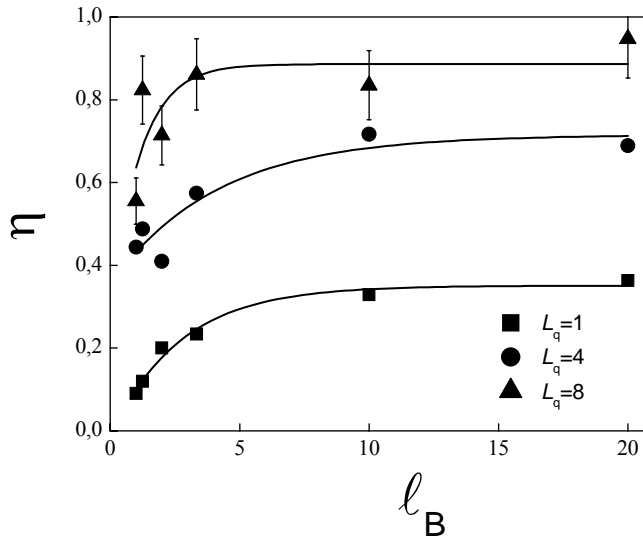
Figure 21. Orientational order parameter for the polyanion bonds as a function of Bjerrum length at L_q = e/σ, $4e/\sigma$, and $8e/\sigma$. Error bars indicate the statistical deviations.
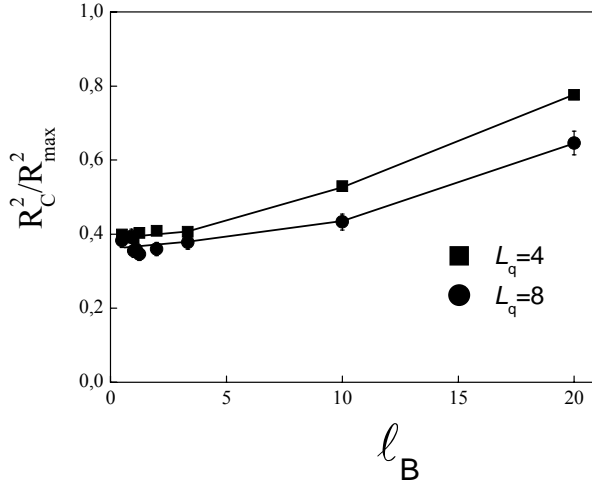
**Figure 22.** Ratio R_C^2 / R_{max}^2 as a function of Bjerrum length for two linear charge densities ($L_q = 4e/\sigma$, and $8e/\sigma$); $R_{max} = b(N_C-1)$. Error bars indicate the statistical deviations.

As it has been noted, with increasing the strength of electrostatic interaction (when the linear charge density is fixed at relatively small $L_q \lesssim 4e/\sigma$), charged half of the copolymer chain is almost perfectly aligned parallel to the polyanion chain forming a train section, while the other neutral half forms a tail. For larger L_q, charged copolymer sections begin to crumple and form turns around the polyanion backbone. Such a behavior is presented in **Fig. 18**. **Figure 22** shows that for $\ell_B \gtrsim 3$, the values of R_C^2 found at $L_q = 4e/\sigma$ exceed those observed at $L_q = 8e/\sigma$. Such a behavior is explained in terms of competition between the electrostatic attraction of unlike charged units and steric repulsion of blocks on the surface of the polyanion chain. Indeed, the higher the charge on polyanion units induces the greater the number of positively charged blocks which can be accommodated in the complex. Hence, a growth in L_q increases the local density of positively charged units near the anion chain, thus creating steric hindrance to their packing. As a result, positively charged blocks begin to wrinkle and to wind the polyanion chain (this behavior is clearly illustrated in **Fig. 17***c*).

A measure of the local organization of oppositely charged monomer units in polyelectrolyte complexes is a pair correlation function $g_{+-}(r)$, which characterizes the spatial distribution of positive and negative charges.
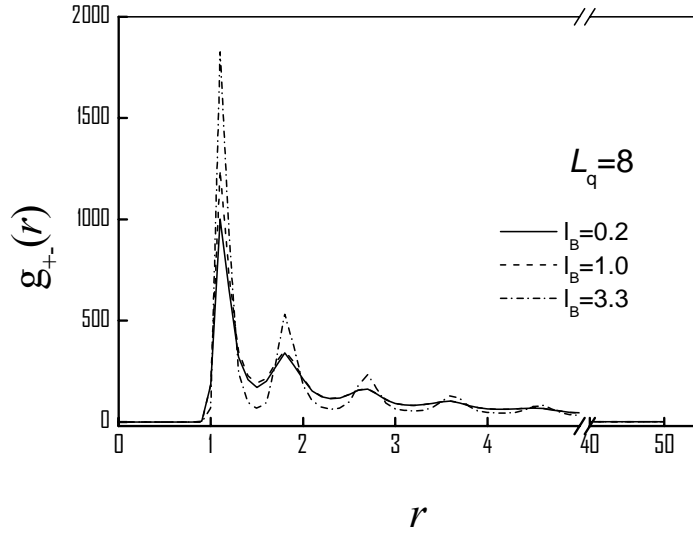
Figure 23. Pair correlation function $g_{+-}(r)$ characterizing the spatial distribution of positive and negative charges in a polyelectrolyte complex at ℓ_B = 0.2, 1.0, and 3.3, for L_q = $8e/\sigma$.

As an example, **Fig. 23** presents a function $g_{+-}(r)$, calculated at $L_q = 8e/\sigma$ for three different Bjerrum lengths. It is seen that $g_{+-}(r)$ exhibits almost regular damping oscillations even at a relatively small ℓ_B. An increase in the strength of electrostatic interactions enhances the local ordering of the complex and indicate a strong aggregation of the oppositely charged chain beads. On the length scale of few monomer units densely packed structures are formed. A similar behavior was observed for compact clusters composed from two oppositely charged chains [175].

Note that the aforementioned stiffening of the polyanion chain is also due to steric repulsion between solvophilic uncharged copolymer blocks. The fact of polymer chain stiffening as a consequence of non-covalent interactions between neutral blocks is well known. There are a number of experimental and theoretical confirmations of this effect for electrically neutral cylindrical polymer brushes [171], and comblike complexes [163,164,181-183].

Effective polyanion-chain stiffening at the complexation with oppositely charged block copolymers allows to make a conclusion that this behavior can be responsible for various self-organization processes in the system. In particular, there are grounds to believe that a rise in the polyanion rigidity and, hence, an increase in the shape anisotropy of the complex must facilitate the orientational ordering of ionic micelles in solution. Thus, we may speak about two levels of hierarchy of the self-organization process: the lower level is associated with the formation of individual ionic micelles and the upper level can involve their spatial ordering.

To study the self-assembly of micellar complexes, we simulated a semidilute solution with a number density of monomer units of $\rho = 2.2 \times 10^{-3} \sigma^{-3}$ at $L_q = 8e/\sigma$. A quantitative characteristic of the ordering process is the collective order parameter η defined by the equation:

$$\eta_{\tau\upsilon} = \frac{1}{2n_p(N_p - 1)} \left\langle \sum_{j=1}^{n_p} \sum_{i=1}^{N_p - 1} \left[3 \frac{b_{i,\tau}^{(j)} b_{i+1,\upsilon}^{(j)}}{b^2} - \delta_{\tau\upsilon} \right] \right\rangle \quad (3.2)$$

Note that as distinct from Eq. 3.1, averaging in Eq. 3.2 is performed for every pair PE chains presented in the system. **Figure 24** shows the order parameter as a function of Bjerrum length. It is seen that η does not exceed 0.4 at $\ell_B \lesssim 0.5$. When $\ell_B > 0.5$, the value of η rapidly grows with increasing the strength of electrostatic interactions. At $\ell_B \approx 1$ the order parameter indicates a sharp transition from a disordered state to an orientationally ordered state, which arises by spontaneous symmetry breaking. Such a behavior indicates the formation of a nematic liquid-crystalline phase in the system of strongly interacting ionic micelles, the process is accompanied by the additional extension of polyanion chains.

Visual inspection of recorded snapshots shows that ionic micelles do not aggregate in a solution, retaining their morphological integrity. The aggregation is impeded by two factors. First and foremost, there is strong steric repulsion between electrically neutral solvophilic shells consisting of DHBC sections which densely cover micelle cores built up from the polyelectrolyte backbone with condensed charged DHBC sections. Due to the fact these core-shell cylindrical brushes are size- and shape-persistent objects; they should maintain their morphological integrity even in rather concentrated solutions where large-scale aggregation is prevented. Second, there is electrostatic repulsion between individual micelles at any non-zero temperature owing to the possibility of spontaneous breaking of stoichiometry of the complexes: when temperature is not too low (or the Bjerrum length is not too large), a part of DHBC molecules is not strongly linked to polyanion chains, thus making ionic micelles negatively charged on average and causing their mutual repulsion (for more detail, see Ref [156]).

Our simulation results are in agreement with available experimental data. Gohy et. al. studied the morphology of water-soluble interpolyelectrolyte complexes formed by poly(2-vinylpyridine)-*block*-poly(ethylene oxide) (P2VP-*b*-PEO) diblocks and poly(4-styrenesulfonate) (PSS) polyanions [184].
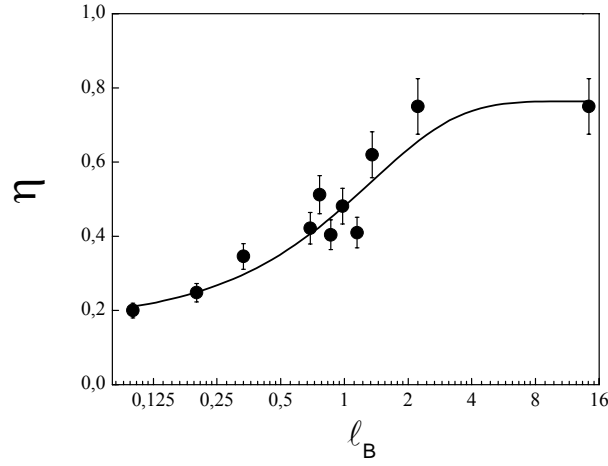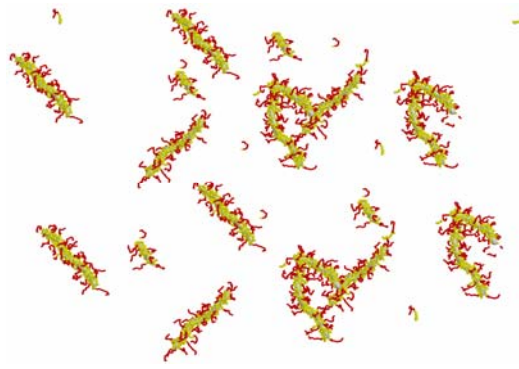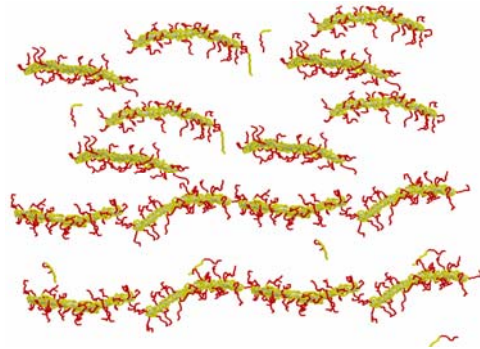
Figure 24. Collective orientational order parameter for the polyanion bonds as a function of Bjer-rum length at $L_q = 8e/\sigma$ and $\rho \cong 2.2 \times 10^{-3} \sigma^{-3}$ (*a*);
(*b*) and (*c*) – snapshots of ionic micelle systems at $\ell_B.0.33$ and 2, respectively.

Aqueous solutions of P2VP-*b*-PEO diblocks were mixed with aqueous solutions of PSS, such that the final number of polyanionic and polycationic chains in the resulting complex was the same. The morphology of these PE-DHBC complexes was analyzed by transmission electron microscopy. It was found that they can have a rod-like shape and also can arrange themselves into isolated and more or less extensively extended buckle-like structures. Such supramolecular assemblies are composed of a solvophobic core, arising as a result of charge neutralization upon complexation, surrounded and stabilized by a solvophilic shell [184]. The formation of such complexes can be explained by the force balance of three factors:

(i) the stretching of the core-forming blocks, (ii) the surface tension between the micelle core and the solvent outside the core, and (iii) the intershell-chain interactions [185]. Extended ionic micelles from DNA and PEO-*block*-PLys were visualized by AFM [186]. These water-soluble PEs were found to be stoichiometric, with hydrophilic PEO block forming the micelle shell. Similar results were reported for PEO-*block*-PLys/oligonucleotide complexes under physiological conditions [160]. These observations are consistent with these simulations.

III.4   Conclusion.

Complexation in solutions of strongly charged polyelectrolytes and diblock copolymers composed of oppositely charged and neutral blocks were studied using the molecular dynamics method. Stoichiometric micellar complexes formed in a dilute solution represent cylindrical brushes whose conformation is determined by the linear charge density on the polyelectrolyte and by temperature. As the concentration of macromolecules increases, the orientational ordering of anisotropic ionic micelles takes place. The complexation can induce the stiffening of the polyelectrolyte chain.

Chapter IV. Network Structures in Solutions of Rigid-Chain Polyelectrolytes.

IV.1 Introduction.

Many synthetic and natural macromolecules are capable of forming branched structures and networks [188-190]. Such reversible structures can emerge upon change in external conditions (e.g., with variation in the pH and ionic strength of solution, temperature, solvent composition, etc.) They also appear in the presence of substances that have an effect on specific interactions between macromolecules (hydrogen bonding, hydrophobic interactions, coordination bonds, π-π stacking). Networks or stacks of rodlike macromolecules, such as F-actin, DNA, and other highly charged polyelectrolyte chains (tobacco mosaic virus, fd-virus), are stabilized by condensed multivalent ions, polyamines, positively charged polypeptides, and proteins with positively charged domains [20,188,191-193]. For example, both structure and dynamics of actin bundles are strongly regulated by interaction with actin-binding proteins in living cell [194]. Some actin-binding proteins, such as Ena/VASP, calponin, and dystrophin induce the formation of actin architectures to be bound to actin by electrostatic interactions [195,196].

A relatively high rigidity of polyelectrolyte molecules provides opportunity for the formation of three-dimensional networks or bundles [189]. For flexible-chain polymers, multivalent ions can cause their collapse [87,93]. In the case of semirigid chains, various compact conformations (tori, cylinders, tennis racket structures) form [101,197,198], as has been discussed in Chapter II.

Effective attraction between likely charged polyelectrolytes was revealed rather long ago [199,200]. This interaction plays a key role in various biological processes, such as compaction of DNA and formation of filaments that compose the cytoskeleton. The fact that an attraction is observed in a variety of rigid PEs and counterions (organic and inorganic) indicates that specific interactions like hydrogen bonding do not determine the behavior of such structures. Therefore, the mechanism of network formation can mainly be due to electrostatic interactions. However, in the systems with strong electrostatic interactions (containing, e.g., strongly charged surfaces or multivalent ions) the physics may be different. The interactions between PEs can be controlled by the structure and charge of condensed ions sur-

rounding PE chains. It has been shown that mean-field Poisson-Boltzmann approach [201] does not explain the effective attraction since in the model the correlations between counterions are not taken into consideration [202]. It was proposed by Kirkwood [203] and was shown by Oosawa [200] by means of approximate analytical model that the attraction between like-charged PEs is possible due to correlated fluctuations of condensed ionic layers around the strongly charged cylindrical chains. Recently, certain anionic biopolymers having the persistence length at 1μm or more (e.g., filaments of bacteriophages, microtubules, F-actin, etc.) have been used as a research system for studying such attraction [20,193]. Because of large persistence length (**Table 1**) these rigid-chain polymers can be considered as idealized rod-like PEs. Based on these systems, a large set of new effects has been demonstrated. For example, in the presence of divalent ions, the actin filaments are condensed to closely packed bundles, but liquid crystal network composed by 1D-lamellar stacks is an intermediate state in the structure formation [204].

The next interesting experimental observation consists in that the charge-mediated attraction typically does not lead to macroscopic phase separation. In this regard this "effective attraction" is different from usual attraction, e.g., solvophobic attraction which leads to phase separation at a sufficiently high concentration of solution. Moreover, the polyelectrolyte chains exhibit a tendency to form of closely packed aggregates with well-defined thickness [205,206].

The question was raised as to whether counterions can induce an attraction between like-charged chains was repeatedly investigated in many theoretical studies, because as already mentioned above, in mean-field classical theory the like-charged objects always repel from each other [207].

Using the integral-equation theory, it was shown that an effective attraction between charged spheres [208] and surfaces appears in the presence of multivalent counterions [209,210]. Today, there are several approaches to the theoretical description of attraction. A simple physical explanation of such interaction (static concept) is given in Refs. [211-214]. At low temperatures, condensed counterions form Wigner crystals near charged surfaces. Effective attraction between likely charged rods decreases as temperature increases and the crystal melts [212]. In the case of rodlike counterions, ideas of this kind were developed on the basis of an exactly solved model [214,215]. Another mechanism (dynamic concept) assumes the existence of correlated fluctuations of counterions [199,200,198, 216,217]. It was shown [200] that

the density fluctuations of opposite charges in the vicinity to a polyelectrolyte chain lead to short-range attraction, which can overcome electrostatic repulsion under certain conditions. This attraction is askin to van der Waals attraction. It is enhanced with a decrease in temperature, since the effective interchain interaction dominates over thermal fluctuations. Dispersion forces and hydrophobic effects may also facilitate the association of macromolecules [199,205, 219-221].

It was found that the transition from dilute regime to dense regime is the first-order phase transition and is similar to isotropic-nematic transition in the system of semirigid chains, where the chains are extended and orientationally ordered at large solution concentration. However, in the latter case it takes place owing to translation entropy gain which induces this transition, whereas in the case at question the transition is caused by competition between binding energy and electrostatic repulsion between like-charged chains [204].

As has already been mentioned, the aggregation of charged polymers was experimentally revealed for F-actin, rodlike viruses, and microtubes [20,193,222-230]. In all discussed instances when the concentration of condensing agents was sufficiently large, polyelectrolyte macromolecules were associated into various structures; e.g., hypercrosslinked networks and parallel "bundles". The subsequent experiments with such objects revealed that the general properties of the aggregates agree well with theoretical predictions, and the main cause of the formation of such complexes is determined by the polyelectrolyte nature of actin [20]. Tang and Janmey [20] also showed that the formation of network structures from polymer bundles in most cases may result from steric hindrances while network cross-links frequently appear in the random way. The role of arisen cross-links in gelation processes have been described in detail in Ref. [231].

Attraction that effectively arises between likely charged rigid-chain PEs as well as the conditions of formation and stability of produced branched structures and networks was studied by computer simulation methods [28, 232-234].

However, it is still unclear how counterions affect the properties of the condensed polyelectrolyte phase and the structural evolution of aggregates containing rigid charged chains. The influence of external parameters (e.g., temperature or solvent) on the stability and morphology of aggregates, likewise, has been studied to an insufficient extent. Thus, studying the behavior of PE chains in solution with multiply charged ions by means of molecular dynamics seems to be of topical interest.

IV.2   Description of Model and Simulation Procedure.

In this Chapter the theoretical study of non-covalently linked structures and the networks formed in solutions of rigid-chain PEs and low-molecular multivalent counterions will be presented. The stability of network structures depending on charge value of counterions will be considered.

As a model, a salt-free solution composed of polyanion chains (with the number of chains $n = 50$ and a chain length of $N = 32$) with the fixed value of charge on each monomer unit was considered. The monomer units of the polyanion are connected with one another by rigid links of a fixed unit length.

The potential energy of the system was written as (2.1). The volume interactions, electrostatic term, as well as PE chain rigidity were modeled by means of potentials described in the methodical part of Chapter II.

Charges q_i on polyions and counterions expressed in the unit charge units e had values of q_i = -1 for the polyanion and +1, +2, +4 for cations. The solvent was considered as a continuum with a prescribed viscosity ($\gamma_0 = 1$), whose value ensured that the temperature remains constant within the limits of ($\pm 5\%$). The number density of polymer units was $\rho = 7.3 \times 10^{-2} \sigma^{-3}$. This value corresponds to a semidilute solution of semirigid chains.

The main calculation parameters were the temperature T and the valence of counterions q_i. For each set of parameters, the system was equilibrated over 2×10^6 time steps. The step of integration was equal $\Delta t = 0.01$. The data averaging was carried out during 2×10^6 steps. The computations were executed in normalized units; the length was measured in σ, the energy in ε and temperature T in ε / k_B.

IV.3   Results and Discussion.

Most calculations were performed for conditions what assumed strong electrostatic interactions and provided the condensation of counterions on macromolecules in the system. A decrease in temperature or permittivity of medium enhanced the electrostatic interaction.

IV.3.1   Characterization of Single Chains in Network Structure.

The temperature dependences of the mean-square radius of gyration of chains R^2_g and the order parameter η are shown in **Figs. 25** and **26**, respectively. As usual, the value η is determined by largest eigenvalue of symmetric matrix with elements (3.2).

It is seen that both quantities have a maximum in the range $0.2 \leq T \leq 0.25$ (T^*_2) and $0.4 \leq T \leq 0.5$ (T^*_4) for q_i = +2 and +4, respectively. This implies that the chains attain their maximal extension and degree of orientation at these temperatures. The systems demonstrate of non-monotonic dependence of R^2_g and η on strength of electrostatic interaction.
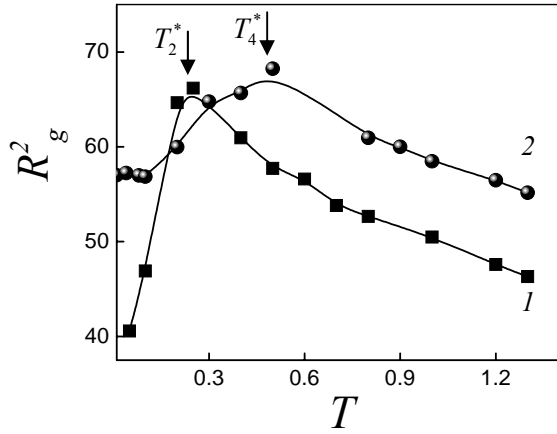
Figure 25. Mean-square radius of gyration of a single polyanion chain as a function of temperature at q_i = +2 (*1*) and q_i = +4 (*2*).
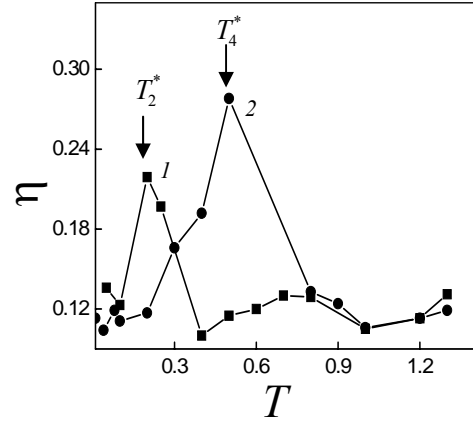
Figure 26. Change in the order parameter of the system with temperature: q_i = +2 (*1*) and q_i = +4 (*2*).

Kwon et al. [235] have also observed an extremal dependence of size of formed aggregates (**Fig. 27**) on electrostatic interaction that was varied by addition of electrolyte. It is seen that these experimental data are well correlated with the results of performed calculations.
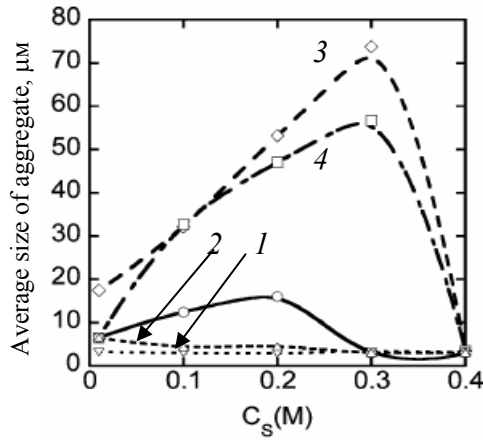
Figure 27. Average size of polycation-actin complexes at various concentration of added electrolyte (KCl), C_s(M).
1 – 0M, *2* – 10^{-6}M, *3* - 10^{-5}M, *4* - 10^{-2}M, *5* - 10^{-1}M are concentration of polycation solution [235].

At large temperatures, i.e. low Bjerrum lengths, many counterions are found in solution, and PE chains remain strongly charged. Another extreme case is a very-low temperature. In this case, practically all counterions are condensed. As a result, the aggregate charge is close to zero. These results agree with the data of theoretical study of hydrophobic-modified poly(p-phenylele sulphonate) [28,236] and experimental observations [237].
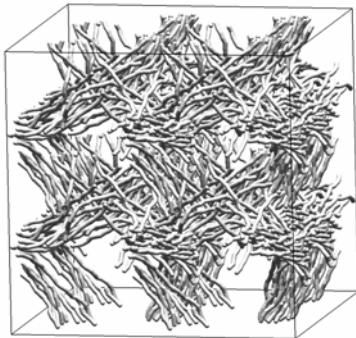
Figure 28. Network superstructure formed at *T* = 0.4 in a rodlike-polyelectrolyte solution at q_i = +4. Counterions are not shown.
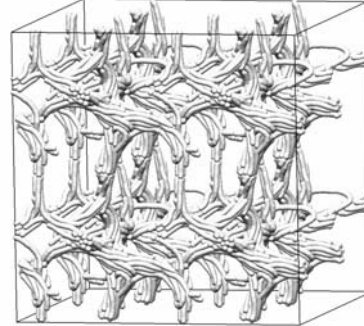
Figure 29. Structure formed at *T* = 0.1 in a rodlike-polyelectrolyte solution at q_i = +4. Counterions are not shown.

From the analysis of snapshots (**Figs. 28** and **29**), it follows that at T^* (ε_r =1) the network structures consist of polymer bundles. In these bundles, the macromolecules are locally ordered in a parallel manner, i.e. anisotropic units are formed. Such anisotropic growth mechanism of actin bundles was also observed in experiment. The conception of anisotropic growth was proposed by Kwon et al. [238]. It should be noted that obtained sharp structural transition is very important because it may be responsible for self-assembly/destruction dy-

namics of actin, which is bioactive substance and serves for cell displacement, adhesion and cytokinesis.

At a lower temperature, a structure composed of chains with arc-like conformation appears (**Fig. 29**). At low temperatures (in a poor solvent or in the presence of a condensing agent), rigid-chain polymers usually take torus-like conformation, as has been shown in Chapter II. In our case, each chain is a part of a united aggregate (network). Therefore, such connectivity impedes the complete collapse of single chains. As a result, we do not observe the formation of torus-like chain conformations, but we observe a tendency to form such conformations.

The conformational transitions of actin associates are also known in the experiment [238]. Typical morphologies of polymer-actin complexes in phases I, II, III, IV, and V as observed by TEM images and fluorescence images are shown in **Fig. 30**. In phase I, actin bundles do not grow. In phase II, the native F-actin and polymer-actin complexes coexist. The polymer-actin complexes are divisible into the cross-linked structures (III), the branched-structures (IV), and parallel-bundles (V) as shown in **Fig. 30**. According to our results, the formed structures (**Figs. 28, 29**) correspond to the so-called III and IV morphologies which were observed experimentally (**Fig. 30**) [238].

It should be pointed out that the energy of the system rapidly decreases when the network structure begins to form (**Fig. 31**). At $T > 0.6$ and 0.8 (for $q_i = +2$ and $+4$, respectively) the chains practically do not experience aggregation.
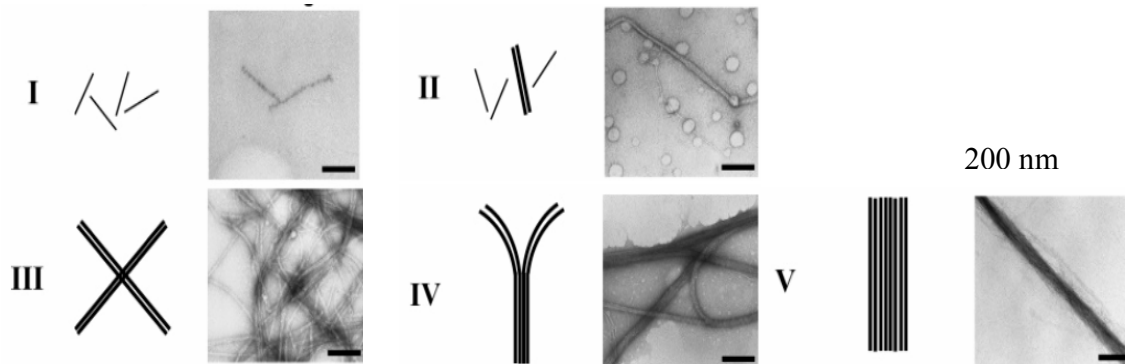
Figure 30. Typical morphologies of polymer-actin complexes in phases I, II, III, IV, and V as observed by TEM images and fluorescence images. Scale bars present 200 nm for TEM images and 25 μm for fluorescence images [238].
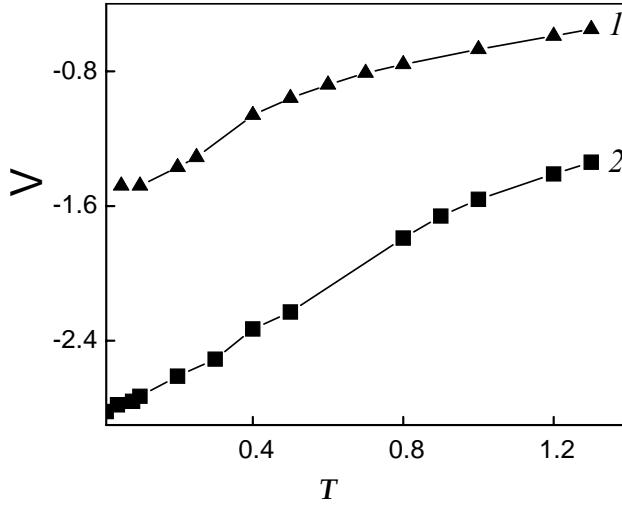
Figure 31. Potential energy of the system as a function of temperature at $q_i = +2$ (*1*) and $q_i = +4$ (*2*).

The formation of network structures (not cylindrical aggregates) occurs for the following reasons. It has been already noted that network cross-links appear in the random manner; i.e., aggregation nuclei — stacks of several polyelectrolyte chains with counterion interlayers between the chains — arise in the system at a certain temperature (T^*). At each momemt, an individual stack in the network structure has an unbalanced charge, inasmuch as counterions experience thermal motion. Consequently, individual bundles can exchange counterions. Being likely charged, the stacks tend to occupy the most distant position with respect to one another. In this case, the formation of network structures is the most favorable at a fixed polymer concentration. It is the reasons for polyelectrolyte chains do not form a single aggregate with the parallel arrangement of all chains with respect to one another.

IV.3.2   Characterization of Network Structures.

To quantitatively characterize the spatial structure of networks produced in solutions of rodlike polyelectrolytes and multivalent counterions, we attempted to determine the distribution of free volume in the systems. For this purpose, hole size differential distribution functions were calculated and the mean hole size depending on the temperature was found for two systems (using counterions with charges of $q_i = +2$ and +4 as condensing agents).

Figure 32 presents pore size distribution functions $W_d(r)$. Three temperature regions which differ in the homogeneity of space filling with polyelectrolyte molecules can be distinguished. At high temperatures, there is a relatively uniform distribution of molecules for both

systems – small holes with a radius of $R = 2\sigma$ are the most probable (the distribution function is more or less symmetrical and has the highest intensity).

As temperature decreases to T^*, less uniform distribution of holes is observed. Namely, at these temperatures, the size of polymer chains and the order parameter have the maximal values (**Fig. 25, 26**). In this case, the snapshots show the formation of network structures (**Fig. 28, 29**). Under these conditions, the probability of occurrence of holes with a large radius (up to $r = 8\sigma$ at $q_i = +4$) increases, and it is manifested in considerable asymmetry of the distribution function. As temperature is further decreased, the probability of occurrence of large voids decreases, but the distribution remains asymmetrical.
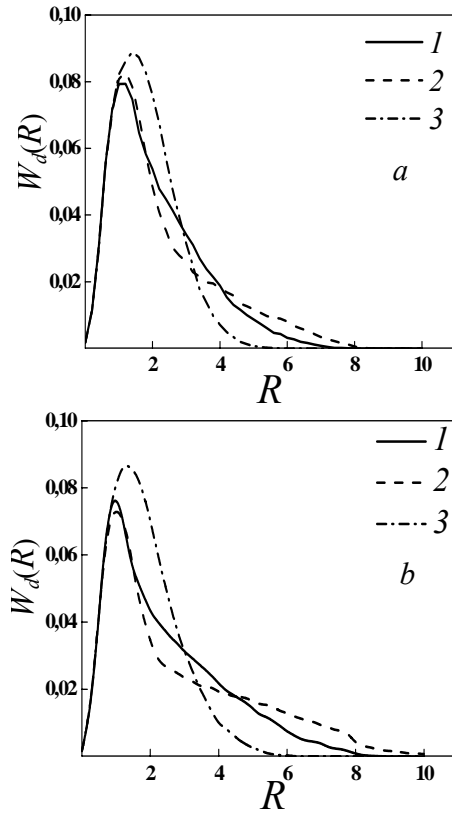
Figure 32. Void-size differential distribution functions at $T = 0.1$ (*1*), 0.25 (*2*), 1.2 (*3*); $q_i = +2$ (*a*), and $T = 0.1$ (*1*), 0. 5 (*2*), 1.2 (*3*); $q_i = +4$ (*b*).

A quantitative characteristic of the three-dimensional networks is the mean hole diameter (**Fig. 33**):

$$\langle D \rangle = 2 \frac{\int\limits_{0}^{\infty} r W_i(r) dr}{\int\limits_{0}^{\infty} W_i(r) dr} \tag{4.1}$$

Here $W_i(r)$ is the integral void-size distribution function.
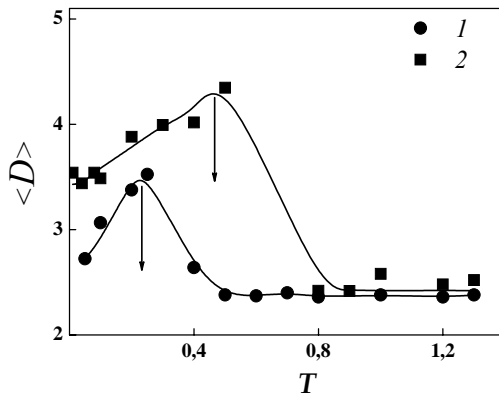
Figure 33. Average free-volume hole diameter as a function of the temperature at $q_i = +2$ (*1*) and $q_i = +4$ (*2*). The arrows mark the maximum attainable dimensions of holes in the systems.

In **Fig. 33**, the average hole diameter, $<D>$ is plotted as a function of temperature for the two systems under study. It is seen that the $<D>$ values have a maximum value at the temperatures corresponding to the formation of stable networks ($T = T^*$). From these plots as well as from **Figs. 25**, **26**, and **32** the network-formation signatures and the stability interval of the networks can also be determined. As shown in **Fig. 33**, the maximum pore diameters are observed also at $T = T^*$. In this case, the inequality $T_2^* < T_4^*$ is valid. As the q_i value increases, the critical temperature T^* is shifted toward higher T, thus indicating that multivalent counterions are better stabilizers of such networks. The same conclusions have been drawn by Yoshikava et al. [115] in their experimental study of interaction of DNA with various polyamines (1,3-diaminopropane, spermine, and spermidine).

IV.4 Conclusions

The results of molecular dynamics simulation of solutions of strongly charged rigid-chain polymers in the presence of multivalent counterions are presented. The processes of self-assembly of macromolecules that occur during the condensation of counterions were studied depending on temperature, dielectric permittivity of the medium, and charge of counterions. Various conformational rearrangements induced by changing the parameters of the medium were examined. The conditions that lead to the formation of network superstructures composed of aggregating polymer chains were found. Size distribution functions for free-volume holes were constructed and the average dimensions of voids in the network structures formed were calculated.

CONCLUDING REMARKS

Self-assembly of soft matter is of fundamental importance in various fields of science, especially including polymer science. It is a widely used term that describes the phenomena of self-organization. In the present thesis, different types of self-assembled polyelectrolyte systems have been addressed. The keywords of the testis are "strongly charged rigid-chain polyelectrolytes" (PE), "polyelectrolyte complexes" (PEC), and "computer simulation". Below, the main results of this study are briefly summarized.

The investigations of conformational behavior of strongly-charged PEs have been performed. To identify and characterisize resulting PECs, the effect of oligocation chain length , N_c and electrostatic interactions was studied. The state diagrams in the "N_c - T" and "N_c - ε_r" variables were constructed. To this end, simulations of equimolar systems containing rigid-chain polyanion and flexible-chain polycations of various lengths were performed. To identify the types of emerging conformations, various energetic and structural criteria (potential energy of complexes, pair correlation functions, etc.) were employed. The snapshots of the complexes were also analyzed. As a result of calculations, the regions of preferential existence of typical conformations were revealed. In stable polyelectrolyte complexes, the observed entities may have the form of bent superhelical bundle (I) (in which oppositely charged chains are braided), folded cylinder (II), tennis racket (III), torus (IV), or double torus (V). It was found that the structures I, II, and IV are the most stable, whereas other structures are most likely metastable.

The numerical simulation of a system of strongly charged polyanions and diblock copolymers composed of a positively charged block and a neutral block (DHBC) has shown that stable ionic micelles in the form of extended cylindrical brushes are formed owing to electrostatic interaction. A decrease in temperature or an increase in the charge density on the polyanion chain leads to its effective stiffening. This outcome is primarily due to steric interactions between diblock copolymers, which are bound to polyanions chain to form complexes of a nearly stoichiometric composition. The orientational ordering of anisotropic ionic micelles, which do not aggregate in solution, takes place at a sufficiently high concentration.

The system of nonaggregating orientationally ordered ionic micelles is interesting from the viewpoint of potential applications in nanotechnology and molecular nanoelectronics. It is known that one of the processes for manufacturing of nanowires is the metallization of an amphipolar, comblike, polymer brush. Although the synthesis of polymer brushes has

been thoroughly studied, this process remains very laborious. An alternative to chemical brushes can be polyelectrolyte complexes formed by a rigid-chain, strongly charged polymer (e.g., DNA) and oppositely charged macromolecules of a doubly hydrophilic block copolymer.

Issues for the further study include determination of various characteristics of electrostatic-based formation of cylindrical brushlike nanostructures at different concentrations of polyelectrolyte and DHBC chains in the presence of small counterions. The question of how the solvent quality and salt concentration influence the aggregation process also is of great interest.

The computer simulation of the systems composed of strongly charged polyanion chains and multivalent ions showed that, at certain temperatures and electrostatic interaction forces, attraction between polymer chains takes place, which results in the formation of branched structures and networks. Under these conditions, the systems are characterized by maximal values for the mean-square radius of gyration of chains and the order parameter of their arrangement. The stability ranges of network structures shift toward higher temperatures with an increase in charge of counterions. The formed porous structures were described in terms of differential void-size distribution functions. The obtained quantitative characteristics (mean hole diameter) of the spatial arrangement of networks can be useful in the application of analogous systems, such as membranes, filters [239], sorbents, and materials for micro-encapsulation.

ZUSAMMENFASSUNG

„Simulation der Nanostrukturbildung der rigiden Polyelektrolytketten in Lösungen"

Die von Olga A. Gus'kova verfasste Doktorarbeit „Simulation der Nanostrukturbildung der rigiden Polyelektrolytketten in Lösungen" ist wie folgt gegliedert: Einleitung, Literaturüberblik, drei Originalteile, Schlußfolgerungen, Danksagung, Liste der Verweise und Anhängen.

Polyelektrolyte (PE) sind Polymere, die ionisierbare Gruppen enthalten, den in polaren Lösungsmitteln (z. B. in Wasser) in geladene Polymerketten, die Makroionen, und kleine Gegenionen dissoziieren. Fast alle biologischen Polymere sind Polyelektrolyte. Obwohl Polyelektrolyte in der Natur und Technik weit verbreitet sind, sind sie theoretisch weit weniger bekannt als neutrale Polymere. Eine Schwachstelle der meisten Theorien von PEn ist, daß sie, zumindest ursprünglich, für einzelne Ketten bei unendlicher Verdünnung entwickelt wurden. Die Einführung einer bestimmten Dichte und damit die Behandlung des Einflusses von Gegenionen und Ketten-Ketten Wechselwirkungen gestaltet sich schwierig. Nichtsdestotrotz ist die Theorie von Polyelektrolyte ein momentan stark bearbeitetes Forschungsgebiet. Wegen der oben genannten Schwierigkeiten bedarf es allerdings der Überprüfung theoretischer Vorhersagen durch andere Methoden. Da auch auf experimenteller Seite Schwierigkeiten bestehen, sind die Ergebnisse von Computersimulationen oftmals das einzige Mittel, die Theorien zu überprüfen.

In der vorliegenden Doktorarbeit werden Struktur und Eigenschaften von rigiden Polyelektrolyte mit Hilfe von Molekulardynamiksimulationen studiert. Die Schwerpunkte liegen in der Untersuchung der Einzelkettenstruktur, der Konformationen der Polyelektrolytkomplexen und der Struktur der Polyelektrolytlösungen.

In der *Einleitung* werden das Interesse an der Untersuchung polyelektrolytischer Systeme, die Besonderheit sowie die Signifikanz der vorliegenden Doktorarbeit beschprochen.

Der *Literaturüberblik* (*Kapitel 1* der vorligenden Doktorarbeit) ist in 4 Teile unterteilt. Der erste Teil ist den ion-haltigen polymerischen Systeme gewidmet. Hier handelt es sich um aktuelle Fragestellungen und Ansätze zur aktuellen experimentellen Forschungen von polyelektrolytischen Systemen. Im zweitem Teil werden die Vorgänge der Selbsorganisation in ion-haltigen polymerischen Systeme detaillieert besprochen, z.B., in Systemen der flussigkristallinen PE und hydrophobischen PE, in PE-Surfaktant Systemen. Im letzten Fall

ergibt sich eine interessante Konkurrenzsituation zwischen der elektrostatischen Abstoßung der geladenen Monomere und der durch das Wasser verursachten effektiven Anziehung. Die wesentlichen theoretischen Arbeiten, die Eigenschaften von Polyelektrolyten behandeln, werden im dritten Teil erwähnt, z.B., Skalentheorie, Renormalisierungstheorie, mittele Feldtheorie, Integralgleichungtheorien). Im vierten Teil werden die Simulationemethoden besprochen. In diesem Teil wird eine besondere Aufmerksamkeit der Berechnung von langreichweitigen Wechselwirkungen zugeteilt (die Behandlung der vollen Coulomb Wechselwirkung und die explizite Berücksichtigung der Gegenionen). Es wurden alle Ionen explizit simuliert und für die Wechselwirkung die volle Ewaldsumme berücksichtigt.

Die nächsten drei Kapitel stellen die neuen Ergebnisse der Doktorarbeit vor, von denen einige schon im Experiment bestätigt wurden.

Kapitel 2 (Erster Originalteil) ist der Untersuchung des Einflusses einer Polykationketten auf die Konformationen der Polyelektrolytkomplexe in verdünnten Lösungen rigider Polyelektrolytketten gewidmet. Dabei wird die Abhängigkeit von Parametern wie Kettenlange von „Gegenionen" (Polykationen) and Bjerrum-Lange behandelt. Die starke Kopplung zwischen Rechnungparametern und Struktur der Komplexen (Koexistenz verschiedener Strukturtypen, z.B. Torus, doppelter Torus u.a.) wird gezeigt und diskutiert. Die Zustandsdiagramme der Komplexen aufgrund der rigiden PE werden berechnet.

Kapitel 3 (Zweiter Originalteil) beschäftigt sich mit den Untersuchungen der Selbstorganization im System der rigiden PE mit doppelten hydrophilen Blockkopolymeren. Es wurde gezeigt, daß in diesem Fall anisotrope zylindrische ionische Micellen entstehen werden. Die Polyelektrolytkettenstruktur in diesen physikalischen Komplexen wurde untersucht. Es wurde vorhergesagt, daß in halbverdünnten Lösungen diese ionischen Micellen eine kristallin-flüssige Anordnung formen können.

Kapitel 4 (Dritter Originalteil) beschreibt die theoretische Untersuchung der Nanostrukturformierung in Systemen der starkgeladenen stabförmigen PE und niedermolekularen multivalenten Gegenionen. Es wurde gezeigt, daß sich nicht kovalentgebunden Strukturen und physikalische Netzwerke in halbverdünnten Lösungen formen können. Die Stabilität der Netzwerke je nach Gegenionladungen wurde untersucht.

Die wichtigsten Ergebnisse der vorligenden Doktorarbeit werden in den *Schußfolgerung* zusammengefasst.

ACKNOWLEDGEMENTS

REFERENCES

1.   Borue V. Yu., Erukhimovich I. Ya. A statistical theory of weakly charged polyelectrolytes: fluctuations, equation of state and microphase separation. // Macromolecules. 1988. v. 21. № 11. pp. 3240 – 3249.

2.   Khokhlov A. R., Khachaturian K. A. On the theory of weakly charged polyelectrolytes. // Polymer. 1982. v. 23. № 12. pp. 1742-1750.

3.   Dobrynin V., Rubinstein M. Theory of Polyelectrolytes in Solutions and at Surfaces. // Progress in Polymer Science. 2005. v. 30. pp. 1049-1118.

4.   Nguyen T. T., Grosberg A. Yu., Shklovskii B. I. Physics of charge inversion in chemical and biological systems. // Rev. Mod. Phys. 2002. v. 74. №2. pp. 329-345.

5.   Potemkin I.I., Limberger R.E., Kudlay A.N., Khokhlov A.R. Rodlike polyelectrolyte solutions: Effect of the many-body Coulomb attraction of similarly charged molecules favoring weak nematic ordering at very small polymer concentration. // Phys Rev. E. 2002. v. 66. № 1. pp. 011802 (1-11).

6.   Khokhlov A.R., Starodubtsev S.G., Vasilevskaya V.V. Conformational Transitions in Polymer Gels: Theory and Experiment. // Adv. Polym. Sci. 1993. V.109. pp. 123-171.

7.   Starodubtsev S.G, Khokhlov A.R. Synthesis of Polyelectrolyte Gels with Embedded Voids Having Charged Walls. // Macromolecules. 2004. v. 37. № 6. pp. 2004-2006.

8.   Deserno M., Holm C. Theory and simulation of rigid polyelectrolytes. // Mol. Phys. 2002. v. 100. № 18. pp. 2941-2956.

9.   Hofmann T., Winkler R.G., Reineker P. Integral equation theory approach to rodlike polyelectrolytes: Counterion condensation. // J. Chem. Phys. 2001. v. 114. pp. 10181-10188.

10.   Khokhlov A. R., Dormidontova E. E. Self-organization in ion-containing polymer systems// Physics-Uspekhi. 1997. v. 40. № 2. pp. 109-124.

11.   Bekturov E.A., Bakaurova Z. Kh. Sinteticheskie vodorastvorimye polimery v rastvorakh (Synthesized Water-Soluble Polymers in Solutions), Alma-Ata: Nauka, 1981. – 248 p.

12.   Staudinger H. Die Hochmolecularen Organischen Verbindungen. Berlin: Springer, 1932. – S. 39.

13.   Kuhn W., Kuhn H. Die Frage nach der Aufrollung von Fadenmolekeln in strömenden Lösungen // Helv. Chim. Acta. 1943. v. 26. № 5. pp. 1394-1465.

14.   Flory P. J. Principles of Polymer Chemistry. Cornell University Press, Ithaca, 1953.

15.   Plate N.A., Shibaev V.P Grebneobraznye Polimery i Zhidkie Kristally (Comb-shaped Polymers and Liquid Crystals). Moscow: Khimiya, 1980.

16.   Strand K. A., Boee A., Dalberg P. S., Sikkeland T., Smidsroed O. Dynamic and static light scattering on aqueous solutions of sodium alginate // Macromolecules. 1982. v. 15. №2. pp. 570-579.

17.   Stokke B. T., Brant D. A. The reliability of wormlike polysaccharide chain dimensions estimated from electron micrographs. // Biopolymers. v. 30. № 13-14. pp. 1161-1181.

18.   Wenner J. R., Williams M. C., Rouzina I., Bloomfield V. A. Salt Dependence of the Elasticity and Overstretching Transition of Single DNA Molecules. // Biophys. J. 2002. v. 82. № 6. pp. 3160-3169.

19.   Sato T., Norisuye T., Fujita H. Double-Stranded Helix of Xanthan in Dilute Solution: Evidence from Light Scattering. // Polymer J. 1984. v. 16. № 4. pp. 341-350.

20.   Tang J.X., Janmey P.A. The Polyelectrolyte Nature of F-actin and the Mechanism of Actin Bundle Formation // J. Biol. Chem. 1996. v. 271. № 15. pp. 8556-8563.

21.   Bockstaller M., Kohler W., Wegner G., Vlassopoulos D., Fytas G. Hierarchical Structures of a Synthetic Rodlike Polyelectrolyte in Water. // Macromolecules. 2000. v. 33. № 11. pp. 3951-3953.

22.   Kassapidou K., Jesse W., Kuil M. E., Lapp A., Egelhaaf S., van der Maarel J. R. C. Structure and Charge Distribution in DNA and Poly(styrenesulfonate) Aqueous Solutions. // Macromolecules. 1997. v. 30. № 9. pp. 2671-2684.

23.   Lee C. C., Chu P., Berry G. C. Studies on dilute solutions of rodlike macroions. I. Light scattering, densitometry, and cryoscopy. // J. Polym. Sci. Polym. Phys. Ed. 1983. v. 21. № 9. pp. 1573-1597.

24.   Brodowski G., Horvath A., Ballauff M., Rehahn M. Synthesis and Intrinsic Viscosity in Salt-Free Solution of a Stiff-Chain Cationic Poly(p-phenylene) Polyelectrolyte. // Macromolecules. 1996. v. 29. № 21. pp. 6962-6965.

25.   Rau I. U., Rehahn M. Rigid-rod polyelectrolytes: carboxylated poly(para-phenylene)s via a novel precursor route. // Polymer. 1993. v. 34. № 13. pp. 2889-2893.

26.   Ballauff M. Kettensteife Polymere - Struktur, Phasenverhalten und Eigenschaften. // Angewandte Chemie. 1989. v. 101. № 3. pp. 261-276.

27.   Rehahn M., Schlüter A. D., Wegner G. Pd-catalyzed polycondensation of aromatic monomers with functional groups. // Makromolekulare Chemie. Rapid Communications. 1990. v. 11. № 11. pp. 535-539.

28.   Limbach H.J., Sayar M., Holm C. Polyelectrolyte bundles // J. Phys.: Cond. Matter 2004. v. 16. pp. 2135-2144.

29.   Rau I. U., Rehahn M. Towards rigid-rod polyelectrolytes via well-defined precursor poly(paraphenylene)s substituted by 6-iodohexyl side chains. // Acta Polymerica. 1994. v. 45. № 1. pp. 3-13.

30.   Kötz J., Kosmella S., Beitz T. Self-assembled polyelectrolyte systems. // Prog. Polym. Sci. 2001. v. 26. pp. 1199-1232.

31.   Nakamura K., Hatakeyama T., Hatakeyama H. Formation of the Glassy State and Mesophase in the Water–Sodium Alginate System. // Polymer J. 1991. v. 23. № 4. pp. 253-258.

32.   Hatakeyama T., Yoshida H., Hatakeyama H. A differential scanning calorimetry study of the phase transition of the water-sodium cellulose sulphate system. // Polymer. 1987. v. 28. № 8. pp. 1282-1286.

33.   Wittmer J., Joanny J. F. Charged diblock copolymers at interfaces. // Macromolecules. 1993. v. 26. № 11. pp. 2691-2697.

34.   Forster S., Hermsdorf N., Leube W., Schnablegger H., Regenbrecht M., Akari S., Lindner P., Bottcher C. Fusion of Charged Block Copolymer Micelles into Toroid Networks. // J. Phys. Chem. B. 1999. v. 103. № 32. pp. 6657-6668.

35.   Shen H., Zhang L., Eisenberg A. Multiple pH-Induced Morphological Changes in Aggregates of Polystyrene-*block*-poly(4-vinylpyridine) in DMF/H_2O Mixtures. // J. Am. Chem. Soc. 1999. v. 121. № 12. pp. 2728-2740.

36.   Netz R. R. Micellar morphologies of charged diblock-copolymers. // Europhys. Lett. 1999. v. 47. № 3. pp. 391-397.

37.   Sinquin A., Hubert P., Dellacherie E. Amphiphilic derivatives of alginate: evidence for intra- and intermolecular hydrophobic associations in aqueous solution. // Langmuir. 1993. v. 9. № 12. pp. 3334-3337.

38.   Glass J. E. Polymers in aqueous media performance through association. Washington, DC: American Chemical Society. 1989.

39.   Hansson P., Almgren M. Interaction of C_nTAB with Sodium (Carboxy-methyl)cellulose: Effect of Polyion Linear Charge Density on Binding Isotherms and Surfactant Aggregation Number. // J. Phys. Chem. 1996. v. 100. № 21. pp. 9038-9046.

40.   Malovikova A., Hayakawa K, Kwak J. C. T. Surfactant-polyelectrolyte interactions. 4. Surfactant chain length dependence of the binding of alkylpyridinium cations to dextran sulfate. // J. Phys. Chem. 1984. v. 88. № 10. pp. 1930-1933.

41.   de Gennes P.G. Scaling concepts in polymer physics. Cornell University Press, Ithaca, 1979.

42.   Barrat J.-L., Joanny J.-F. Theory of polyelectrolyte solutions. // Advances in Chemical Physics. 1996. v. 54, pp. 1-78.

43.   Manning G. S. // J. Chem.. Phys. 1969. v. 51. pp. 954.

44.   Odijk T., houwaart A.C. // J. Polym. Sci. 1978. v. 16. pp. 627.

45.   Kuhn W., Künzle O., Katchalsky A. Verhalter polyvalenter Fadenmolukülionen in Lösung. // Helv. Chim. Acta. 1994. v. 31. pp. 1994-2037.

46.   Khokhlov A.R. // J. Phys. A. 1980. v. 13. p. 979.

47.   Jonsson B., Peterson T., Soderberg B. // J. Phys. Chem. 1994. v. 99. pp. 1251.

48.   Bouchaud J.-P., Mézard M., Parisi G., Yedidia J.S. // J. Phys. A 1992. v. 24. p. L1025.

49.   Fuoss R.M., Katchalsky A., Lifson S. // Proc. Natl. Acad. Sci. USA. 1951. v. 37. p. 579.

50.   Zherenkova L.V., Khalatur P.G., Khokhlov A.R. Solution properties of charged quasi-random copolymers: Integral equation theory. // J. Chem. Phys. 2003. v. 119. №13. pp.6959-6972.

51.   Freed K.F. Renormalization Group Theory of Macromolecules. New York: Wiley, 1987.

52.   Shirvanyanz D. G., Khalatur P. G. Computer simulation of polymers. - Tver, 2000. – 156 p.

53.   Verdier P. H., Stockmayer W. H. Monte Carlo Calculations on the Dynamics of Polymers in Dilute Solution // J. Chem. Phys. 1962. v. 36. № 1. pp. 227-235.

54.   Baumgärtner A. Simulations of polymer models // Application of the Monte Carlo method in statistical physics/ (Ed. K. Binder). – N.Y.: Springer Verlag, 1984. pp. 145.

55.   Shaffler J. S. Effects of chain topology on polymer dynamics: Bulk melts. // J. Chem. Phys. 1994. v. 101. № 5. pp. 4205-4213.

56.   Khalatur P. G., Shirvanyanz D. G., Starovoitova N. Yu., Khokhlov A. R. Conformational properties and dynamics of molecular bottle-brushes: a cellular-automation-based simulation // Macromol. Theory Simul. 2000. v. 9. № 3. pp. 141-155.

57.   Flory P.J. Statistical Mechanics of Chain Molecules. New York, Interscience, 1969.

58.   Kratky O., Porod G. Röntgenuntersuchungen gelöster Fadenmoleküle. // Recueil Trav. Chim. Pays-Bas. 1949. v. 68. pp. 1106-1122.

59.   Skolnick J., Fixman M. Electrostatic Persistence Length of a Wormlike Polyelectrolyte. // Macromolecules. 1977. v. 10. № 5. pp. 944-948.

60.   Odijk T. J. Polyelectrolytes near the rod limit // Polym. Sci. Polym. Phys. Ed. 1977. v. 15. № 3. pp. 477-483.

61.   Rapaport D C. The Art of Molecular Dynamics Simulation. Cambridge, 2004.

62.   McQuarrie D., Statistical Mechanics. -New York: Harper Collins, 1976. – 640 p.

63.   Hünenberger P. H., McCammon J. A. Ewald artifacts in computer simulations of ionic solvation and ion–ion interaction: A continuum electrostatics study. // J. Chem. Phys. 1999. v. 110. № 4. pp. 1856-1872.

64.   Allen M. P., Tildesley D. J. Computer simulation of liquids. – Oxford: Clarendon Press, 1987.

65.   Smith A. E. R., Perram J. W. Periodic boundary conditions and dipolar interactions in statistical mechanics. // Physics Letters A. 1975. v. 53. № 2. pp. 121-123.

66.   Heyes D. M. Electrostatic potentials and fields in infinite point charge lattices. // J. Chem. Phys. 1981. v. 74. № 3. pp. 1924-1929.

67.   Eastwood J. W., Hockney R. W., Lawrence D. N. P3M3DP — The three-dimensional periodic particle-particle/ particle-mesh program. // Computer Physics Communications. 1980. v. 19. № 2. pp. 215-261.

68.   Leach A.R. Molecular Modelling: Principles and Applications. 2001.

69.   Onsager L. Electric Moments of Molecules in Liquids. // J. Am. Chem. Soc. 1936. v. 58. № 8. pp. 1486-1493.

70.   Verlet L. Computer "Experiments" on Classical Fluids. I. Thermodynamical Properties of Lennard-Jones Molecules. // Phys. Rev. 1967. v. 159. № 1. pp. 98-114.

71.   Hockney R.W., Eastwood J.W. Computer Simulation Using Particles. Adam Hilger, Philadelphia, 1988.

72.   Kriksin Yu. A., Khalatur P. G., Khokhlov A. R. Reconstruction of Protein-Like Globular Structure for Random and Designed Copolymers. // Macromolecular Theory and Simulations. 2002. v. 11. № 2. pp. 213-221.

73.   Kabanov A.V., Bronich T.K., Kabanov V.A., Eisenberg Yu.K. Spontaneous Formation of Vesicles from Complexes of Block Ionomers and Surfactants // J. Am. Chem. Soc. 1998. v. 120. № 38. pp. 9941-9942.

74.   Kabanov V.A. In Macromolecular Complexes in Chemistry and Biology: Dubin P.L., Eds.: Springer – Verlag: New York; 1994. p. 151.

75.   Felgner P.L., Gadek T.R., Holm M., Roman R., Chan H.W., Wenz M., Northrop J.P., Ringold G.M., Danielsen M. Lipofection: A Highly Efficient, Lipid-Mediated DNA-Transfection Procedure // Proc. Natl. Acad. Sci. USA. 1987. v. 84. № 21. pp. 7413-7417.

76.   Starodoubtsev S. G., Yoshikawa K. Intrachain Segregation in single giant DNA Mlecules indused by poly(2-vinylpyrrolidone). // J. Phys. Chem. 1996. v. 100. № 50. pp. 19702-19705.

77.   Chen W., Turro N.J., Tomalia D.A. Using Ethidium Bromide To Probe the Interactions between DNA and Dendrimers // Langmuir. 1999. v. 16. № 1. pp. 15-19.

78.   Kabanov V.A., Zezin A.B., Rogacheva V.B., Gulyaeva Zh.G., Zansochova M.F., Joosten, J.G.H., Brackman J. Dendrimer-Polyelectrolyte Complexation: A Model Guest-Host System // Macromolecules. 1999. v. 32. № 6. pp. 1904-1909.

79.   Welch P., Muthukumar M. Dendrimer-Polyelectrolyte Complexation: A Model Guest-Host System // Macromolecules. 2000. v. 33. № 16. pp. 6159-6167.

80.   Gossl I., Shu L., Schluter A.D., Rabe J.P. Molecular Structure of Single DNA Complexes with Positively Charged Dendronized Polymers // J. Am. Chem. Soc. 2002. v. 124. № 24. pp. 6860-6865.

81.   Stevens M., Kremer K. The nature of flexible linear polyelectrolytes in salt free solution: A molecular dynamics study // J. Chem. Phys. 1995. v. 103. № 4. P. 1669-1690.

82.   Stigter D. Evaluation of the counterion condensation theory of polyelectrolytes// Biophys J. 1995. v. 69. № 2. pp. 380-388.

83.   Winkler R. Universal properties of complexes formed by two oppositely charged flexible polyelectrolytes // New J. Phys. 2004. v. 6. pp. 11.

84.   Srivastava D. Muthukumar M. Interpenetration of Interacting Polyelectrolytes // Macromolecules. 1994. v. 27. № 6. pp. 1461-1465.

85. Imbert J.B., Victor J., Tsunekawa N., Hiwatari Y. Conformational transitions of a diblock polyampholyte in 2 and 3 dimensions // Phys. Lett. A. 1999. v. 258. № 2-3. pp. 92-98.

86. Hayashi Y., Magnus U., Linse P. A Monte Carlo study of solutions of oppositely charged polyelectrolytes // J. Chem. Phys. 2002. v. 116. № 15. pp. 6836-6845.

87. Dias R.S., Pais A.A.C.C., Miguel M.G., Lindman B. Modeling of DNA compaction by polycations // J. Chem. Phys. 2003. v. 119. № 15. pp. 8150-8157.

88. Lyubartsev A.P., Nordenskiöld N. Monte Carlo Simulation Study of DNA Polyelectrolyte Properties in the Presence of Multivalent Polyamine Ions // J. Phys. Chem. B. 1997. v. 101. № 21. pp. 4335-4342.

89. Akitaya T., Tsumoto K., Yamada A., Makita N., Kubo K., Yoshikawa K. NTP Concentration Switches Transcriptional Activity by Changing the Large-Scale Structure of DNA // Biomacromolecules. 2003. v. 4. № 5. pp. 1121-1125.

90. Yoshikawa Yu., Velichko Y.S., Ichiba Yu., Yoshikawa K. Self-assembled pearling structure of long duplex DNA with histone H1 // Eur. J. Biochemistry. 2001. v. 268. № 9. pp. 2593-2599.

91. Ueda M., Yoshikawa K. Phase Transition and Phase Segregation in a Single Double-Stranded DNA Molecule // Phys. Rev. Lett. 1996. v. 77. № 10. pp. 2133-2136.

92. Vasilevskaya V.V., Khokhlov A.R., Matsuzawa Y., Yoshikawa K. Collapse of single DNA molecule in poly(ethylene glycol) solutions // J. Chem. Phys. 1995. v. 102. № 16. pp. 6595-6602.

93. Grosberg A. Yu., Khokhlov A.R. Statistical Physics of Macromolecules. M.: Nauka, 1989.

94. Lifshitz M., Grosberg A. Y., Khokhlov A. R. Some problems of the statistical physics of polymer chains with volume interaction // Rev. Mod. Phys. 1979. v. 50. № 3. pp. 683-713.

95. Dobrynin A. V., Rubinstein M., Obukhov S. P. Cascade of Transitions of Polyelectrolytes in Poor Solvents // Macromolecules. 1996. v. 29. № 8. pp. 2974-2979.

96. Grosberg A. Yu. // Biofizika. 1979. v. 24. pp. 32-37.

97. Grosberg A. Y., Khokhlov A.R. Statistical theory of polymeric lyotropic liquid crystals // Adv. Polym. Sci. 1981. v. 41. pp. 53-97.

98. Cohen A.E., Mahadevan L. Kinks, rings, and rackets in filamentous structures // Proc. Natl. Acad. Sci. USA. 2003. v. 100. № 21. pp. 12141-12146.

99. Schnurr B., Gittes F., MacKintosh F.C. Metastable intermediates in the condensation of semiflexible polymers // Phys. Rev. E. 2002. v. 65. № 6. pp. 0619041(1-13).

100. Martemyanova J.A., Stukan M.R., Ivanov V.A., Muller M., Paul W., Binder K. Dense orientationally ordered states of a single semiflexible macromolecule: An expanded ensemble Monte Carlo simulation // J. Chem. Phys. 2005. v. 122. pp. 174907(1-10).

101. Bloomfield V. A. DNA condensation. // Curr. Opin. Struct. Biol. 1996. v. 6. № 3. pp. 334-341.

102. Lambert O., Letellier L., Gelbart W.M., Rigaud J.-L. DNA delivery by phage as a new strategy for encapsulating toroidal condensates of arbitrary size into liposomes. // Proc. Natl. Acad. Sci. USA. 2000. v. 97. № 13. pp. 7248-7253.

103. Lin Z., Wang C., Feng X., Liu M., Li J., Bai C. The observation of the local ordering characteristics of spermidine-condensed DNA: atomic force microscopy and polarizing microscopy studies // Nucleic Acids Res. 1998. v. 26. № 13. pp. 3228-3234.

104. Fang Y., Hoh J. H. Surface-directed DNA condensation in the absence of soluble multivalent cations // Nucleic Acids Res. 1998. v. 26. № 2. pp. 588-593.

105. Ubbink J., Odijk T. Polymer- and salt-induced toroids of hexagonal DNA. // Biophys. J. 1995. v. 68. № 1. pp. 54-61.

106. Ubbink J., Odijk T. Deformation of toroidal DNA condensates under surface stress // Europhys. Lett. 1996. v. 33. № 5. pp. 353-358.

107. Park S.Y., Harries D., Gelbart W.M. Topological Defects and the Optimum Size of DNA Condensates // Biophys. J. 1998. v. 75. № 2. pp. 714-720.

108. Vasilevskaya V.V., Khokhlov A.R, Kidoaki S., Yoshikawa K. Structure of collapsed persistent macromolecule: Toroid vs. spherical globule // Biopolymers. 1997. v. 41. № 1. pp. 51-60.

109. Miller I.C.B., Keentok M., Pereira G.G., Williams D.R.M. Semiflexible polymer condensates in poor solvents: Toroid versus spherical geometries // Phys. Rev. E. 2005. v. 71. pp. 031802 (1-9).

110. Noguchi H., Yoshikawa K. Morphological variation in a collapsed single homopolymer chain // J. Chem. Phys. 1998. v. 109. № 12. pp. 5070-5077.

111. Stevens M.J. Simple Simulations of DNA Condensation // Biophys. Soc. 2001. v. 80. № 1. pp. 130-139.

112.   Stukan M.R, Ivanov V.A, Grosberg A.Y, Paul W., Binder K. Chain length dependence of the state diagram of a single stiff-chain macromolecule: Theory and Monte Carlo simulation // J. Chem. Phys. 2003. v. 118. № 7. pp. 3392-3400.

113.   Conwell C.C., Vilfan I.D., Hud N.V. Controlling the size of nanoscale toroidal DNA condensates with static curvature and ionic strength // Proc. Natl. Acad. Sci. USA. 2003. v. 100. № 16. pp. 9296-9301.

114.   Cherstvy A.G. Structure of DNA toroids and electrostatic attraction of DNA duplexes // J. Phys.: Cond. Matt. 2005. v. 17. № 8. pp. 1363-1374.

115.   Yoshikawa K., Takahashi M., Vasilevskaya V.V., Khokhlov A.R. Large Discrete Transition in a Single DNA Molecule Appears Continuous in the Ensemble // Phys. Rev. Lett. 1996. v. 76. № 16. pp. 3029-3031.

116.   Arscott P.G., Li A.Z., Bloomfield V.A. Condensation of DNA by trivalent cations. 1. Effects of DNA length and topology on the size and shape of condensed particles // Biopolymers. 1990. v. 30. № 5-6. pp. 619-630.

117.   Golan R., Pietrasanta L.I., Hsieh W., Hansma H.G. DNA Toroids: Stages in Condensation // Biochemistry. 1999. v. 38. № 42. pp. 14069-14076.

118.   Laemmli U.K. Characterization of DNA Condensates Induced by Poly(ethylene oxide) and Polylysine // Proc. Natl. Acad. Sci. USA. 1975. v. 72. № 11. pp. 4288-4292.

119.   Inman R.B. Some factors affecting electron microscopic length of deoxyribonucleic acid // J. Mol. Biol. 1967. v. 25. № 2. pp. 209-214.

120.   Blessing T., Remy J.S., Behr J.P. Monomolecular collapse of plasmid DNA into stable virus-like particles // Proc. Natl. Acad. Sci. USA. 1998. v. 95. № 4. pp. 1427-1431.

121.   Sitko J.C., Mateescu E.M., Hansma H.G. Sequence-Dependent DNA Condensation and the Electrostatic Zipper // Biophysical J. 2003. v. 84. № 1. pp. 419-431.

122.   Maurstad G., Danielsen S., Stokke B. T. Analysis of compacted semiflexible polyanions visualized by atomic force microscopy: influence of chain stiffness on the morphologies of polyelectrolyte complexes. // J. Phys. Chem B. 2003. v. 107. № 32. pp. 8172-8180.

123.   Khalatur P.G. // Vysokomol. soed. A. 1980. v. 22. № 9. pp. 2050-2057.

124.   Khalatur P.G. // Vysokomol. soed. A. 1980. v. 22. № 10. pp. 2226-2233.

125.   Danielsen S., Varum K.M., Stokke B.T. Structural Analysis of Chitosan Mediated DNA Condensation by AFM: Influence of Chitosan Molecular Parameters // Biomacromolecules. 2004. v. 5. № 3. pp. 928-936.

126. Maurstad G., Stokke B.T. Metastable and stable states of xanthan polyelectrolyte complexes studied by atomic force microscopy // Biopolymers. 2004. v. 74. № 3. pp. 199-213.

127. Darden T. A., York D. M., Pedersen L. G. Particle mesh Ewald: An $N\cdot\log(N)$ method for Ewald sums in large systems // J. Chem. Phys. 1993. v. 98. № 12. pp. 10089-10092.

128. Essmann U., Perera L., Berkowitz M.L., Darden T., Lee H., Pedersen L.G. A smooth particle mesh Ewald method // J. Chem. Phys. 1995. v. 103. № 19. pp. 8577-8593.

129. Khalatur P. G., Khokhlov A. R., Mologin D. A., Reineker P. Aggregation and counterion condensation in solution of charged proteinlike copolymers: A molecular-dynamics study // J. Chem. Phys. 2003. v. 119. № 2. pp. 1232-1247.

130. Mologin D. A., Khalatur P. G., Khokhlov A. R., Reineker P. Charged designed copolymers in the presence of multivalent counterions: a molecular dynamics study // New J. Phys. 2004. v. 6. pp. 133 (1-21).

131. Smith S.B., Bendich A.J. Electrophoretic charge density and persistence length of DNA as measured by fluorescence microscopy // Biopolymers. 1990. v. 29. № 8-9. pp. 1167-1173.

132. Kuhn H. Restricted Bond Rotation and Shape of Unbranched Saturated Hydrocarbon Chain Molecules // J. Chem. Phys. 1947. v. 15. № 11. pp. 843-844.

133. Doi M., Edwards S.F. The Theory of Polymer Dynamics; Oxford University Press, Oxford, 1986.

134. Wesson L., Eisenberg D. Atomic solvation parameters applied to molecular dynamics of proteins in solution // Protein Sci. 1992. v. 1. № 2. pp. 227-235.

135. Augspurger J.D., Scheraga H.A. An efficient, differentiable hydration potential for peptides and proteins // J. Comput. Chem. 1996. v. 17. № 13. pp. 1549-1558.

136. Khalatur P. G., Novikov V. V., Khokhlov A. R. Conformation-dependent evolution of copolymer sequences // Phys. Rev. E 2003. v. 67. № 5. pp. 051901 (1-10).

137. Andersen H. C. Rattle: A "velocity" version of the shake algorithm for molecular dynamics calculations // J. Comput. Phys. 1983. v. 52. № 1. pp. 24-34.

138. Takahashi M., Yoshikawa K., Vasilevskaya V. V., Khokhlov A. R. Discrete Coil-Globule Transition of Single Duplex DNAs Induced by Polyamines // J. Phys. Chem. B 1997. V. 101. № 45. pp. 9396-9401.

139. Shen H., Zhang L., Eisenberg A. Multiple pH-Induced Morphological Changes in Aggregates of Polystyrene-*block*-poly(4-vinylpyridine) in DMF/H_2O Mixtures. // J. Am. Chem. Soc. 1999. v. 121. № 12. pp. 2728-2740.

140. Cölfen H. Double-Hydrophilic Block Copolymers: Synthesis and Application as Novel Surfactants and Crystal Growth Modifiers // Macromol. Rapid Commun. 2001. v. 22. № 4. pp. 219-252.

141. Konradi R., Zhang H., Biesalski M., Rühe J. Weak Polyelectrolyte Brushes: Complex Formation and Multilayer Build-up with Oppositely Charged Polyelectrolytes. In: Polymer Brushes, Eds., Advincula R. C., Brittain W. J., Caster K. C., Rühe J. Wiley-VCH Verlag, Weinheim, 2005.

142. Seymour L. W., Kataoka K., Kabanov A. v. Cationic Block Copolymers as Self-Assembling Vectors for Gene Delivery, In: Self Assembling Complexes for Gene Delivery: From Laboratory to Clinical Trial; A. v. Kabanov, P. L. Felgner, L. W. Seymour, Eds., John Wiley & Sons, Chichester, New York, Weinheim, Brisbane, Singapore, Toronto 1998, p. 219.

143. Lemieux P., Vinogradov S. V., Gebhart C. L., Guerin N., Paradis G., Nguyen H., Ochietti K. B., Suzdaltseva Y. G., Bartakova E. V., Bronich T. K., St-Pierre Y., Alakhov V. Y., Kabanov A. v. Block and Graft Copolymers and Nanogel™ Copolymer Networks for DNA Delivery into Cell // J. Drug Target. 2000. v. 8. № 2. pp. 91-105.

144. Yu S. H., Cölfen H. Bio-inspired crystal morphogenesis by hydrophilic polymers // J. Mater. Chem. 2004. v. 14. № 5. pp. 2124-2147.

145. Sidorov S. N., Bronstein L. M., Valetsky P. M., Hartmann J., Cölfen H. Stabilization of Metal Nanoparticles in Aqueous Medium by Polyethyleneoxide–Polyethyleneimine Block Copolymers // J. Colloid&Interf. Sci. 1999. v. 212. № 2. pp. 197-211.

146. McKnight W. J., Ponomarenko E. A., Tirrell D. A. Self-Assembled Polyelectrolyte-Surfactant Complexes in Nonaqueous Solvents and in the Solid State // Acc. Chem. Res. 1998. v. 31. № 12. pp. 781-788.

147. Zezin A. B., Rogacheva V. B., Novoskoltseva O. A., Kabanov V. A. Self-assembly in ternary systems: cross-linked polyelectrolyte, linear polyelectrolyte and surfactant // Macromol. Symp. 2004. v. 211. № 1. pp. 157-174.

148. Ponomarenko E. A., Waddon A. J., Bakeev K. N., Tirrell D. A., MacKnight W. J. Self-Assembled Complexes of Synthetic Polypeptides and Oppositely Charged Low Molecular Weight Surfactants. Solid-State Properties // Macromolecules. 1996. v. 29. № 12. pp. 4340-4345.

149.	Guillot S., McLoughlin D., Jain N., Delsanti M., Langevin D. Polyelectrolyte-surfactant complexes at interfaces and in bulk // J. Phys.: Condens. Matter. 2003. v. 15. № 1. pp. 219-224.

150.	Sokolov E., Yeh F., Khokhlov A.R., Grinberg V. Ya., Chu B. Nanostructure Formation in Polyelectrolyte-Surfactant Complexes // J. Phys. Chem. B. 1998. v. 102. № 37. pp. 7091-7098.

151.	Zhou S., Yeh F., Burger C., Hu H., Liu T., Chu B. SAXS study on complexes formed by anionic poly(sodium methacrylate-co-N-isopropylacrylamide) gels with cationic surfactants // Polym. Adv. Technol. 2000. v. 11. № 5. pp. 235-241.

152.	Ikkala O., Ruokolainen J., ten Brinke G., Torkkeli M., Serimaa R. Mesomorphic State of Poly(vinylpyridine)-Dodecylbenzenesulfonic Acid Complexes in Bulk and in Xylene Solution // Macromolecules. 1995. v. 28. № 21. pp. 7088-7094.

153.	Akiba I., Masunaga H., Sasaki K., Jeong Y., Sakurai K. Phase Behavior of Hydrogen-Bonded Polymer-Surfactant Mixtures in Selective Solvent // Macromolecules. 2004. v. 37. № 26. pp. 10047-10051.

154.	Bakeev K. N., Shu Y. M., Zezin A. B., Kabanov V. A., Lezov A. V., Mel'nikov A. B., Kolomiets I. P., Rjumtsev E. I., MacKnight W. J. Structure and Properties of Polyelectrolyte-Surfactant Nonstoichiometric Complexes in Low-Polarity Solvents // Macromolecules. 1996. v. 29. № 4. pp. 1320-1325.

155.	Holm C., Joanny J.P., Kremer K., Netz R.R., Reineker P., Seidel C., Vilgis T.A., Winkler R.G. Polyelectrolyte theory // Adv. Polym. Sci. 2004. v. 166. pp. 67-111.

156.	Khokhlov A. R., Khalatur P. G. Solution properties of charged hydrophobic/hydrophilic copolymers // Curr. Opin. Colloid Interface Sci. 2005. v. 10. № 1-2. pp. 22-29.

157.	Harada A., Kataoka K. Formation of Polyion Complex Micelles in an Aqueous Milieu from a Pair of Oppositely-Charged Block Copolymers with Poly(ethylene glycol) Segments // Macromolecules. 1995. v. 28. № 15. pp. 5294-5299.

158.	Kabanov A. V., Vinogradov S. V., Suzdaltseva Y. G., Alakhov V. Y. Water-Soluble Block Polycations as Carriers for Oligonucleotide Delivery // Bioconjug. Chem. 1995. V. 6. № 6. pp. 639-643.

159.   Kabanov A. V., Bronich T. K., Kabanov V. A., Yu K., Eisenberg A. Soluble Stoichiometric Complexes from Poly(*N*-ethyl-4-vinylpyridinium) Cations and Poly(ethylene oxide)-*block*-polymethacrylate Anions // Macromolecules. 1996. v. 29. № 21. pp. 6797-6802.

160.   Kataoka K., Togawa H., Harda A., Yasugi K., Matsumoto T., Katayose S. Spontaneous Formation of Polyion Complex Micelles with Narrow Distribution from Antisense Oligonucleotide and Cationic Block Copolymer in Physiological Saline // Macromolecules. 1996. v. 29. № 26. pp. 8556-8557.

161.   Kramarenko E.Yu., Khokhlov A.R., Reineker P. Micelle formation in a dilute solution of block copolymers with a polyelectrolyte block complexed with oppositely charged linear chains // J. Chem. Phys. 2003. v. 119. № 9. pp. 4945-4952.

162.   Groot R.D. Mesoscopic Simulation of Polymer-Surfactant Aggregation // Langmuir. 2000. v. 16. №19. pp. 7493-7502.

163.   von Ferber C., Lowen H. Complexes of polyelectrolytes and oppositely charged ionic surfactants // J. Chem. Phys. 2003. v. 118. № 23. pp. 10774-10779.

164.   von Ferber C., Lowen H. Polyelectrolyte–surfactant complex: phases of self-assembled structures // Faraday Discuss. 2005. v. 128. pp. 389-405.

165.   Laguecir A., Stoll S., Kirton G., Dubin P. L. Interactions of a Polyanion with a Cationic Micelle: Comparison of Monte Carlo Simulations with Experiment // J. Phys. Chem. B. 2003. v. 107. № 32. pp. 8056-8065.

166.   Zanuy D., Alemán C. Molecular Dynamics Simulations of Surfactant·Poly(α,L-glutamate) Complexes in Chloroform Solution: Influence of the Chemical Constitution of the Surfactant in the Molecular Organization // Langmuir. 2003. v. 19. № 9. pp. 3987-3995.

167.   Molnar F., Rieger J. "Like-Charge Attraction" between Anionic Polyelectrolytes: Molecular Dynamics Simulations // Langmuir. 2005. v. 21. № 2. pp. 786-789.

168.   Shusharina N.P., Saphonov M.V., Nyrkova I.A., Khalatur P.G., Khokhlov A.R. The Critical Micelle Concentration for the Solution of Polyelectrolyte/Neutral Block-Copolymers // Ber. Bunsenges. Phys. Chem. 1996. v. 100. pp. 857.

169.   ten Brinke G., Ikkala O. Ordered structures of molecular bottlebrushes // Trends Polym. Sci. 1997. v. 5. № 7. pp. 213-217.

170.   Ruokolainen J., ten Brinke G., Ikkala O., Torkkeli M., Serimaa R. Mesomorphic Structures in Flexible Polymer-Surfactant Systems Due to Hydrogen Bonding: Poly(4-vinylpyridine)-Pentadecylphenol // Macromolecules 1996. v. 29 № 10. pp. 3409-3415.

171.   Stepanyan R., Subbotin A., ten Brinke G. Strongly adsorbed comb copolymers with rigid side chains // Phys. Rev. E: Stat. Phys., Plasmas, Fluids, Relat. Interdiscip. Top. 2001. v. 63. № 6. pp. 061805(1-9).

172.   Kramarenko E. Yu., Pevnaya O. S., Khokhlov A. R. Stoichiometric polyelectrolyte complexes as comb copolymers // J. Chem. Phys. 2005. v. 122. pp. 084902 (1-10).

173.   Komarov P. V., Zherenkova L. V., Khalatur P. G. Ribbonlike nanostructures from stiff polyanions and short cationic chains // Chem. Phys. Lett. 2006. v. 420. № 1-3. pp. 29-34.

174.   Komarov P. V., Zherenkova L. V., Khalatur P. G., Reineker P. The formation of planar ribbonlike aggregates from stiff polyanions in the presence of anisotropic cations // J. Chem. Phys. 2006. v. 125. pp. 154906 (1-11).

175.   Winkler R.G., Steinhauser M.O., Reineker P. Complex formation in systems of oppositely charged polyelectrolytes: A molecular dynamics simulation study // Phys. Rev. E. 2002. v. 66. № 2. pp. 021802 (1-7).

176.   Schulz S.F., Maier E. E., Weber R. Light scattering studies on solutions of charged rod-like fd-virus at very low ionic strength // J. Chem. Phys. 1989. v. 90. № 1. pp. 7-10.

177.   Maier E. E., Schulz S. F., Weber R. Static Light Scattering Studies of Suspensions of Charged Rodlike Tobacco Mosaic Virus // Macromolecules. 1988. v. 21. № 5. pp. 1544-1546.

178.   Jeon J., Dobrynin, A.V. Monte Carlo simulations of polyampholyte-polyelectrolyte complexes: Effect of charge sequence and strength of electrostatic interactions // Phys. Rev. E 2003. v. 67. № 6. pp. 061803 (1-15).

179.   Winkler R. G.; Gold M.; Reineker P. Collapse of Polyelectrolyte Macromolecules by Counterion Condensation and Ion Pair Formation: A Molecular Dynamics Simulation Study // Phys. Rev. Lett. 1998. v. 80. № 17. pp. 3731-3734.

180.   Zherenkova L. V., Khalatur P. G., Yoshikawa K. Self-Consistent Integral Equation Theory for Semiflexible Polyelectrolytes in Poor Solvent // Macromol. Theory Simul. 2003. v. 12. № 5. pp. 339-353.

181.   Fredrickson G. H. Surfactant-induced lyotropic behavior of flexible polymer solutions // Macromolecules. 1993. v. 26. № 11. pp. 2825-2831.

182.   Kato T., Frechet J.M.J. Stabilization of a liquid-crystalline phase through noncovalent interaction with a polymer side chain // Macromolecules. 1989. v. 22. № 9. pp. 3818-3819.

183.   Drummond R.K., Klier J., Alameda J.A., Peppas N.A. Preparation of Poly(methacrylic acid-g-ethylene oxide) Microspheres // Macromolecules. 1989. v. 22. № 9. pp. 3816-3818.

184. Gohy J.-F., Varshney S. K., Jérôme R. Morphology of Water-Soluble Interpolyelectro-lyte Complexes Formed by Poly(2-vinylpyridinium)-*block*-poly(ethylene oxide) Diblocks and Poly(4-styrenesulfonate) Polyanions // Macromolecules. 2001. v. 34. № 9. pp. 2745-2747.

185. Zhang L., Eisenberg A. Multiple Morphologies of "Crew-Cut" Aggregates of Polysty-rene-b-poly(acrylic acid) Block Copolymers // Science. 1995. v. 268. pp. 1728-1731.

186. Wolfert M.A., Schacht E.H., Toncheva V., Ulbrich K., Nazarova O., Seymour L.W. Characterization of vectors for gene therapy formed by self-assembly of DNA with synthetic block co-polymers // Hum. Gene Therapy. 1996. v. 7. № 17. pp. 2123-2133.

187. Djalali R., Li S.Y., Schmidt M. Amphipolar Core-Shell Cylindrical Brusches as Tem-plates for the Formation of Gold Clusters and Nanowires. // Macromol. 2003. v. 35. № 11. pp. 4282-4288.

188. Angelini T.E., Sanders L.K., Liang H., Wriggert W., Tang J.X., Wong G.C.L. Structure and dynamics of condensed multivalent ions within polyelectrolyte bundles: a combined x-ray diffraction and solid-state NMR study // J. Phys.: Condens. Matter. 2005. v. 17. № 14. pp. 1123-1137.

189. Sayar M., Stupp S.I. Assembly of one-dimensional supramolecular objects: From monomers to networks // Phys. Rev. E. 2005. v. 72. pp. 011803 (1-7).

190. Gardel M.L., Shin J.H., MacKintosh F.C., Mahadevan L., Matsudaria P., Weitz D.A. Elastic behavior of Cross-Linked and Bundled Actin Networks // Science. 2004. v. 304. pp. 1301-1305.

191. Deng H., Bloomfield V.A. Structural Effects of Cobalt-Amine Compounds on DNA Condensation // Biophys. J. 1999. v. 77. № 3. pp. 1556-1561.

192. McLoughlin D., Delsanti M., Tribet C., Langevin D. DNA bundle formation induced by cationic surfactants // Europhys. Lett. 2005. v. 69. № 3. pp. 461-468.

193. Tang J.X., Ito T., Tao T., Traub P., Janmey P.A. Opposite Effects of Electrostatics and Steric Exclusion on Bundle Formation by F-Actin and Other Filamentous Polyelectrolytes // Biochemistry. 1997. v. 36. № 41. pp. 12600-12607.

194. Bartles J. R. Parallel actin bundles and their multiple actin-bundling proteins. // Curr. Opin. Cell Biol. 2002. v. 12. № 1. pp. 72-78.

195. Hüttelmaier S., Harbeck B., Steffens N.O., Meßerschmidt T., Illenberger S., Jockusch B.M. Characterization of the actin binding properties of the vasodilator-stimulated phospho-protein VASP. // FEBS Letters. 1999. v. 451. № 1. pp. 68-74.

196.   Tang J. X, Szymanski P. T., Janmey P. A., Tao T. Electrostatic Effects of Smooth Muscle Calponin on Actin Assembly. // Eur. J. Biochem. 1997. v. 247. № 1. pp. 432-440.

197.   Maurstad G., Stokke B.T. Toroids of stiff polyelectrolytes // Curr. Opin. Coll.&Interf. Sci. 2005. v. 10. № 1-2. pp. 16-21.

198.   Ha B.-Y., Liu A.J. Counterion-mediated, non-pairwise-additive attractions in bundles of like-charged rods // Phys. Rev. E. 1999. v. 60. № 1. pp. 803-813.

199.   Oosawa F. Polyelectrolytes; Marcel Dekker Inc.: New York, 1971.

200.   Oosawa F. A theory on the effect of low molecular salts on the dissociation of linear polyacids // Biopolymers. 1968. v. 6. № 1. pp. 135-144.

201.   Israelachvili J. Intremolecular and surface forces. London: Academic. 1992.

202.   Le Bret M., Zimm B. H. Distribution of counterions around a cylindrical polyelectrolyte and Manning's condensation theory. // Biopolymers. 1984. v. 23. № 2. pp. 287-312.

203.   Kirkwood J. G., Shumaker J. B. Forces between Protein Molecules in Solution Arising from Fluctuations in Proton Charge and Configuration // Proc. Natl Acad. Sci. USA. v. 38. № 10. pp. 863-871.

204.   Borukhov I., Lee K.-C., Bruinsma R. F., Gelbart W.M., Liu A. J., Stevens M. J. Association of two semiflexible polyelectrolytes by interchain linkers: theory and simulations. // J. Chem. Phys. 2002. v. 117. № 1. pp. 462-480.

205.   Bloomfield V.A. Condensation of DNA by multivalent cations: considerations on mechanism. // Biopolymers. 1991. v. 31. № 13. pp. 1471-1481.

206.   Tang J.X., Wong S.E., Tran P.T., Janmey P.A. Counterion induced bundle formation of rodlike polyelectrolytes. // Berichte der Bunsen Gesellschaft – Physical Chemistry, Chemical Physics. 1996. v. 100. № 6. pp. 796-806.

207.   Ohnishi T., Imai N., Oosawa F. Interaction between Rod-like Polyelectrolytes // J. Phys. Soc. Jpn. 1960. v. 15. № 5. pp. 896-905.

208.   Patey G.N. The interaction of two spherical colloidal particles in electrolyte solution. An application of the hypernetted-chain approximation // J. Chem. Phys. 1980. v. 72. № 10. pp. 5763-5771.

209.   Kjellander R., Marcelja S. Correlation and image charge effects in electric double layer // Chem. Phys. Lett. 1984. v. 112. № 1. pp. 49-53.

210.   Marcelija S. Electrostatics of membrane adhesion // Biophys. J. 1992. v. 61. № 5. pp. 1117-1121.

211. Rouzina I., Bloomfield V.A. Macroion attraction due to electrostatic correlation between screening counterions. I: mobile surface-adsorbed ions and diffuse ion cloud // J. Phys. Chem. 1996. v. 100. № 23. pp. 9977-9989.

212. Grønbech-Jensen N., Mashl R.J., Bruinsma R.F., Gelbart W.M. Counterion-Induced Attraction between Rigid Polyelectrolytes // Phys. Rev. Lett. 1997. v. 78. № 12. pp. 2477-2480.

213. Shklovskii B.I. Screening of a macroion by multivalent ions: Correlation-induced inversion of charge // Phys. Rev. E 1999. v. 60. № 5. pp. 5802-5811.

214. Arenzon J.J., Levin Y., Stilck J.F. The mean-field theory for attraction between like-charged macromolecules // Physica A. 2000. v. 283. № 1-2. pp. 1-5.

215. Korynshev A.A., Leikin S. Theory of interaction between helical molecules // J. Chem. Phys. 1996. v. 107. № 9. pp. 3656-3674.

216. Barrat J.L., Joanny J.F. Theory of polyelectrolyte solutions // Adv. Chem. Phys. 1996. v. 94. pp. 45-66.

217. Ha B.-Y., Liu A.J. Effect of Non-Pairwise-Additive Interactions on Bundles of Rodlike Polyelectrolytes // Phys. Rev. Lett. 1998. v. 81. № 5. pp. 1011-1014.

218. Ha B.-Y., Liu A.J. Physical Questions Posed by DNA Condensation. In: Physical chemistry of polyelectrolytes. (Ed. by Radeva T.) New York : Marcel Dekker, 2001. pp. 163-180.

219. Ray J., Manning G.S. An attractive force between two rodlike polyions mediated by the sharing of condensed counterions // Langmuir 1994. v. 10. № 7. pp. 2450-2461.

220. Marquet R., Houssier C. Thermodynamics of cation-induced DNA condensation // J. Biomol. Struct. Dynam. 1991. v. 9. № 1. pp. 159-167.

221. Rau D.C., Parsegian V.A. Direct measurement of forces between linear polysaccharides xanthan and schizophyllan // Science 1990. v. 249. pp. 1278-1281.

222. Tang J.X., Wen Q., Bennett A., Kim B., Sheils C.A., Bucki R., Janmey P.A. Anionic poly(amino acid)s dissolve F-actin and DNA bundles, enhance DNase activity, and reduce the viscosity of cystic fibrosis sputum // Am. J. Physiol. Lung. Cell Mol. Physiol. 2005. v. 289. № 4. pp. 599-605.

223. Tang J.X., Janmey P.A., Lyubartsev A., Nordenskiöld L. Metal Ion-Induced Lateral Aggregation of Filamentous Viruses fd and M13 // Biophys. J. 2002. v. 83. № 1. pp. 566-581.

224.   Needleman D.L., Ojeda-Lopez M.A., Raviv U., Miller H.P., Wilson L., Safinya C.R. Higher-order assembly of microtubules by counterions: From hexagonal bundles to living necklaces // Proc. Natl. Acad. Sci. 2004. v. 101. № 46. pp. 16099-16103.

225.   Kawamura M., Maruyama K. Electron Microscopic Particle Length of F-Actin Polymerized in *Vitro* // J. Biochem. 1970. v. 67. № 3. pp. 437-457.

226.   Flower W.E., Aebi U. Polymorphism of actin paracrystals induced by polylysine // J. Cell Biol. 1982. v. 93. № 2. pp. 452-458.

227.   Grant N.J., Oriol-Audit C., Dickens M.J. Supramolecular forms of actin induced by polyamines; an electron microscopic study. // Eur. J. Cell Biol. 1983. v. 30. № 1. pp. 67-73.

228.   Owen C.H., DeRosier D.J., Condeelis J. Actin crosslinking protein EF-1α of *Dictyostelium discoideum* has a unique bonding rule that allows square-packed bundles // J. Struct. Biol. 1992. v. 109. № 3. pp. 248-254.

229.   Stokes D.L., DeRosier D.J. Growth conditions control the size and order of actin bundles in vitro // Biophys J. 1991. v. 59. № 2. pp. 456-465.

230.   Yang L., Sept D., Carlsson A. E. Energetics and Dynamics of Constrained Actin Filament Bundling // Biophys. J. 2006. v. 90. № 12. pp. 4295-4304.

231.   Zilman A. G., Safran S. A. Role of cross-links in bundle formation, phase separation and gelation of long filaments // Europhys. Lett. 2003. v. 63. № 1. pp. 139-145.

232.   Stevens M.J. Bundle Binding in Polyelectrolyte Solutions // Phys. Rev. Lett. 1999. v. 82. № 1. pp.101-104.

233.   Deserno M., Arnold A., Holm C. Attraction and Ionic Correlations between Charged Stiff Polyelectrolytes // Macromolecules. 2003. v. 36. № 1. pp. 249-259.

234.   Yu X., Carlsson A.E. Kinetics of Filament Bundling with Attractive Interactions // Biophys. J. 2004. v. 87. № 6. pp. 3679-3689.

235.   Kwon H. J., Tanaka Y., Kakugo A., Shikinaka K., Furukawa H., Osada Y., Gong J. P. Anisotropic Nucleation Growth of Actin Bundle: A Model for Determining the Well-Defined Thickness of Bundles. // Biochemistry. 2006. v. 45. № 34. pp. 10313-10318.

236.   Hess B., Sayar M., Holm C. Stability of hydrophobically modified poly(*p*-phenylenesulfonate) bundles as observed by molecular dynamics simulation// Macromolecules. 2007. v. 40. № 5. pp. 1703-1707.

237.   Kroeger A., Belack J., Larsen A., Fytas G., Wegner G. Supramolecular Structures in Aqueous Solutions of Rigid Polyelectrolytes with Monovalent and Divalent Counterions. // Macromolecules. 2006. v. 39. № 20. pp. 7098 – 7106.

238.   Kwon H. J., Kakugo A., Shikinaka K., Osada Y., Gong J. P. Morphology of actin assemblies in response to polycation and salts. // Biomacromolecules. 2005. v. 6. № 6. pp. 3005-3009.

239.   Berg M.C., Zhai L., Cohen R. E., Rubner M. F. Controlled drug release from porous polyelectrolyte multilayers // Biomacromolecules. 2006. v. 7. № 1. pp. 357-364.

ERKLÄRUNG

Diese Dissertation wurde im Zeitraum von Januar 2005 bis Dezember 2007 im Institut Polymer Science der Universität Ulm erstellt.

Hiermit erkläre ich, dass ich diese Arbeit selbständig und nur mit den angegebenen Hilfsmitteln angefertigt habe. Alle Stellen, die dem Wortlaut oder dem Sinn gemäss Arbeiten entnommen wurden, sind durch Angabe der Quellen kenntlich gemacht.

Ulm, den 27.05.2008

Olga Gus'kova

CURRICULUM VITAE

PERSONAL INFORMATION

Name:	M. Sc. **Olga A. Gus'kova**
Citizenship:	Russian
Date and place of birth:	October 30, 1981, Tver (Russia)
Marital status:	single
Business address:	Department of Polymer Science University of Ulm Albert Einstein Allee 11, Ulm 89069, Germany **Phone:** +49(731)50-31391 **Fax:** +49(731)50-31399
Home address:	Ochsensteige, 18/2, 89075, Ulm, Germany
Phone:	+49(731)50-31-383
e-mail:	olga.a.guskova@googlemail.com

PROFESSIONAL SKILLS

Languages:	Deutsch, English, Russian (native)
Scientific skills:	Computer simulation of polymer systems; Physical chemistry of polyelectrolytes; Coil-globule transition; Computer simulation of conjugated polymers and bioinspired polymer hybrids; Self-organization of peptide hybrids near surface.

EDUCATION and RESEARCH EXPERIENCE

2004-present **Moscow, Russia / Ulm, Germany**

- Laboratory of Physical Chemistry of Polymers, A.N. Nesmeyanov Institute of Organoelement Compounds, RAS, and Department of Polymer Science, University of Ulm
"*Simulation of Nanostructure Formation in Rigid-Chain Polyelectrolyte Solutions*"

PhD student

1998-2004 **Tver, Russia**

- Department of Physical Chemistry, Tver State University, Tver
  "*Computer Simulation of Coil-to-globule Transition in Charged Macromolecular Systems*"

- Qualification of Master's Degree of Chemistry with the Specialization of "Macromolecular Chemistry"

GRANTS

02/2007-12/2007 **Scientific scholarship (Russian Science Support Foundation)**
The laureate of program "Best PH.D. students of RAS"

AWARDS

05/2002-12/2002 Scholarship of President of Russia

01/2003-10/2002 Scholarship of Government of Russia

10/2004-08/2002 Scholarship of President of Russia

09/2007 Best article prize of editorial office "Nauka-Interperiodika"

Ulm, 27.05.2008

Olga Gus'kova

Appendix A
List of abbreviations and symbols

DHBC	Double hydrophilic bock copolymer
LC	Liquid-crystal
MD	Molecular dynamics
MC	Monte Carlo method
PE	Polyelectrolyte
PEC	Polyelectrolyte complex
RF	Reaction field method

A	Kuhn segment
$<D>$	Average free-volume hole diameter
e	Elementary charge
$g(r)$	Pair correlation function
I	Ionic strength
k_B	Boltzmann constant
$l_{p,0}$	Intristic persistence length
ℓ_B	Bjerrum length
ℓ_p	Persistence length
$l_{p,e}$	Electrostatic persistence length
L_C	Counter length
L_q	Linear charge density
r_C	Cutoff radius
R^2_g	Mean-square radius of gyration
q_i, z_i	Charge
T	Temperature
V	Potential energy
V_{LJ}, V_{ev}	Lennard-Jones potential
V_C	Coulomb potential
$W_d(R)$	Void-size differential distribution function
$z(r)$	Coordination number

Δt	Integration step
$\delta_{\tau\eta}$	Kronecker delta
ε_r	Solvent permittivity
η	Order parameter
θ	Valence angle
λ_D	Screening radius
ξ	Manning parameter
ρ	Solution density
σ	Monomer radius

Appendix B
List of selected publications

1.   L.V. Zherenkova, P.V. Komarov, <u>O.A. Gus'kova</u>. Influence of polyelectrolyte and salt on the structure of dispersions containing charged colloidal particles // J. Structural Chemistry. 2006. v. 47. №1. pp. 157-163.

2.   <u>O.A. Gus'kova</u>, A.S. Pavlov, P.G. Khalatur. Ionic micelles in solutions of a polyelectrolytes and block copolymers with an oppositely charged block: computer simulation //Polymer Science. Ser. A. 2006. v. 48. №11. pp. 1211-1217.

3.   <u>O.A. Gus'kova</u>, A.S. Pavlov, P.G. Khalatur. Complexes based on rigid-chain polyelectrolytes: computer simulation. // Polymer Science. Ser. A. 2006. v. 48. №7. pp. 763-770.

4.   <u>O.A. Gus'kova</u>, A.S. Pavlov, P.G. Khalatur. Network structures in solutions of rigid-chain polyelectrolytes: computer simulation. // Polymer Science. Ser. A. 2007. v. 49, №5. pp. 611-616.

5.   <u>O.A. Gus'kova</u>, A.S. Pavlov, P.G. Khalatur, A.R. Khokhlov. Molecular bottle-brushes in a solution of semiflexible polyelectrolytes and block copolymers with an oppositely charged block: A molecular dynamics simulation // J. Phys. Chem. B 2007. v. 111. № 29. pp. 8360-8368.

6.   <u>O.A. Gus'kova</u>, E. Mena-Osteritz, E. Schillinger, P.G. Khalatur, P. Bäuerle, A.R. Khokhlov. Self-assembled monolayers of β-alkylated oligothiophenes on graphite substrate: molecular dynamics simulation. // J. Phys. Chem. C. 2007. v. 111. №19. pp. 7165-7174.

7.   <u>O.A. Gus'kova</u>, P.G. Khalatur. Structure of adsorption layers of oligothiophene derivatives: effect of substitutents. // Polymer Science. Ser. A. 2007. v. 48. №8. pp. 939-943.

8.   <u>O.A. Gus'kova</u>, P.G. Khalatur, P. Bäuerle, A. R. Khokhlov. Silk-Inspired "Molecular Chimeras": Atomistic Simulation of Nanoarchitectures Based on Thiophene-Peptide Copolymers. // Chem. Phys. Lett. 2008. v. 461. №1-3. pp. 64-70.

9.   <u>O.A. Gus'kova</u>, P.G. Khalatur, A. R. Khokhlov. "Molecular chimeras": new design strategies of functional materials. // Nanotechnologies in Russia. 2008. v. 3. №7-8. pp. 481-493.

10.   <u>O.A. Gus'kova</u>, E. Schillinger, P.G. Khalatur, P. Bäuerle, A.R. Khokhlov. Bioinspired hybrid systems based on oligothiophene and peptides (Ala-Gly)$_N$: computer simulation of adsorption layers. // Polymer Science. Ser. A. 2008 (in Press).

Appendix C
List of selected conferences

1. **Conference "Trends in Nanoscience", February 24-28, 2007, Kloster Irsee, Germany.**
Gus'kova O.A., Mena-Osteritz E., Schillinger E., Khalatur P.G., Bäuerle P., Khokhlov A.R. Self-assembled monolayers of β - Alkylated oligothiophenes on graphite substrate: molecular dynamics simulation. Book of abstracts, p. 23. (poster).

2. **The 4th All-Russian Kargin Conference "Polymers Science to 21 century", January 29 – February 2, 2007**
Gus'kova O.A., Khalatur P.G. Self-assembled monolayers of alkylated oligothiophenes on graphite surface: molecular dynamics simulation. Book of abstracts, v.3, p. 321.

3. **Second SFB 569 Young Researcher Meeting, July 26-28, 2006, Kleinwalsertal – Austria.**
Gus'kova O.A. Tetrathiophene on Graphite: Molecular Dynamics Simulations. Austria, Kleinwalsertal (talk).

4. **Small Polymer Congress, 2005, INEOS RAS, Moscow, Russia.**
Gus'kova O.A. Self-organization in solution of thiophene-peptide diblock copolymers. Book of abstracts. p. 78 (poster, talk).

5. **The 3rd All-Russian Kargin Conference "Polymers -2004", January 27 – February 1, 2004, Moscow, MSU**.
Gus'kova O.A., Ryabova O.A., Khalatur P.G. Simulation of polyelectrolytes with various distributions of charged units. Book of abstracts, p. 183.

6. **The 2nd All-Russian Yung Researcher Conference IOCh RAS, April 13-14, 2006, Moscow, Russia.**
Gus'kova O.A., Khalatur P.G. The adsorbed layer structure of thiophene derivatives near graphite surface. Book of abstracts, pp.106-108 (poster).

7. **The 3rd STIPOMAT Conference, 14-18 October 2007, Lausanne, Switzerland.**
A.R. Khokhlov, O.A. Gus'kova, P.G. Khalatur, P. Bäuerle.Bioinspired oligothiophene-oligopeptide hybrid nanostructures: an atomistic simulation.

8. **XIV International Young Researcher Conference «Lomonosov-2007» - Chemistry**, April 11-13, 2007, Moscow, Russia.
Gus'kova O.A. Structure of adsorption layers of oligothiophene derivatives: effect of substitutents. Book of abstracts, p. 113 (talk).

9. **International Workshop on Dynamics of Complex Fluids, 2004, Kyoto, Japan.**
Gus'kova O.A, Ryabova O. A., Pavlov A.S, Zherenkova L.V. Molecular Dynamics Simulation of Hydrophobic Flexible Polyelectrolytes and Polyampholytes (Poster).

10. **Second Saint-Petersburg International Conference on NanoBiotechnologies "NanoBio'08", 16-18 June, 2008, Saint-Petersburg, Russia**.
Gus'kova O.A. Peptide-functionalized oligothiophene hybrids: computational modeling of bioinspired materials (Poster).

11. **Advanced Polymeric Materials for the Energy Resources Exploitation: Synthesis Properties and Applications, June 1-5, 2008, Gargnano, Lake Garda, Italy.**
Gus'kova O.A., Khalatur P.G., Bäuerle P., Khokhlov A.R. Computational modeling of bioinspired polypeptide/π-conjugated polymer block copolymers (poster).

12. **International Workshop Statistical Mechanics of Polymers: New Developments, June 6-11, 2006, Moscow, Russia**
Berezkin A.V., Lazutin A.A., Gus'kova O.A. (poster).

13. **International School "Computer simulations of macromolecules and biomacromolecules" June 13-16, 2005, Petrozavodsk, Russia**.
Gus'kova O.A. Network structures in solutions of rigid-chain polyelectrolytes: computer simulation (poster).

14. **European Polymer Congress. June 27-Jule 1, 2005, Moscow, Russia**.
Guskova O.A, Pavlov A.S., Khalatur P.G. Computer Simulation of Interactions between Rigid Polyelectrolytes and Hydrophobic-Hydrophilic Copolymers. Book of abstracts, p. 208 (poster).
15. **IASTED International Conference on Nanotechnology and Applications NANA-2008, 2008.**
O.A. Gus'kova, E. Schillinger, P.G. Khalatur, P. Bäuerle, A.R. Khokhlov. Nanoarchitectures based on biomimetic thiophene-peptide copolymers: an atomistic simulation. 2008 (poster).